TECHNICAL REPORT BRL-TR-3078

BRL

BOROHYDRIDE CATALYSIS OF NITRAMINE THERMAL DECOMPOSITION AND COMBUSTION. II. THERMAL DECOMPOSITION OF CATALYZED AND UNCATALYZED HMX PROPELLANT FORMULATIONS

MICHAEL A. SCHROEDER

FEBRUARY 1990

U.S. ARMY LABORATORY COMMAND

BALLISTIC RESEARCH LABORATORY
ABERDEEN PROVING GROUND, MARYLAND

DESTRUCTION NOTICE

Destroy this report when it is no longer needed. DO NOT return it to the originator.

Additional copies of this report may be obtained from the National Technical Information Service, U.S. Department of Commerce, Springfield, VA 22161.

The findings of this report are not to be construed as an official Department of the Army position, unless so designated by other authorized documents.

The use of trade names or manufacturers' names in this report does not constitute indorsement of any commercial product.

UNCLASSIFIED

SECURITY CLASSIFICATION OF THIS PAGE

REPORT DOCUMENTATION PAGE

Form Approved OMB No. 0704-0188

1a. REPORT SECURITY CLASSIFICATION: Unclassified	1b. RESTRICTIVE MARKINGS
2a. SECURITY CLASSIFICATION AUTHORITY	3 DISTRIBUTION / AVAILABILITY OF REPORT: Approved for public release; distribution unlimited.
2b. DECLASSIFICATION / DOWNGRADING SCHEDULE	
4. PERFORMING ORGANIZATION REPORT NUMBER(S): BRL-TR-3078	5. MONITORING ORGANIZATION REPORT NUMBER(S)
6a. NAME OF PERFORMING ORGANIZATION: US Army Ballistic Research Laboratory; 6b. OFFICE SYMBOL (If applicable): SLCBR-IB	7a. NAME OF MONITORING ORGANIZATION
6c. ADDRESS (City, State, and ZIP Code): Aberdeen Proving Ground, MD 21005-5066	7b. ADDRESS (City, State, and ZIP Code)
8a. NAME OF FUNDING / SPONSORING ORGANIZATION; 8b. OFFICE SYMBOL (If applicable)	9. PROCUREMENT INSTRUMENT IDENTIFICATION NUMBER
8c. ADDRESS (City, State, and ZIP Code)	10. SOURCE OF FUNDING NUMBERS: PROGRAM ELEMENT NO. 61102A; PROJECT NO. AH43; TASK NO.; WORK UNIT ACCESSION NO.

11. TITLE (Include Security Classification)
BOROHYDRIDE CATALYSIS OF NITRAMINE THERMAL DECOMPOSITION AND COMBUSTION. II. THERMAL DECOMPOSITION OF CATALYZED AND UNCATALYZED HMX PROPELLANT FORMULATIONS

12. PERSONAL AUTHOR(S)
Michael A. Schroeder

13a. TYPE OF REPORT	13b. TIME COVERED	14. DATE OF REPORT (Year, Month, Day)	15. PAGE COUNT
Final	FROM Jan 87 TO Dec 87		

16. SUPPLEMENTARY NOTATION

17 COSATI CODES			18. SUBJECT TERMS (Continue on reverse if necessary and identify by block number)
FIELD	GROUP	SUB-GROUP	
07	03		HMX, Nitramines, Borohydrides, Boron Hydrides, Catalysis Mechanisms, Catalysis, Propellants, Explosives, Thermal Decomposition, Gun Propellants, VHBR Propellants, Combustio
07	04		

19. ABSTRACT (Continue on reverse if necessary and identify by block number)

This report describes GC-MS studies on thermal decomposition of HMX, RDX and propellants, with and without catalysis by $K_2B_{12}H_{12}$ or $K_2B_{10}H_{10}$. This work differs from previous work in that it emphasizes the less-volatile decomposition products. Pyrolysis-GC-MS on HMX-GAP and HMX-PEG compositions with and without $K_2B_{10}H_{10}$ has been carried out. Identification of products is in progress; identification of a number of products is discussed. To date, the most mechanistically important product identified is probably 1,3,5-triazine. This is beleived to be formed from HMX via 1,3,5,7-tetraazacycloocta-tetraene; this is consistent with the known thermal decomposition behavior of cyclooctatetraene and its azaderivatives. 1,3,5-triazine formation by trimerization of HCN is believed to be relatively unimportant. There is also an unknown component whose highest mass peak is at m/e 70.

(CONT'D)

20. DISTRIBUTION / AVAILABILITY OF ABSTRACT: ☐ UNCLASSIFIED/UNLIMITED ☒ SAME AS RPT ☐ DTIC USERS	21 ABSTRACT SECURITY CLASSIFICATION: Unclassified
22a. NAME OF RESPONSIBLE INDIVIDUAL: DR. MICHAEL A. SCHROEDER	22b TELEPHONE (Include Area Code): 301-278-6105; 22c. OFFICE SYMBOL: SLCBR-IB-I

DD Form 1473, JUN 86 *Previous editions are obsolete.*

SECURITY CLASSIFICATION OF THIS PAGE

UNCLASSIFIED

19. Abstract (Cont'd):

In addition, further analysis of results from earlier runs on RDX and RDX-$K_2B_{12}H_{12}$ mixtures has been carried out. Based on all of the above, it appears that formation of the m/e 70 unknown decreases with increasing temperature. Most interesting is the effect of $K_2B_{12}H_{12}$ on formation of this material; it varies with decomposition temperature. Added catalyst appears to decrease m/e 70 (1,2,4-oxadiazole?) formation at low temperature, but to increase it slightly at the higher temperatures. This shift suggests the possibility of a change in catalysis mechanism on going from low to high temperature; some possible chemical mechanisms are discussed.

TABLE OF CONTENTS

INTENTIONALLY LEFT BLANK.

LIST OF FIGURES

LIST OF FIGURES (CONT'D)

LIST OF FIGURES (CONT'D)

LIST OF FIGURES (CONT'D)

LIST OF FIGURES (CONT'D)

LIST OF FIGURES (CONT'D)

LIST OF FIGURES (CONT'D)

LIST OF FIGURES (CONT'D)

LIST OF TABLES

LIST OF TABLES (CONT'D)

I. INTRODUCTION

Very high burning rate (VHBR) propellants are needed for such applications such as the monolithic charge and the traveling charge. These propellants generally contain HMX or RDX, and/or triaminoguanidine nitrate (TAGN) together with a borohydride such as one of the HIVELITES (Teledyne-McCormick-Selph). The borohydride greatly accelerates the burning rate of the propellant. The purpose of the present work is to elucidate the chemical mechanisms responsible for the burning rate acceleration, with the ultimate goal of optimizing propellant formulations for actual use, e.g., maximum "catalytic" effects with minimum sensitivity.

This report describes gas chromatography-mass spectrometry (GC-MS) studies of thermal decomposition of nitramines and nitramine propellant formulations, both uncatalyzed and catalyzed with $B_{10}H_{10}^{=}$ and $B_{12}H_{12}^{=}$ salts. The compositions being studied are experimental VHBR formulations being tested as part of the BRL VHBR and monolithic charge programs. The goal of the present work is to correlate observed pyrolysis behavior with performance. This report describes GC-MS studies on some HMX propellant compositions and their ingredients. The present author has previously described[1] GC-MS studies on RDX and on mixtures of RDX with $K_2B_{12}H_{12}$. Reference 1 is considered to be Part I in this series of reports.

The approach employed involves GC-MS studies on the pyrolysis products of pure RDX and HMX, of propellant compositions and of mixtures of HMX and RDX with $K_2B_{10}H_{10}$ and $K_2B_{12}H_{12}$. A number of previous studies (reviewed in References 2-9) have reported detailed analysis of the permanent gaseous products from HMX (octahydro-1,3,5,7-tetranitro-1,3,5,7-tetrazocine) and RDX (hexahydro-1,3,5-trinitro-1,3,5-triazine) decomposition. Therefore, the present work concentrates mainly on the less-volatile products, namely those whose retention times and volatilities are intermediate between those of the more-commonly-studied permanently gaseous products and those of unreacted RDX. Because of their possible mechanistic significance, the effect of such factors as temperature and catalyst on formation of 1,3,5-triazine and Unknown A (1,2,4-oxadiazole?) were also studied.

II. EXPERIMENTAL

The HMX-GAP and HMX-PEG compositions were prepared at Teledyne-McCormick-Selph by Dr. Abdul Helmy, and contained 10% by weight of the indicated binder (glycidyl azide polymer (GAP) or polyethylene glycol (PEG)); as oxidizer a mixture containing five parts by weight HMX and three parts TAGN; and between 0% (uncatalyzed) and 15% $K_2B_{10}H_{10}$. Thus the PEG formulation identified as PEG 5-3-0 has 10% PEG, 56.3% HMX, 33.8% TAGN, and 0% (none) of $K_2B_{10}H_{10}$, while the formulation identified as PEG 5-3-15 has 10% PEG, 46.9% HMX, 28.1% TAGN, and 15% $K_2B_{10}H_{10}$. The GAP formulations are designated in a similar way.

The apparatus used consists of a Hewlett-Packard 5890 GC, coupled to a 5970 Mass Selective Detector. Pyrolysis is carried out by means of a Chemical Data Systems (CDS) Pyroprobe, which is interfaced to the GC-MS apparatus with a Chemical Data Systems (CDS) 330 concentrator.

To carry out a run, a small amount (ca 0.1-1 mg) of the sample is placed between two quartz-wool plugs in a quartz tube 25 mm long, and pyrolyzed in a

coil Pyroprobe at a known temperature, generally in the range 250 to 800°C, and usually either 325 or 800°C, in the desorber inlet of the CDS 330 concentrator. Temperatures given are Pyroprobe set temperatures and are believed to be somewhat (possibly as much as 100-200°) higher than the actual temperature. The products pass to trap A of the concentrator, where the less volatile ones are held at -50° (liquid N_2 cooling) until the pyrolysis event is complete. Then trap A is heated and the products are directed to trap B of the concentrator; this is a cryofocuser which focuses them onto the GC column. The GC column (crosslinked methyl silicone gum, 12 meter x 0.2 mm, 0.33 μm film thickness) is programmed from 70°C to 250°C over 9 minutes with an initial 3 minute hold time. The products are held on trap B at -50° (liquid nitrogen cooling) for several minutes to assure that as many products as possible are carried over from trap A; this adds ca 5-6 minutes to the apparent retention time, since the mass spectrometer was kept on during this time in order to obtain any information that might become available as the gaseous and other poorly-retained products passed through trap B and the GC column.

The runs involving RDX and RDX-$K_2B_{12}H_{12}$ mixtures were carried out in the course of the work reported[1] previously, using the apparatus and procedures described.

III. RESULTS

The results of this part of the study are summarized in Figures 1-136 and in Tables 1-27.

Typical chromatograms for catalyzed and uncatalyzed PEG and GAP compositions at each of the two temperatures (325 and 800°C) employed are given in Figures 1-8. Typical chromatograms for each of the pure ingredients PEG, TAGN, HMX, and H498 at 325 and 800° are given in Figures 9-16. The retention times given should be corrected by subtracting five minutes in order to take account of the trap B cooling time. A sample of pure GAP is on order but was not received in time to be included here.

It can be seen that these chromatograms (Figures 1-16) are extremely complex. Note that the chromatography is greatly improved over that described in our previous report;[1] this is a result of the cryofocusing provided by trap B of the concentrator.

The formation in this work of two compounds seems particularly significant. These include: (a) 1,3,5-triazine, the formation of which from RDX decomposition we have previously described;[1] and (b) an unknown compound, possibly 1,2,4-oxadiazole, whose mass spectrum has its highest-mass peak at m/e 70.

The 1,3,5-triazine was formed in all of the runs on the compositions (Figures 1-16, Table 27), regardless of temperature or catalyst content.

Although it was formed to a quite noticeable degree in most of the runs on pure HMX and RDX, the m/e 70 unknown (Unknown A) was much less noticeable in the runs on the formulations, and in many cases was not seen in these runs. The cases in which a peak at m/e 70 was discernible at 5-6 minutes were

mostly low-temperature (325°C) runs, although it was weakly discernible in a very few catalyzed runs at 800°C.

Tables of retention times (and for the more obvious or important peaks, spectral information and/or comments on possible identitiies) for the less-volatile products, compiled with the aid of the software from chromatograms such as those given in Figures 1-16, are given in Tables 1-21 and Figures 18-136. The numbers in the first columns of these tables give the retention times in minutes; note that five minutes should be subtracted from these numbers to allow for the cooling time of trap "B" of the concentrator. The letters following these numbers are abbreviations denoting the relative intensity of the respective peaks and have the following meanings: s - Strong; m - Medium; w - Weak, v - Variable; vi - Variable Intensity; vo - Variable Occurrence. The spectra from all peaks are on hand and further work on identification is in progress.

Formation of Unknown A (1,2,4-oxadiazole?) in the runs reported earlier[1] was studied by reconstructing m/e 70 ion chromatograms, integrating the peak at ca 0.5.-1.0 minute and normalizing these integrated intensities against the integrated intensities of the total gaseous-product peak and the gaseous-product peak at m/e 44 (N_2O + CO_2) (Tables 22-26).

The information in Tables 22-26 suggests that formation of the m/e 70 unknown (1,2,4-oxadiazole?) exhibits an interesting dependence on both decomposition temperature and presence of catalyst: First, the extent of its formation appears to first increase, then decrease with temperature; and second, the effect of $K_2B_{12}H_{12}$ varies with temperature. At low temperatures, borohydride causes a decrease in formation of this material and at high temperatures an increase in its formation is observed over what is observed in the absence of catalyst.

Table 27 represents an attempt to roughly quantify trends in formation of 1,3,5-triazine from decomposition of the formulations; the heights of the 1,3,5-triazine peaks at m/e 54 and m/e 81 (columns 4 and 5) were normalized by dividing them by the heights of the most intense peaks in the respective chromatograms; the results of these normalizations are given in columns 6 and 7. The first three columns give respectively the run number, the sample and the pyroprobe set temperature at which the decompositions were carried out.

Note the large run-to-run variations in both the original (columns 4 and 5) and the normalized (columns 6 and 7) peak heights; these are apparently due to the approximate nature of the data. Nevertheless it is possible to discern that the presence of $K_2B_{10}H_{10}$ as catalyst appears in most cases to decrease the amount of 1,3,5-triazine formed (Table 27). Any effects of temperature and of binder (PEG vs. GAP) are apparently obscured due to the approximate nature of the data in Table 27.

An attempt was made at checking for the possibility of destruction of 1,3,5-triazine by $K_2B_{10}H_{10}$; this involved vaporization of 1,3,5-triazine in a pyroprobe at 400°C in the presence and absence of $K_2B_{10}H_{10}$ and analyzing the effluent by gas chromatography-infrared spectroscopy (GC-IR). In some runs, both with and without $K_2B_{10}H_{10}$, the effluent appeared to be reasonably pure 1,3,5-triazine. However, the results are still considered inclusive because of the use of unweighed samples, and because in many runs, both with and

without $K_2B_{10}H_{10}$, the samples appeared to have decomposed while being prepared, possibly as a result of atmospheric moisture. However, injection of liquid samples of acetone solutions of 1,3,5-triazine invariably gave good GC-IR and GC-MS chromatograms of 1,3,5-triazine.

IV. DISCUSSION

A. Identification of Chromatographic Peaks

Among the most noticeable features of the chromatograms (Figures 1-16) from thermal decomposition of HMX, RDX, and the formulations are the relatively intense peaks at the beginning of the temperature-programmed region of the chromatogram. Substances emerging in this region include 1,3,5-triazine, N,N-dimethylaminoacetonitrile and some possibly related compounds, and an unidentified material (Unknown A) apparently having a molecular weight of 70 (1,2,4-oxadiazole?). Since these are also probably among the most mechanistically significant of the less-volatile products, it seems worthwhile to describe in some detail the evidence for their structures.

1,3,5-Triazine. Identification of 1,3,5-triazine from RDX decomposition was described in our previous report.[1] In the present work, the occurrence of 1,3,5-triazine with retention time ca 0.5-1.0 minute after release of the products from trap B was detected by carrying out ion chromatograms for its characteristic peaks at m/e 54 and 81; this was confirmed by comparing its spectrum with spectra[1] of authentic 1,3,5-triazine obtained on our instrument. 1,3,5-triazine was found in nearly all runs involving decomposition of HMX and HMX-containing propellant formulations. Possible mechanisms for its formation in these systems will be discussed below.

N,N-Dimethylaminoacetonitrile and Related Compounds. A peak of variable intensity with retention time of ca 5.9-6.0 minutes (ca 0.9-1.0 minutes after correction for the 5-minute cooling time of trap B) was tentatively identified from mass spectra (see for example Figures 76, 82, 91) as $(CH_3)_2NCH_2CN$ (N,N-dimethylaminoacetonitrile). This was confirmed by the spectrum and retention time obtained from injection of an authentic sample (Figure 137). This peak occurs in many runs, and appears to be strongest in those carried out in the presence of $K_2B_{10}H_{10}$ as catalyst (Tables 1-10), although it does occur in runs on HMX alone (Tables 11-15).

There are several other peaks which may be related to $(CH_3)_2NCH_2CN$. Some of these appear to be characterized by components with highest-mass peaks at m/e 70 and strong M-1 peaks at m/e 69. These include peaks with retention times 6.98 - 5.0 = 1.98 minutes (Table 6, Figure 58); 6.46 - 5.0 = 1.46 minutes (Table 8, Figure 70); 6.64 - 5.0 = 1.64 minutes (Table 8, Figure 71); and 6.38 - 5.0 = 1.38 minutes (Table 9, Figure 77). In addition, there is at least one peak (7.70 - 5.0 = 2.70 minutes) (Table 14, Figure 100) with highest mass at m/e 109; and finally a second (7.34 - 5.0 = 2.34 minutes) peak with highest mass at m/e 84 (Table 11, Figure 88). All of these chromatographic peaks are characterized by M - 26 (loss of CN), M - 42 (loss of CH_2CN) and in some cases M - 15 (loss of CH_3). Possible structures include $(CH_3)_2N-CN$ and $CH_3-NH-CH_2-CN$ for M = 70, $CH_3-NH-CH_2CH_2CN$ and $CH_3CH_2-NH-CH_2CN$ for M = 84 and $CH_3-N(-CH_2-CN)_2$ for M = 109. Authentic comparison samples of the first three compounds are on order; unfortunately the last two are apparently not commercially available.

Unknown A (1,2,4-Oxadiazole?). Another strong peak at the beginning of the temperature-programmed region of the chromatogram has the spectrum shown in Figure 17. The structure of this material is at present uncertain. However it seems worth mentioning that unknowns containing peaks at m/e 70 have been reported[10-14] previously among the products from HMX and RDX decomposition. In some cases[10,12,13] the structure 1,2,4-oxadiazole has been mentioned in connection with these peaks. This seems at least consistent with the following:

(a) Ion chromatograms for m/e 70 for the pure-HMX and pure-RDX runs in which this compound occurs show a single strong peak at a point about one-half minute after release of the products from the cryofocuser.

(b) The isotope peak at m/e 71 had an intensity 2.93% of that of the apparent parent-ion peak at m/e 70; this is in reasonable agreement with the value of 2.99% calculated[15] for $C_2H_2N_2O$.

(c) The index of hydrogen deficiency[15] (equal to total number of rings and double bonds) for this molecular formula is 3, in agreement with the 1,2,4-oxadiazole structure which has one ring and two double bonds.

(d) By analogy with the mass spectra of 3,5-disubstituted 1,2,4-oxadiazoles,[16,17] the unsubstituted parent compound should be capable of cleaving in two possible ways, one yielding an m/e 29 (HCO) and an m/e 41 (NCHN) fragment and the other yielding an m/e 27 (HCN) and an m/e 43 (HCNO). There is a problem here, since while the m/e 43 peak of our spectrum is the strongest in that part of the spectrum, the other strong peak in the region occurs not at m/e 41 but at m/e 40; however it does not seem unreasonable to suppose that increased resonance stabilization in NCN (m/e 40) might be a driving force for loss of a hydrogen from m/e 41 (NCHN).

(e) In the pure-HMX and pure-RDX runs, which were less "busy" than the composition runs, the peak which we tentatively attribute to 1,2,4-oxadiazole appeared homogeneous; the spectra were the same throughout the peak.

(f) Integration of ion chromatograms for m/e 26, 27, 28, 29, 30, 38, 39, 40, 41, 42, and 43 showed peaks in the 5.5-6 region within ca 0.001 minute of each other and of the only intense peak in the m/e 70 chromatogram.

(g) In a footnote in Reference 13, it is stated that a fragment of m/e 70 appeared in pyrolysis/ms studies on HMX at 573 K (300°C). When ring-labeled (with ^{15}N) was used the peak shifted to m/e 72. It was stated (experimental details not given) that the mass spectrum of this compound was similar to a known spectrum of 1,2,4-oxadiazole. The present work apparently differs from this in that we used chromatography to separate the products.

It seems unlikely that the m/e 70 peak reported by Juhasz[11] is identifiable with the m/e 70 peak mentioned here. This follows from the fact that the substance reported earlier[11] had a peak at m/e 69 as well as 70; no such peak appeared in our Unknown A (Figure 17). We did see at least one other unknown with m/e 70 that was accompanied by a peak at m/e 69 (Tables 8 and 9, Figures 71 and 77); the structure of this peak is under investigation. It is also unlikely that the m/e 70 peak mentioned by Behrens[14] is identifiable with Unknown A from the present work, since that

peak appears to result from decomposition of a compound with parent ion at 97, whereas the parent ion of Unknown A in the present work appears to be 70.

Identification of the compounds responsible for the remainder of the peaks in the chromatograms pictured in Figures 1-136 is in progress.

B. Preliminary Observations Conerning Catalyst and Temperature Effects on Formation of Products

1,3,5-Triazine. In Table 27 are presented the results of an attempt to quantify at least the trends in formation of 1,3,5-triazine. Ion chromatograms for the 1,3,5-triazine mass peaks at m/e 54 and m/e 81 were taken, and the heights of their peaks at ca 5.8 - 5.0 = 0.8 minutes (retention time of 1,3,5-triazine) were normalized by dividing them by the heights of the highest peaks in the respective chromatograms.

Several trends emerge from the data in Table 27. First, although 1,3,5-triazine is formed from decomposition of HMX, there seems to be much more 1,3,5-triazine formed from RDX decomposition than from HMX decomposition (Runs 107-113, 172-175 and 186). This is as expected, since RDX and 1,3,5-triazine both include six-membered ring structures while in the case of HMX the six-membered structure must be formed from the eight-membered ring present in HMX.

Second, at least for consecutive runs there seems to be a tendency for 1,3,5-triazine formation to be reduced in the presence of catalyst (Runs 114-156 and 161-166), although runs 114, 155 and 162 are exceptions. This is in agreement with results obtained earlier[1] on RDX and RDX-$K_2B_{12}H_{12}$ mixtures. However it is harder to discern any effect of temperature.

It is interesting to note that while at 800°C even less (none at all in many runs) of the 1,3,5-triazine peaks at m/e 54 and m/e 81 are seen from decomposition of TAGN than from HMX, these peaks become a little more intense when decomposition of TAGN is carried out at 325°C (Runs 157-60, 167-71, 184-185). There is no obvious explanation as to why HMX at 325°C, in contrast to the higher temperatures, forms little if any 1,3,5-triazine. Possibly (see below, Section IV.C.) the 1,3,5-triazine forms from HMX via an intermediate 1,3,5,7-tetraazacyclooctatetraene which decomposes only at higher temperatures than reached by our samples at a set temperature of 325°C. It is also hard to see why, in contrast to pure TAGN and pure HMX, some runs on the compositions seem to give appreciable amounts of m/e 54 and m/e 81 on decomposition at 325°C.

Unknown A. Tables 22-26 show some further results taken from total ion chromatograms (plots of total ion intensity vs. time) obtained in the course of our earlier work,[1] as well as results obtained from single-ion chromatograms. A single ion chromatogram is a plot of intensity vs. time for a single ion mass; these can be obtained using the software that came with our equipment.

Columns 4-6 of Tables 22-26 contain summaries of integrated total intensities of the almost-unretained (retention times less than ca 0.8 minute) products, as well as of the peaks at ca 0.5 minute corresponding to m/e 44 (believed to be mostly N_2O and CO_2), and 70 (used as an index of Unknown A (1,2,4-oxadiazole?) formation). The last three columns of Tables 22-26

contain the ratios of the areas of the peaks of m/e 44 and 70 to the total ion area and of the integrated area of the m/e 70 ion chromatogram to that of the m/e 44 ion chromatogram. The object of the ratioing was to compensate at least partially for the fact that the samples were unweighed, thereby obtaining at least a crude normalized estimate of the relative amounts of Unknown A (1,2,4-oxadiazole?) formed in the various runs. This seemed worthwhile because of the possible mechanistic significance of the formation of Unknown A (1,2,4-oxadiazole?). Note however the uncertainty due to such factors as possible changes with temperature or degree of catalyst in the relative amounts of gaseous products.

Increasing the decomposition temperature (Tables 22-26) in the absence of catalyst caused some increase until at least the 600°C region is reached, but by the time 800°C is reached, the intensity ratios for m/e 70 have decreased to a fraction of their value at 250°C. This suggests that in the absence of catalyst, formation of Unknown A decreases at the higher temperatures, although it is also possible that the decrease is due to boron-hydride catalyzed decomposition of Unknown A (1,2,4-oxadiazole?) after formation.

In the presence of $K_2B_{12}H_{12}$ catalyst (Tables 22-26), the temperature effect appears to be the following: Unknown A (1,2,4-oxadiazole?) formation seems to remain more or less constant with temperature, with some signs of a maximum in the 400°C - 600°C region.

The effect of catalyst at the various temperatures appears to be as follows. At 250°C and at 400°C, added $K_2B_{12}H_{12}$ causes a decrease in Unknown A (1,2,4-oxadiazole?) formation. At 600°C, the situation does not seem clear-cut and at 800°C, there is actually some increase in Unknown A (1,2,4-oxadiazole?) formation due to added $K_2B_{12}H_{12}$. This shift with temperature in the effect of presence of catalyst on the amount of Unknown A detected seems of considerable interest, since it could indicate a change in catalysis mechanism as temperature increases. This is true regardless of the exact nature of any chemical structure that may ultimately be assigned to Unknown A.

C. Chemical Mechanisms

Mechanisms for 1,3,5-Triazine Formation from HMX. Most if not all of the 1,3,5-triazine observed from the decomposition of the HMX formulations presumably results from decomposition of HMX, since decomposition of HMX alone gives some 1,3,5-triazine and none of the other ingredients contain any obvious source or precursor for 1,3,5-triazine. Mechanisms that should be considered for its formation include (a) further decomposition of 1,3,5,7-tetraazacyclooctatetraene formed from HMX decomposition by mechanisms similar to those written[1] for formation of 1,3,5-triazine from RDX decomposition (Scheme I); and (b) trimerization of HCN formed[5-8] in HMX decomposition (Scheme II).

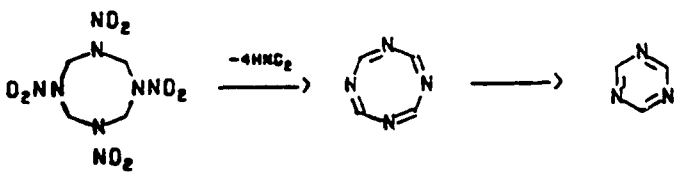

SCHEME I

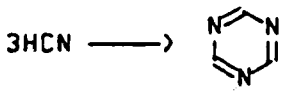

SCHEME II

It seems unlikely that more than a small amount of the 1,3,5-triazine could have been formed from pathway (b), HCN trimerization. It formed in almost every decomposition of HMX, RDX, and of the formulations. However when TAGN, the decomposition products of which include HCN,[18] was decomposed at 800°C under the same conditions, the runs gave very little 1,3,5-triazine as measured by the peaks at m/e 54 and 81. The runs at 325°C on TAGN did give a little more intensity at m/e 54 and 81, but still much less than did the formulation runs at the same temperature. The compositions were only about 30% TAGN. Thus it appears that while it is possible that at 325°C a little of the 1,3,5-triazine may have been formed by HCN trimerization, little if any of the 1,3,5-triazine seen at 800°C was formed via this route. However, it seems difficult to rule out HCN trimerization conclusively except by scrambling studies on mixtures of fully-ring-labeled and unlabeled RDX; such studies are planned.

Most, and at the higher temperature (800°C) essentially all, of the 1,3,5-triazine formed in these runs presumably arose from further decomposition of 1,3,5,7-tetraazacyclooctatetraene formed in decomposition of HMX. HMX would give this species after loss of the elements of four molecules of HONO by pathways (Scheme I) analogous to those involved in formation of 1,3,5-triazine directly from RDX.[1] By analogy with the known chemistry of cyclooctatetraene, azocine and di- and triazocines (which are known[19] to yield respectively benzene and azabenzenes on thermolysis), 1,3,5,7-tetraazacyclooctatetraene should decompose further with formation of 1,3,5-triazine.

Possible Chemical Mechanism for Formation of Unknown A (1,2,4-Oxadiazole?). The structure of Unknown A is not yet established firmly. However the possibility of its being identifiable with the earlier[13] m/e 70 unknown (which was described as having a mass spectrum similar to that of 1,2,4-oxadiazole) seems sufficiently reasonable to at least mention a possible mechanism by which 1,2,4-oxadiazole might be formed, as well as its possible implications for combustion catalysis by borohyrdide catalysts. Another reason for such a discussion is to help make the point for the importance of continued study of Unknown A, including its true structure, the mechanisms by which it is formed, and the factors affecting its formation. This importance is based mainly on the fact that the shift with temperature in the effect of $K_2B_{12}H_{12}$ on its formation suggests a difference in catalysis mechanism between high and low temperatures.

A possible mechanism for formation of 1,2,4-oxadiazole is given in Scheme III.

According to this mechanism, the HMX (or RDX) loses NO_2 by N-NO_2 cleavage, then recombines with attack by oxygen instead of nitrogen. N-O cleavage of the resulting hydroxylamine nitrite leaves a nitroxide; nitroxides of this type have actually been observed in HMX and RDX decompositions.[20]

The nitroxide could have a hydrogen and its adjacent nitro group stripped away either inter- or intramolecularly (the position next to the nitroxide should be favored for this due to resonance) and loses one (RDX) or two (HMX) molecules of $H_2C{=}N{-}NO_2$ possibly by ring-opening and beta-cleavage. The resulting nitroso-containing radical could cyclize with attack of the radical center on the nitroso oxygen to give a cyclic radical which could yield 1,2,4-oxadiazole by loss of a hydrogen atom.

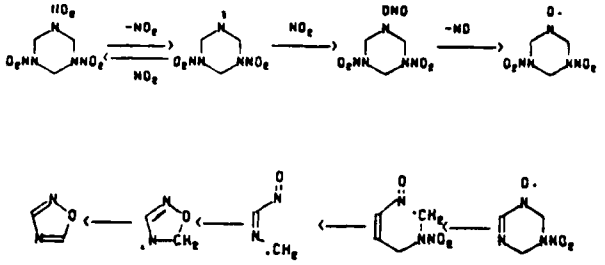

SCHEME III

Nitroxides of the type shown have actually been observed[20] in HMX and RDX decomposition. The mechanism of Scheme III also accounts for the fact[12,13] that the m/e 70 peak sometimes written as 1,2,4-oxadiazole is replaced by one at m/e 72 when the decomposition is carried out on fully ring-labeled HMX: both nitrogens in the species must therefore have been ring nitrogens of the original HMX or RDX molecule.

The following suggestions are obviously highly speculative. They are being put forward at this time for two reasons: First, there seems to be considerable interest in understanding the chemical mechanisms responsible for borohydride catalysis of HMX and RDX decomposition and combustion. Second, it seems worthwhile to make a case for the importance of continued study of Unknown A.

The effects of temperature and of $K_2B_{12}H_{12}$ or $K_2B_{10}H_{10}$ catalyst on the amount of Unknown A (1,2,4-oxadiazole?) detected were discussed above. They included the following: At high temperatures, the amount of Unknown A detected was decreased. Addition of $K_2B_{12}H_{12}$ or $K_2B_{10}H_{10}$ catalyst causes a decrease in amount of Unknown A detected at low temperature, and an increase in amount detected at high temperature. The temperature effect can be explained in terms of increased reaction of NO_2 with, for example, CH bonds in molecules such as $H_2C{=}O$ or unreacted HMX/RDX at higher temperatures relative to the recombination mechanism that according to Scheme III would lead to formation of oxadiazole. This makes sense since such reactions as H-abstraction might be expected to have higher activation energies than a simple recombination mechanism such as the first step of Scheme III.

Possibly the most obvious way for added $K_2B_{12}H_{12}$ or $K_2B_{10}H_{10}$ to influence the formation of oxadiazole would be for it to influence the amount of NO_2 present, possibly either by (a) reacting with it or by (b) promoting or retarding a reaction in which it is formed.

The following, highly speculative suggestion is based on the preceding three paragraphs. Possibly added $K_2B_{12}H_{12}$ or $K_2B_{10}H_{10}$ accelerates HMX/RDX decomposition at low temperatures by reacting with NO_2, possibly to give

radicals which acclerate decomposition, for example by reacting with unreacted HMX/RDX faster than does NO_2 itself. At higher temperatures, possibly the added $K_2B_{12}H_{12}$ or $K_2B_{10}H_{10}$ causes a mechanism shift in which the added $K_2B_{12}H_{12}$ or $K_2B_{10}H_{10}$ induces generation of more NO_2. To give only one example, the shift might be from the low-temperature thermolysis mechanism to a mechanism involving an initial hydrogen transfer or electron transfer followed by steps which generate NO_2 faster than the low-temperature mechanism.

V. SUGGESTIONS FOR FUTURE WORK

Many possibilities for future work suggest themselves. A number of these actually arise out of the fact that funding for this work ended too suddenly for the examination and interpretation of the data to be completed satisfactorily. For one thing, there is considerable room for further work simply analyzing the chromatograms from which Tables 1-21 and Figures 18-137 were made, examining spectra and library searches from each peak.

Another possibility would involve identification of the material referred to above as "Unknown A". Two aids in identification might involve (a) use of a concentrator similar to that used in this work, together with Gas Chromatography-Fourier Transform Infrared Spectroscopy (GC-FTIR) equipment to provide high-resolution chromatograms based on infrared spectra. This would be useful if a reference infrared spectrum of 1,2,4-oxadiazole could be located. (b) Another possible approach might be to prepare an authentic sample of 1,2,4-oxadiazole and obtain its mass spectrum for comparison with that of Unknown A. The preparation of 1,2,4-oxadiazole has been described,[21] but we have not been able to locate an authentic mass spectrum of 1,2,4-oxadiazole.

Another way of obtaining information on mechanisms operating in catalysis of nitramine decomposition and combustion would involve studies of isotope scrambling during decomposition of mixtures of unlabeled and fully-^{15}N-labeled HMX or RDX, followed by analysis of the products (N_2O, N_2, nitrosoamines, and unreacted RDX). This approach has been discussed earlier[3,5,7] for the case of uncatalyzed HMX or RDX; information on the effect of boron hydride catalysts such as $K_2B_{10}H_{10}$ and $K_2B_{12}H_{12}$ could be obtained by comparing results obtained presence and in the absence of such materials.

Another variation on this general theme would involve scrambling studies on mixtures of ring-^{15}N-labeled and unlabeled HMX and RDX; this would make it possible to distinguish between intermolecular (e.g., HCN trimerization) and intramolecular formation of 1,3,5-triazine.

Finally, it would be of considerable interest to check for deuterium isotope effects by carrying out decompostion and combustion studies on $K_2B_{10}D_{10}$ and $K_2B_{12}D_{12}$, and comparing the results with those from parallel studies on $K_2B_{10}H_{10}$ and $K_2B_{12}H_{12}$. Hopefully this would yield information on the role of the hydrogen atoms in $K_2B_{10}H_{10}$ and $K_2B_{12}H_{12}$ in catalysis of HMX and RDX decomposition and combustion. Deuterium isotope-effect studies (see for example References 13 and 22) on decomposition of pure HMX and RDX have revealed that the hydrogen atoms play a significant role in the combustion and explosion behavior of these materials. However, as far as this writer is aware such studies have not been carried out on mixtures involving deuterated boron hydrides.

REFERENCES

1. M.A. Schroeder, "Thermal Decomposition of RDX and RDX-$K_2B_{12}H_{12}$ Mixtures", Proceedings of 23rd JANNAF Combustion Meeting, CPIA Publication No. 457, Vol. II, pp. 43-54, October 1986; "Thermal Decomposition of RDX and RDX-$K_2B_{12}H_{12}$ Mixtures," BRL Memorandum Report BRL-MR-3699, September 1988, AD-A199 371.

2. M.A. Schroeder, "Critical Analysis of Nitramine Decomposition Data: Some Suggestions for Needed Research Work", BRL Memorandum Report ARBRL-MR-3181, June 1982, AD-A116 194.

3. M. A. Schroeder, "Critical Analysis of Nitramine Decomposition Data: Preliminary Comments on Autoacceleration and Autoinhibition in HMX and RDX Decomposition in HMX and RDX Decomposition", Memorandum Report ARBRL-MR-03370, August 1984, AD-A146 570.

4. M.A. Schroeder, "Critical Analysis of Nitramine Decomposition Data: Activation Energies and Frequency Factors for HMX and RDX Decomposition", Technical Report BRL-TR-2673, September 1985, AD-A160 543.

5. M.A. Schroeder, "Critical Analysis of Nitramine Decomposition Data: Product Distributions from HMX and RDX Decomposition", Technical Report BRL-TR-2659, June 1985, AD-A159 325.

6. M.A. Schroeder, "Critical Analysis of Nitramine Decomposition Results: Some Comments on Chemical Mechanisms", Proceedings of 16th JANNAF Combustion Meeting, CPIA Publication No. 308, Vol. II, pp. 17-34, September 1979.

7. M.A. Schroeder, "Critical Analysis of Nitramine Decomposition Data: Update, Some Comments on Pressure and Temperature Effects and Wrap-Up Discussion of Chemical Mechanisms", Proceedings of 21st JANNAF Combustion Meeting, CPIA Publication 412, Vol. II, pp. 595-614, October 1984.

8. R.A. Fifer, "Chemistry of Nitrate Ester and Nitramine Propellants", in "Fundamentals of Solid Propellant Combustion", K.K. Kuo and M. Summerfield, Eds., Vol 90 of Progress in Astronautics and Aeronautics Series, AAIA, New York, 1984.

9. T.L. Boggs, "The Thermal Behavior of Cyclotrimethylenetrinitramine (RDX) and Cyclotetramethylenetetranitramine (HMX)", Chapter 3 in K.K. Kuo and M. Summerfield, Eds., "Fundamentals of Solid Propellant Combustion", American Institute of Aeronautics and Astronautics, Inc., New York, p. 121, 1984.

10. B.B.Goshgarian, "The Thermal Decomposition of Cyclotrimethylenetrinitramine (RDX) and Cyclotetramethylenetetranitramine (HMX)", AFRPL-TR-78-76, October 1978 (AD-B032 275).

11. A.A. Juhasz, "Nitramine Pyrolysis Mechanisms", Proceedings of the 1975 Review of the Ignition and Combustion Programs, BRL Report No. 1883 (AD-B011 644L).

12. R.J. Powers, AFATL, Eglin AFB, Florida, Private Communication, 1980.

13. S.A. Shackleford, M.B. Coolidge, B.B. Goshgarian, B.A. Loving, R.N. Rogers, J.L. Janney, and M.H. Ebinger, "Deuterium Isotope Effects in Condensed-Phase Thermochemical Decomposition Reactions of Octahydro-1,3,5,7-Tetranitro-1,3,5,7-Tetrazocine", J. Phys. Chem., Vol. 89, p. 3118, 1985.

14. R. Behrens, Jr., "Simultaneous Thermogravimetric Modulated Beam Mass Spectrometry and Time-of-Flight Velocity Spectra Measurements: Thermal Decomposition Mechanisms of RDX and HMX", in Combustion of Energetic Materials, Semiannual Progress Report, October 1986 - March 1987, Sandia National Laboratories, Livermore, California.

15. R.M. Silverstein, G.C. Bassler, and T.C. Morrill, "Spectrometric Identification of Organic Compounds", 4th ed., Wiley, New York, p. 10, 1981.

16. L.B. Clapp, "1,2,3- and 1,2,4-Oxadiazoles", in "Comprehensive Heterocyclic Chemistry", Vol. 6, Part 4B, A.R. Katritzky, C.W. Rees, and K.T. Potts, Eds., Pergamon Press, New York.

17. Q.N. Porter and J. Baldas, "Mass Spectrometry of Heterocyclic Compounds", Wiley-Interscience, New York, p. 529, 1971.

18. A.E. Axworthy, J.E. Flanagan, and J.C. Gray, "Interaction of Reaction Kinetics and Nitramine Combustion", AFATL-TR-80-58, May 1980, AD-B052 861L.

19. (a) S. Yogi, K. Hokama, and O. Tsuge, "A Stable 1,2-Diazocine System: 3,8-Diphenyl-1,2-Diazacycloocta-2,4,6,8-Tetraenes", Chemistry Letters, pp. 1579-1582, 1982; (b) B.M. Trost, P.H. Scudder. R.M. Cory, N.J. Turro, V. Ramanurthy, and T.J. Katz, "1,2-Diaza-2,4,6,8-Cyclooctatetraene", J. Org. Chem., Vol. 44, pp. 1264-1269, 1979; (c) D. Dudek, K. Glanzer and J. Troe, "Pyrolysis of 1,3,5,7-Cyclooctatetraene, Semibullvalene and 1,5-Dihydropentalene in Shock Waves and in a Flow System (Part I)", Ber. Bunsenges. Phys. Chem., Vol. 83, pp. 776-788, 1979.

20. (a) M.D. Pace, "Thermal Decomposition of RDX: Evidence of a Nitronylnitroxyl Free Radical Intermediate", Journal of Energetic Materials, Vol. 3, pp. 279-291, 1985; (b) M.D. Pace, A.D. Britt, W.B. Moniz, and D. Stec, III, "Paramagnetic Decomposition Products from Energetic Materials", Preprints of papers to be presented at the Eighth Symposium (International) on Detonation, Albuquerque, Vol. I, pp. 441-448, 15-19 July 1985.

21. C. Moussebois, R. Lenaers, and F. Eloy, "Synthese de l'Oxadiazole-1,2,4," Helvetica Chimica Acta, Vol. 45, pp. 446-449, 1962.

22. S. Bulusu, D.I. Weinstein, J.R. Autera, and R.W. Velicky, "Deuterium Kinetic Isotope Effect in the Thermal Decomposition of 1,3,5-Trinitro-1,3,5-Triazacyclohexane and 1,3,5,7-Tetraazacyclooctane: Its Use as an Experimental Probe for Their Shock-Induced Chemistry," J. Phys. Chem., Vol. 90, pp. 4121-4126, 1986.

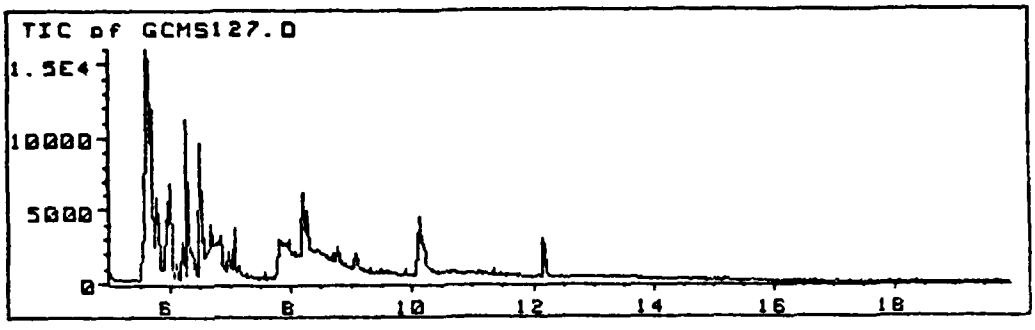

Figure 1. Total Ion Chromatogram from PEG 5-3-0 Decomposed 20 Sec at 325°C

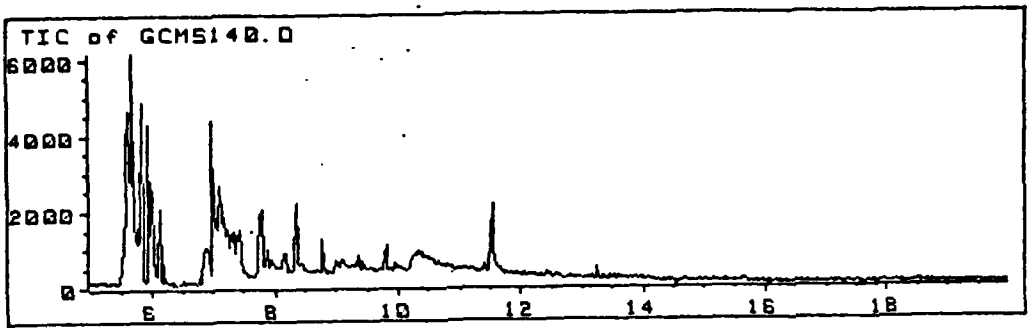

Figure 2. Total Ion Chromatogram from PEG 5-3-0 Decomposed 20 Sec at 800°C

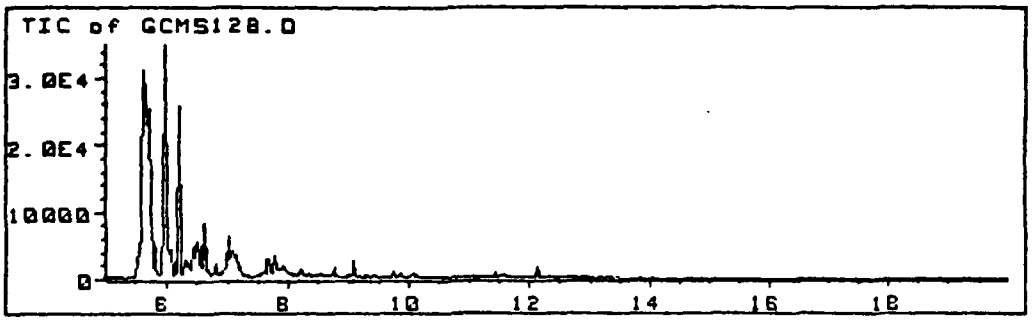

Figure 3. Total Ion Chromatogram from PEG 5-3-15 Decomposed 20 Sec at 325°C

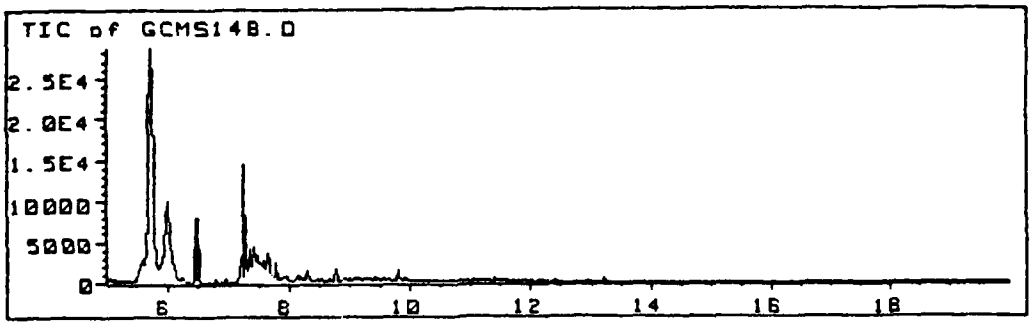

Figure 4. Total Ion Chromatogram from PEG 5-3-15 Decomposed 20 Sec at 800°C

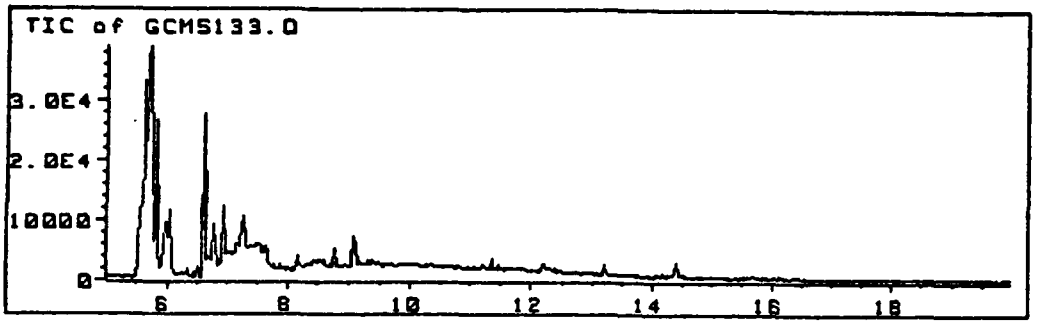

Figure 5. Total Ion Chromatogram from GAP 5-3-0 Decomposed 20 Sec at 325°C

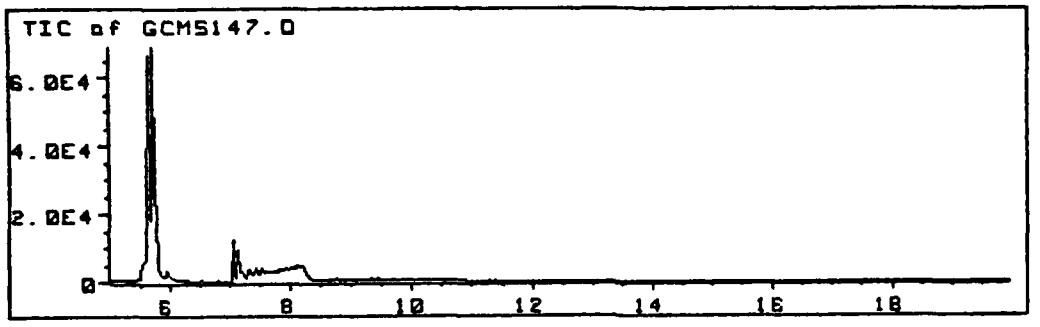

Figure 6. Total Ion Chromatogram from GAP 5-3-0 Decomposed 20 Sec at 800°C

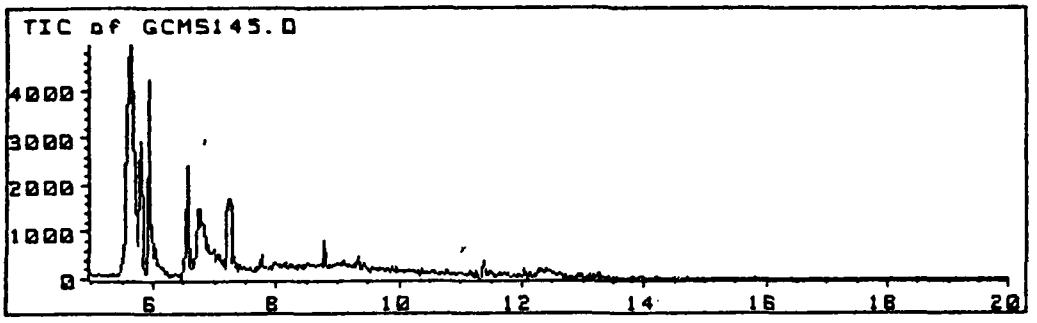

Figure 7. Total Ion Chromatogram from GAP 5-3-15 Decomposed 20 Sec at 325°C

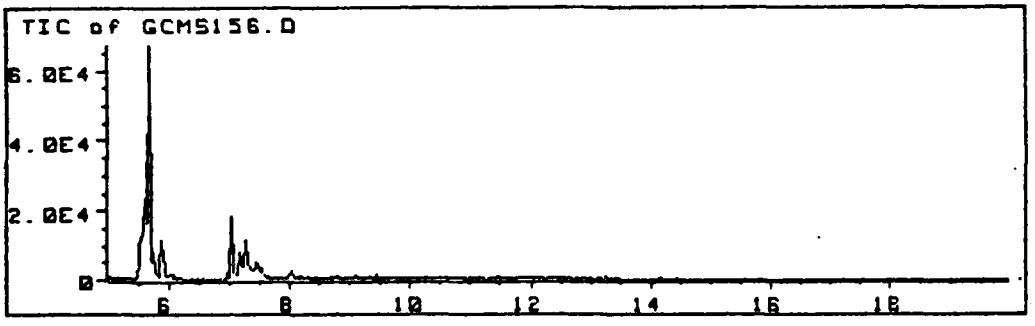

Figure 8. Total Ion Chromatogram from GAP 5-3-15 Decomposed 20 Sec at 800°C

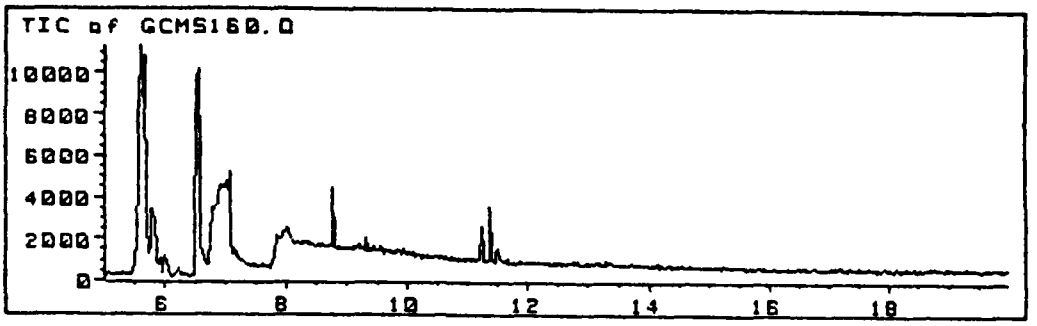

Figure 9. Total Ion Chromatogram from TAGN Decomposed 20 Sec at 325°C

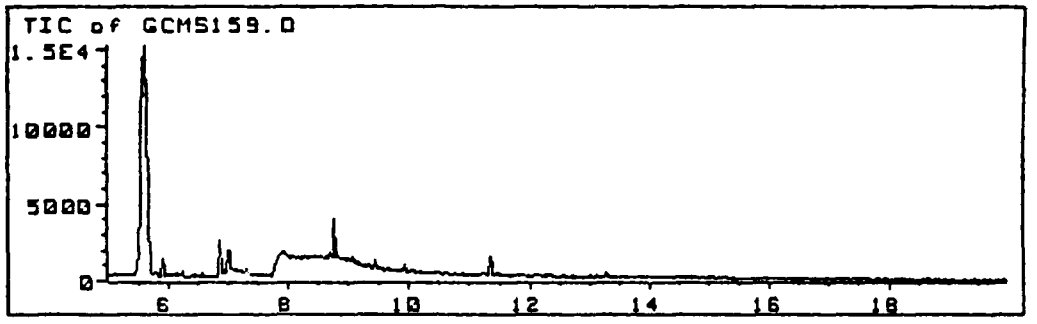

Figure 10. Total Ion Chromatogram from TAGN Decomposed 20 Sec at 800°C

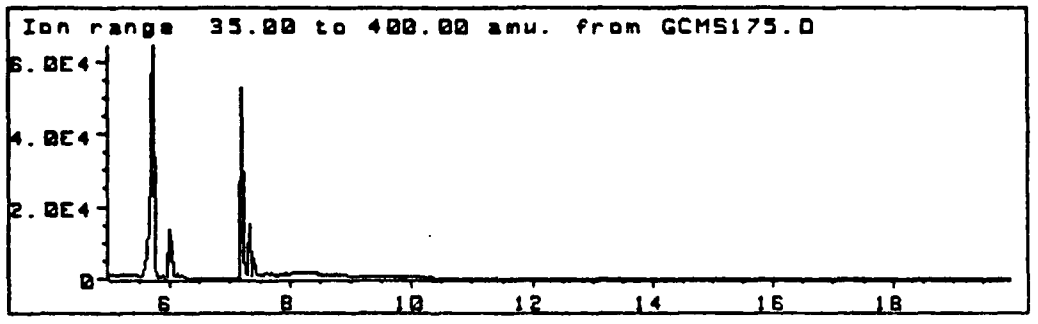

Figure 11. Total Ion Chromatogram from HMX Decomposed 20 Sec at 325°C

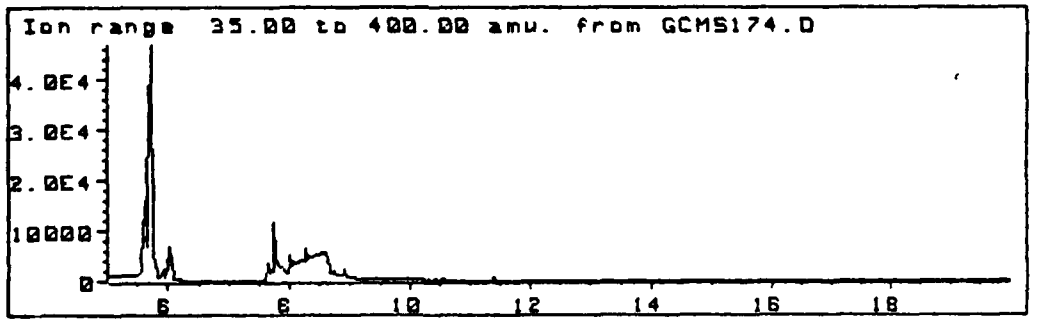

Figure 12. Total Ion Chromatogram from HMX Decomposed 20 Sec at 800°C

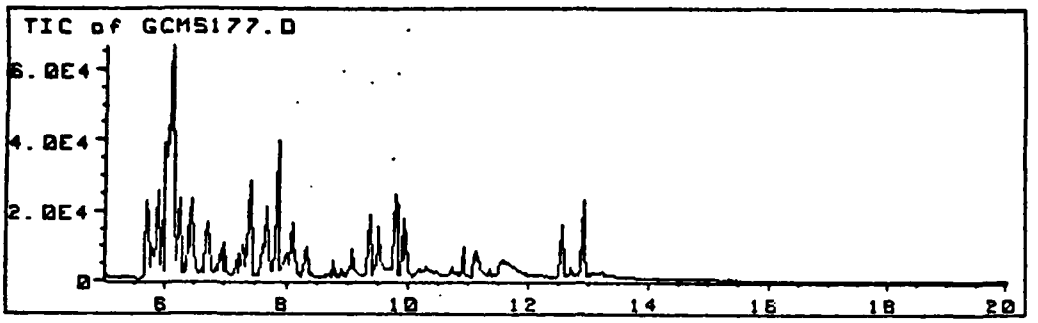

Figure 13. Total Ion Chromatogram from PEG Decomposed 20 Sec at 325°C

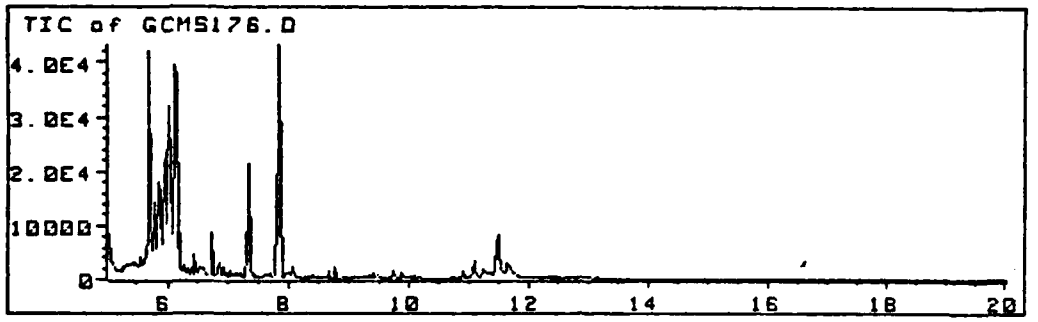

Figure 14. Total Ion Chromatogram from PEG Decomposed 20 Sec at 800°C

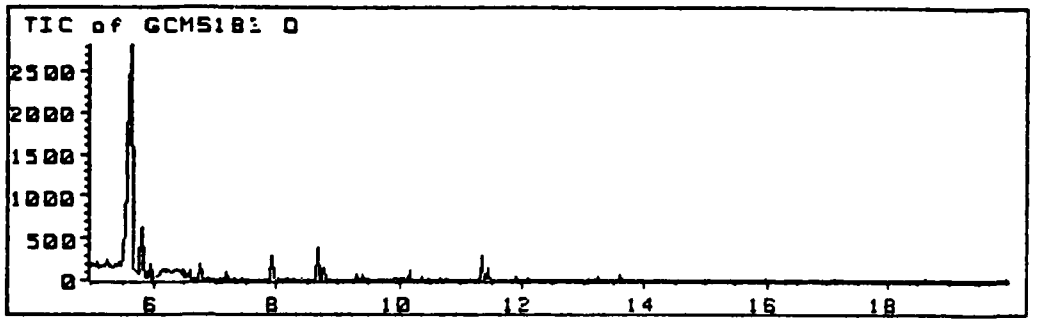

Figure 15. Total Ion Chromatogram from $K_2B_{10}H_{10}$ Decomposed 20 Sec at 325°C

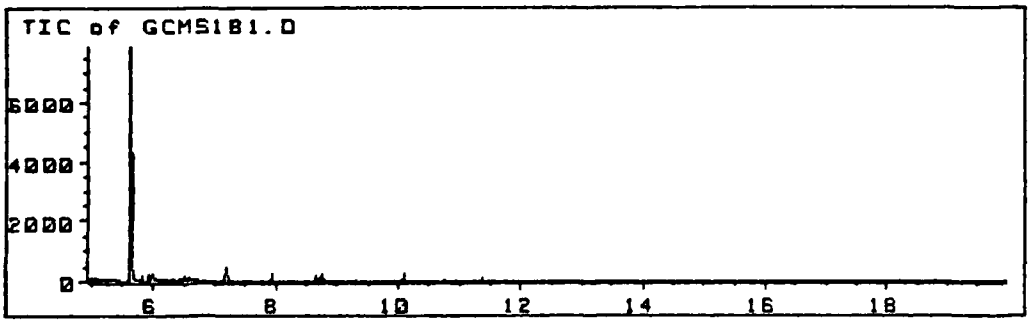

Figure 16. Total Ion Chromatogram from $K_2B_{10}H_{10}$ Decomposed 20 Sec at 800°C

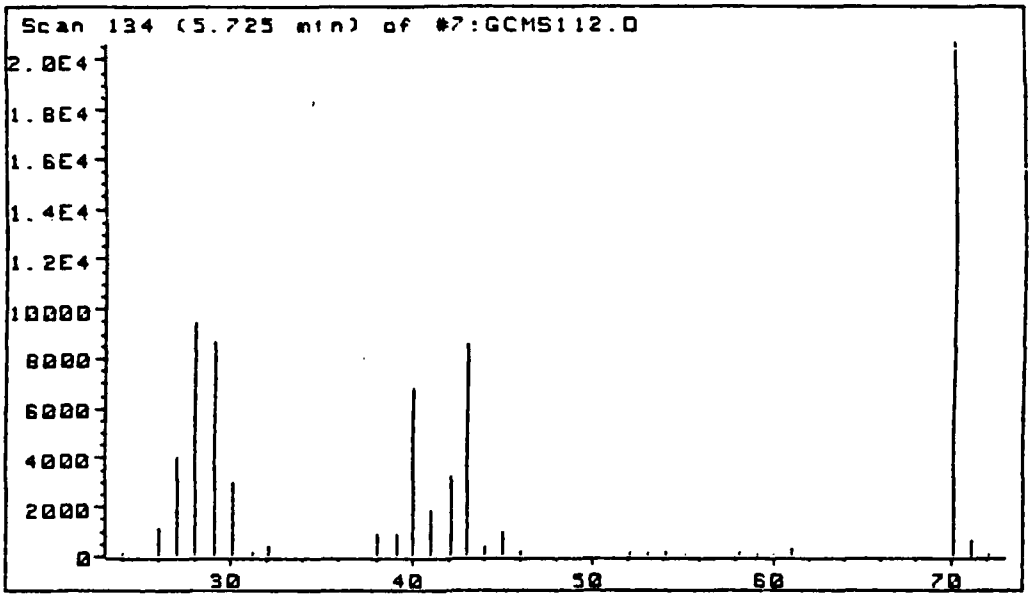

Figure 17. Spectrum of Unknown A (1,2,4-Oxadiazole?), from HMX Decomposition

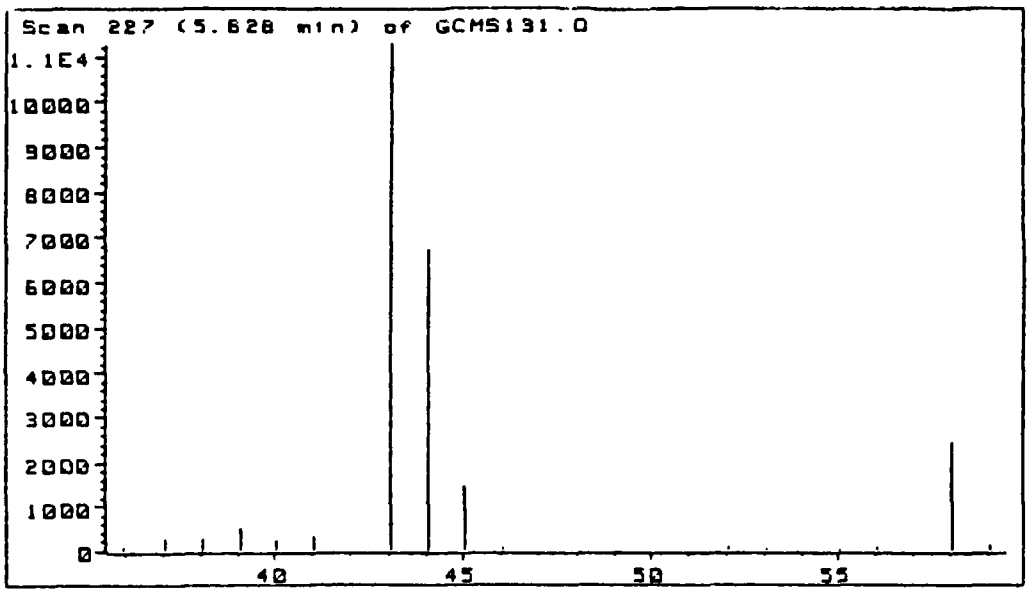

Figure 18. Typical Mass Spectrum of Chromatographic Peak at ca 5.6 Minutes, GAP 5-3-0, 325°C

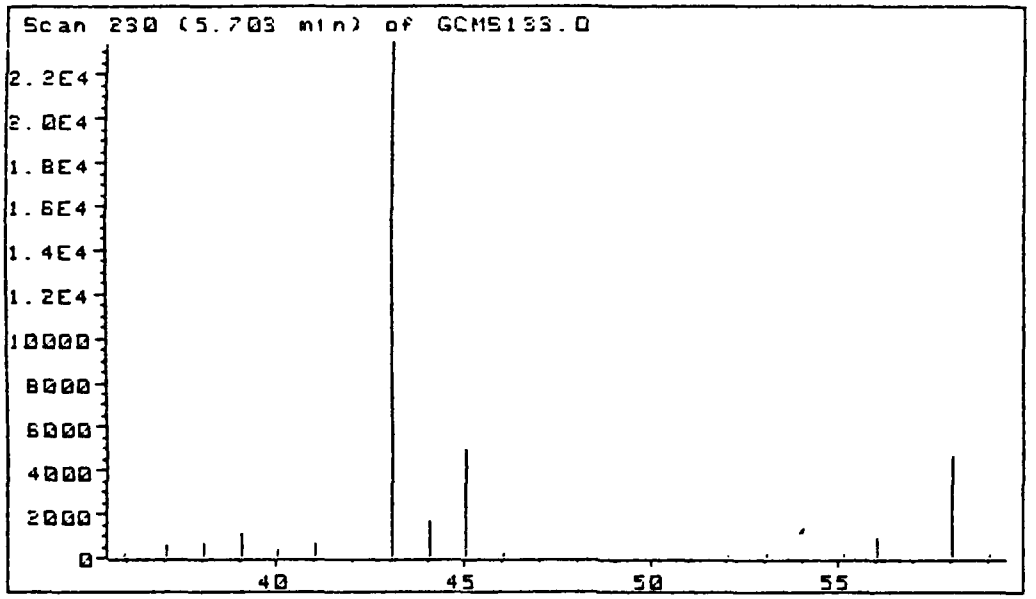

Figure 19. Typical Mass Spectrum of Chromatographic Peak at ca 5.7 Minutes, GAP 5-3-0, 325°C

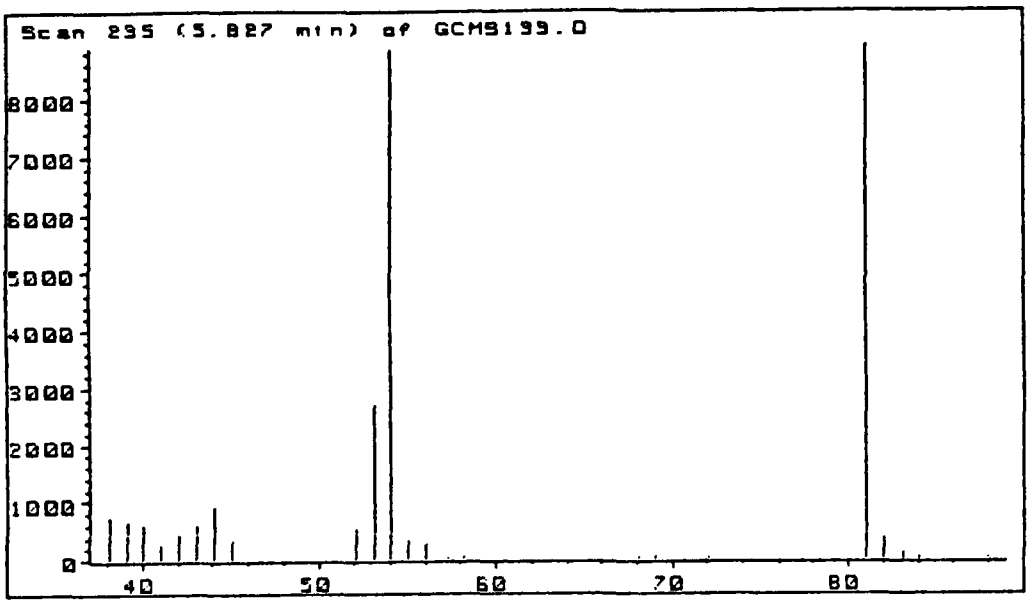

Figure 20. Typical Mass Spectrum of Chromatographic Peak at ca 5.8 Minutes, GAP 5-3-0, 325°C

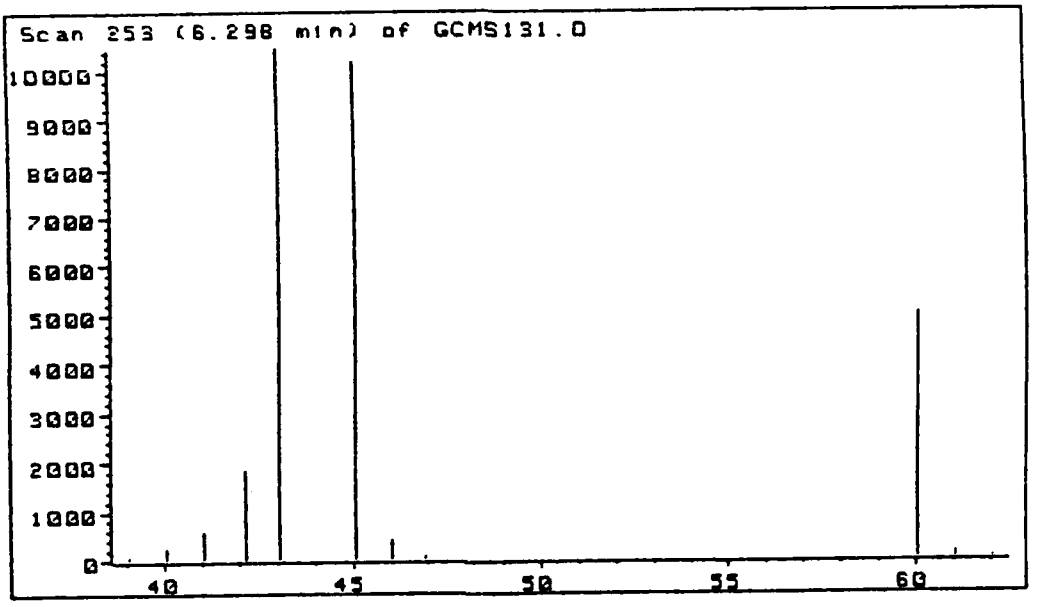

Figure 21. Typical Mass Spectrum of Chromatographic Peak at ca 6.3 Minutes, GAP 5-3-0, 325°C

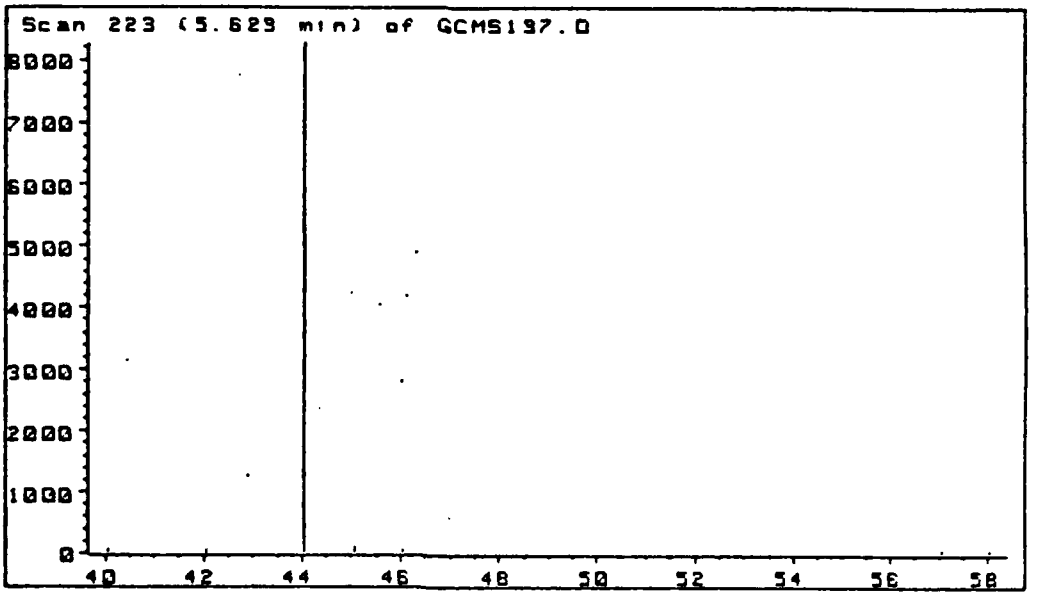

Figure 22. Typical Mass Spectrum of Chromatographic Peak at ca 5.6 Minutes, GAP 5-3-0, 800°C

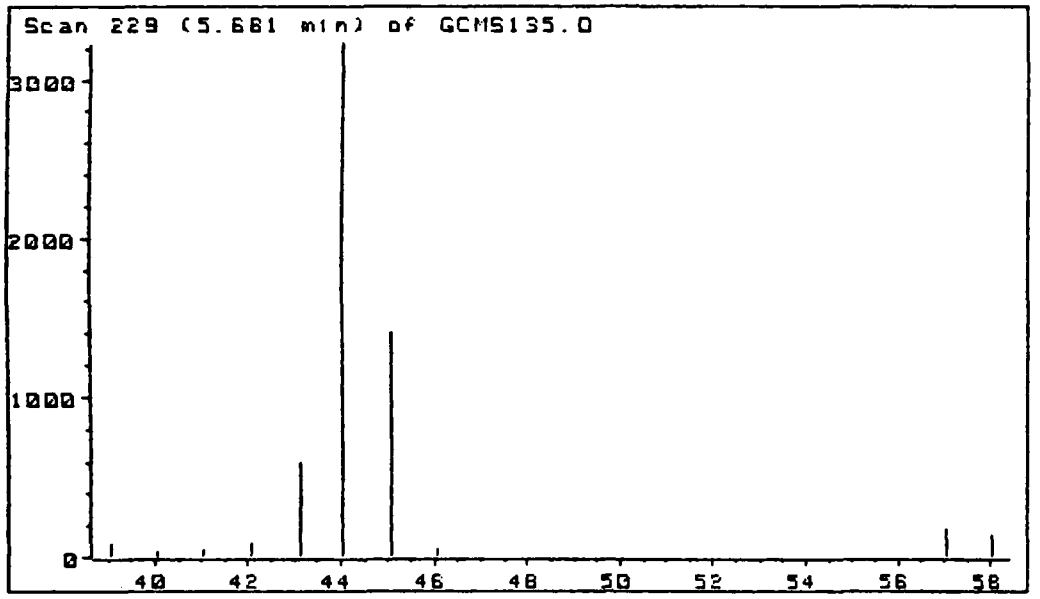

Figure 23. Typical Mass Spectrum of First Chromatographic Peak at ca 5.7 Minutes, GAP 5-3-0, 800°C

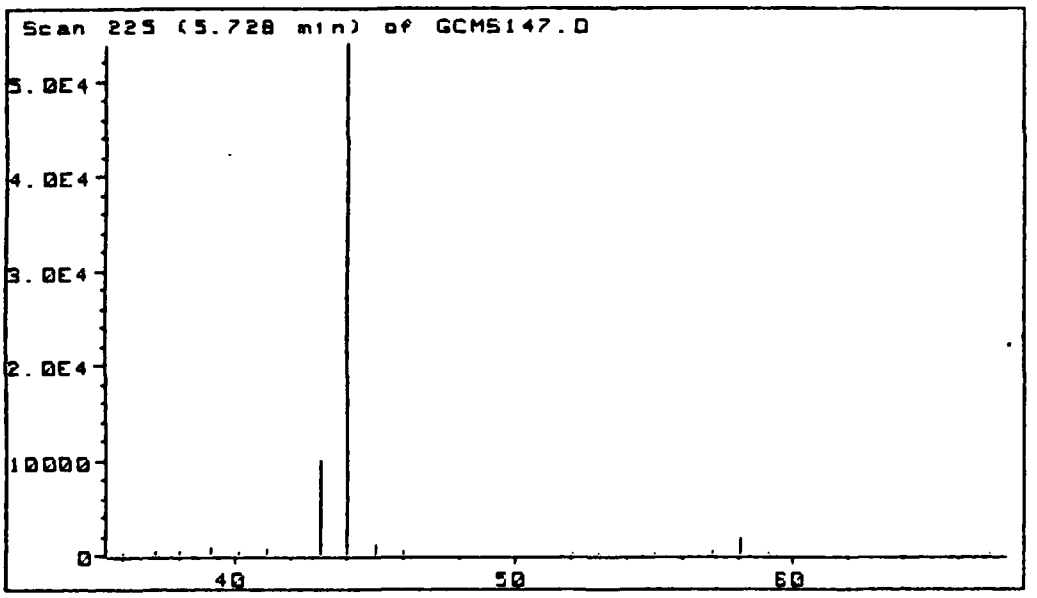

Figure 24. Typical Mass Spectrum of Second Chromatographic Peak at ca 5.7 Minutes, GAP 5-3-0, 800°C

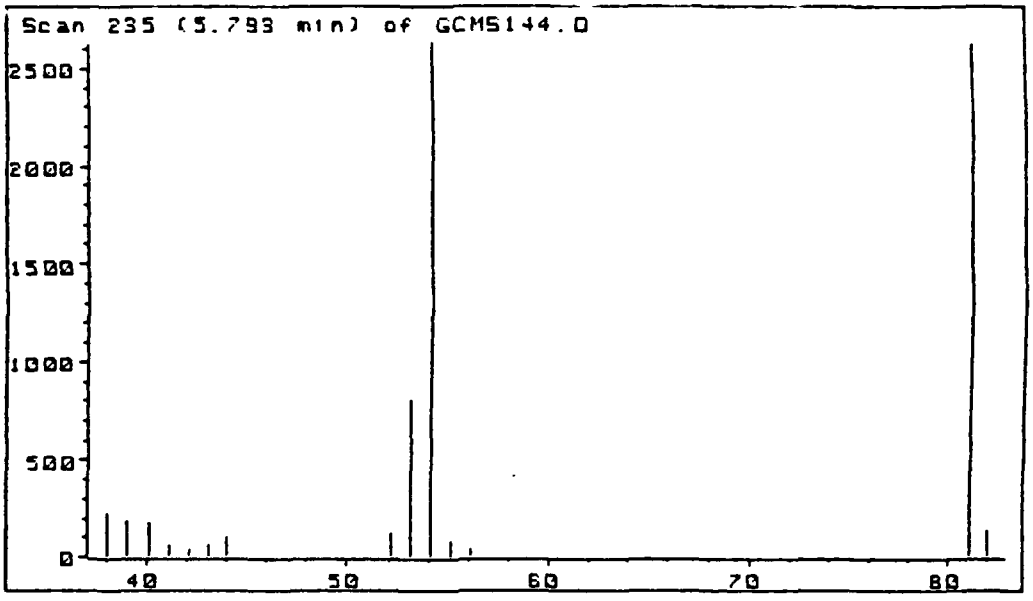

Figure 25. Typical Mass Spectrum of Chromatographic Peak at ca 5.8 Minutes, GAP 5-3-0, 800°C

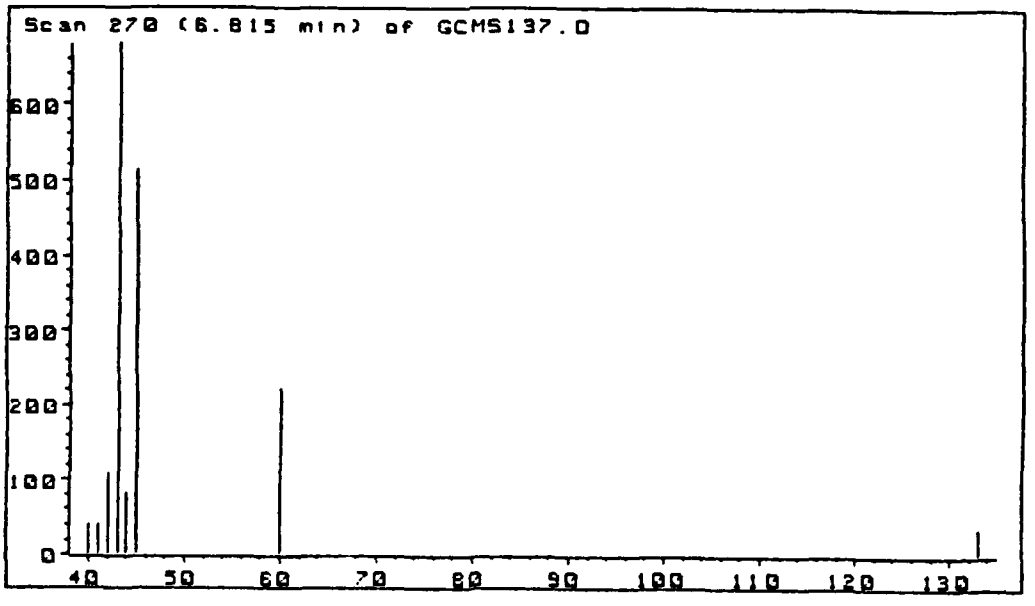

Figure 26. Typical Mass Spectrum of Chromatographic Peak at ca 6.8 Minutes, GAP 5-3-0, 800°C

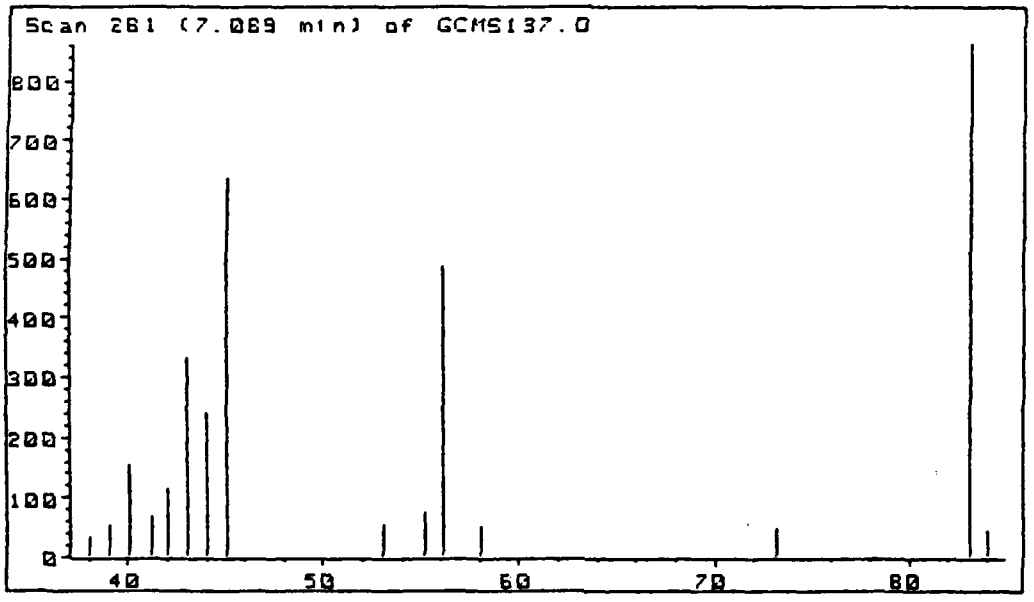

Figure 27. Typical Mass Spectrum of Chromatographic Peak at ca 7.1 Minutes, GAP 5-3-0, 800°C

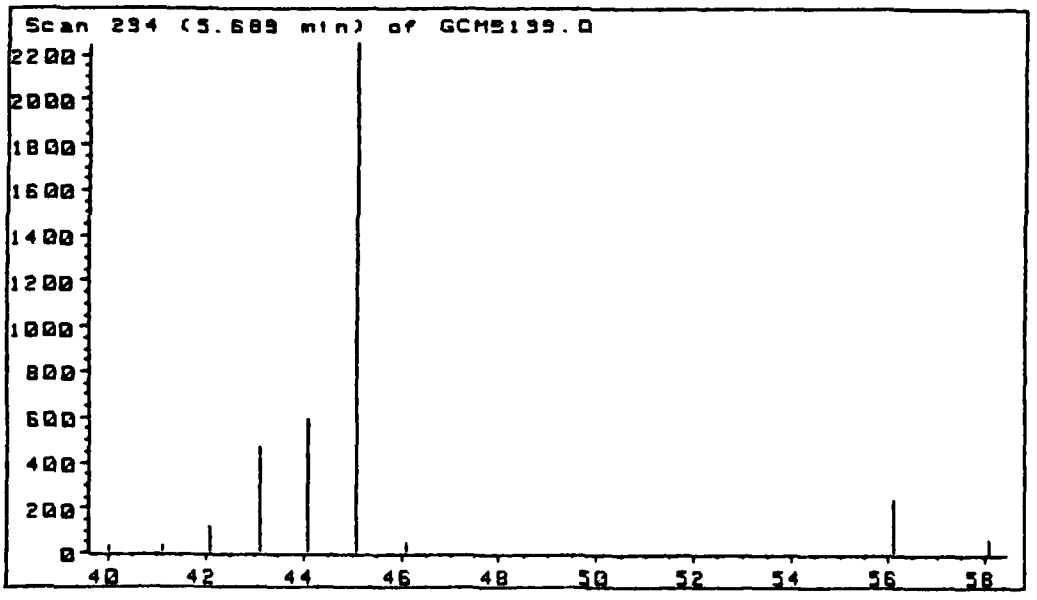

Figure 28. Typical Mass Spectrum of Chromatographic Peak at ca 5.7 Minutes, PEG 5-3-0, 325°C

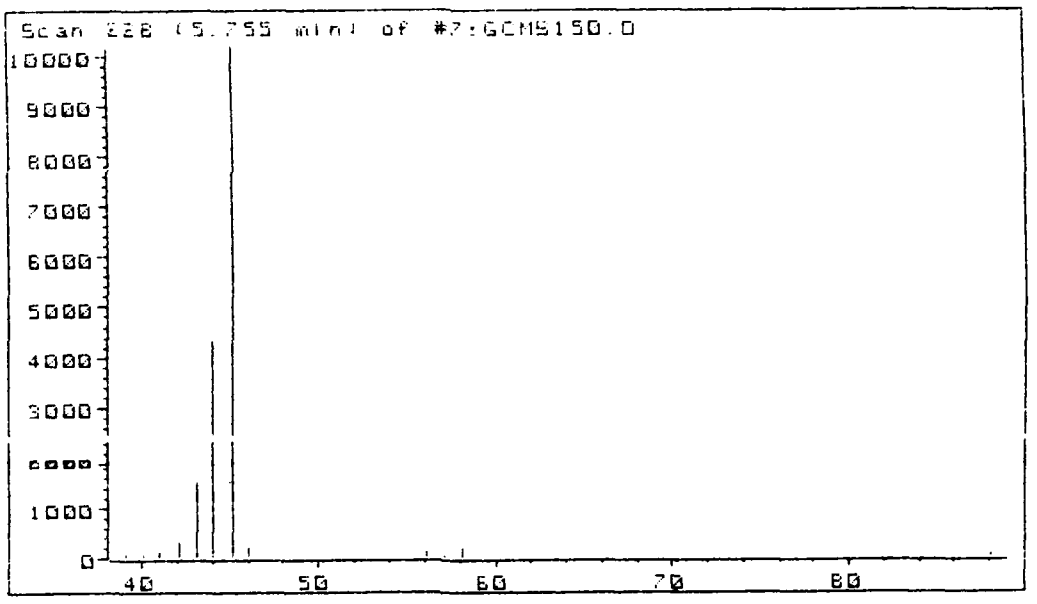

Figure 29. Typical Mass Spectrum of First Chromatographic Peak at ca 5.8 Minutes, PEG 5-3-0, 325°C

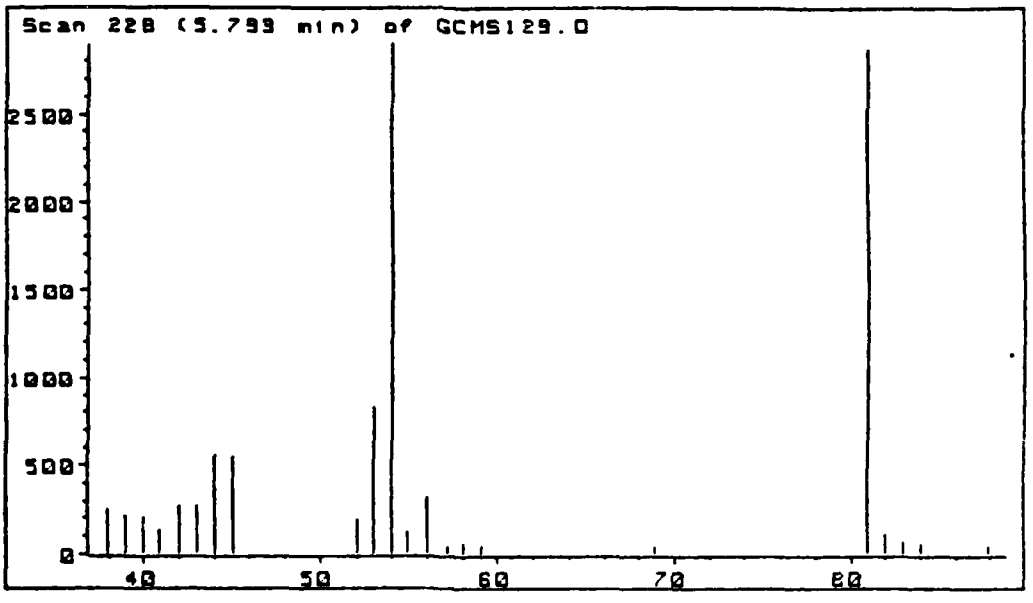

Figure 30. Typical Mass Spectrum of Second Chromatographic Peak at ca 5.8 Minutes, PEG 5-3-0, 325°C

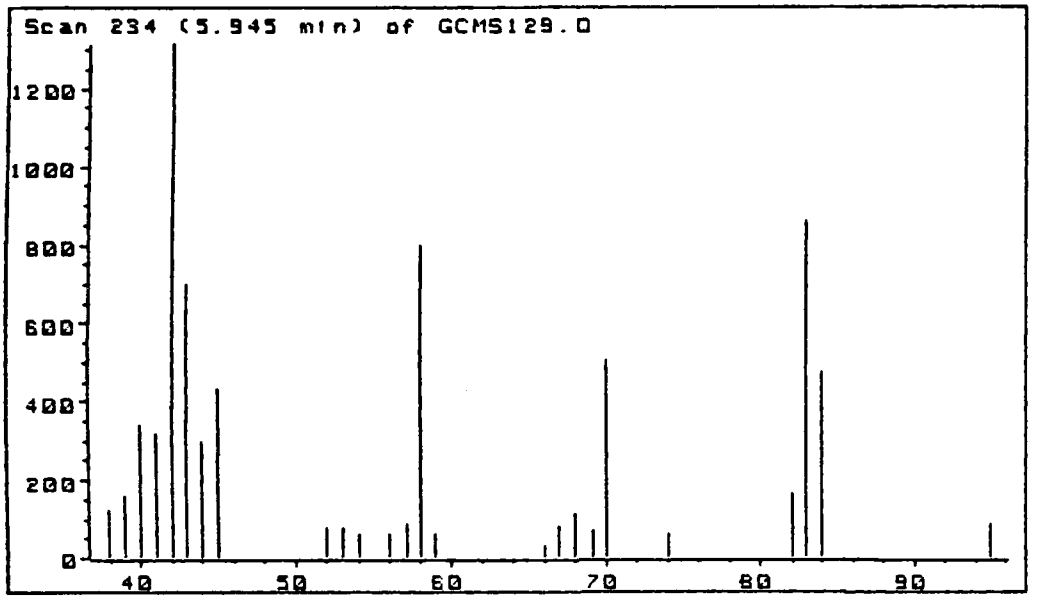

Figure 31. Typical Mass Spectrum of First Chromatographic Peak at ca 6.0 Minutes, PEG 5-3-0, 325°C

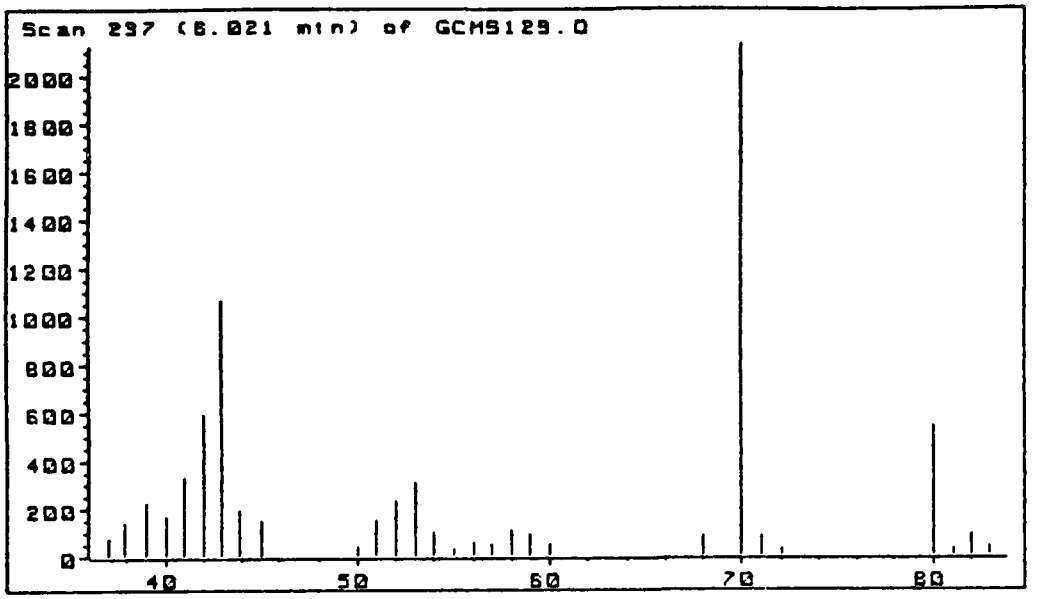

Figure 32. Typical Mass Spectrum of Second Chromatographic Peak at ca 6.0 Minutes, PEG 5-3-0, 325°C

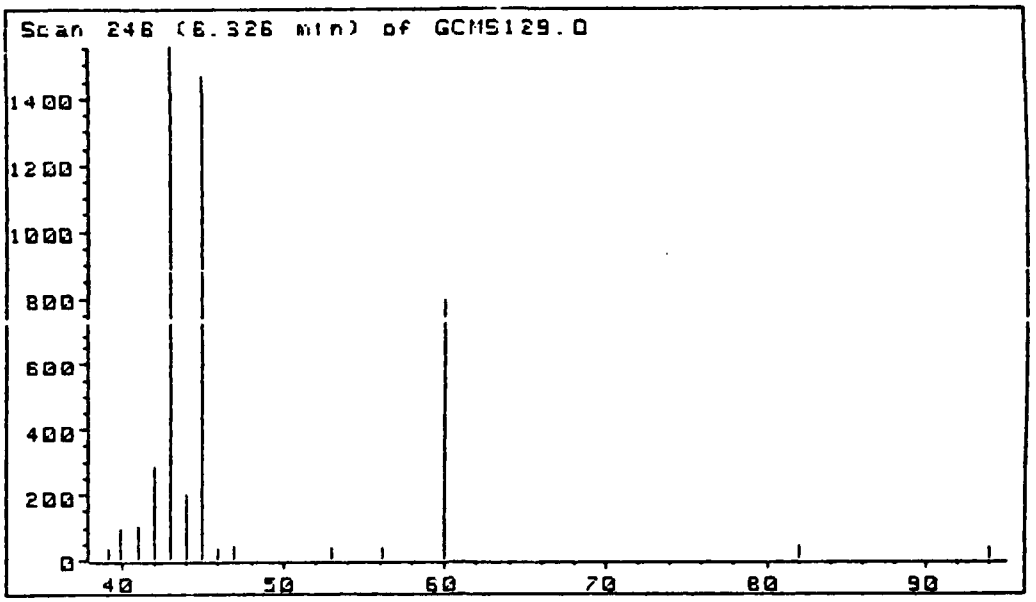

Figure 33. Typical Mass Spectrum of Chromatographic Peak at ca 6.3 Minutes, PEG 5-3-0, 325°C

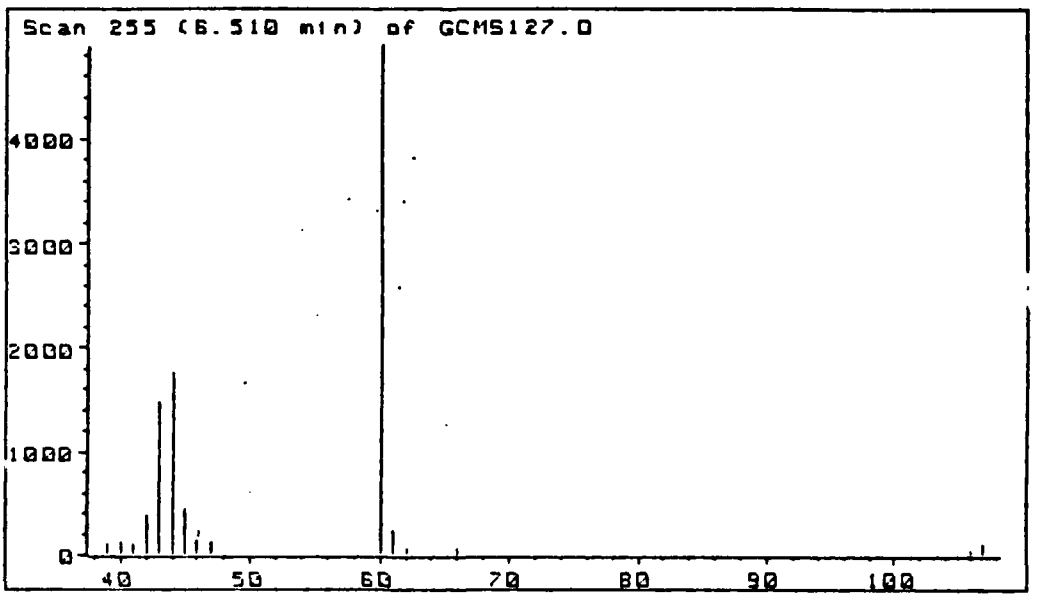

Figure 34. Typical Mass Spectrum of Chromatographic Peak at ca 6.5 Minutes, PEG 5-3-0, 325°C

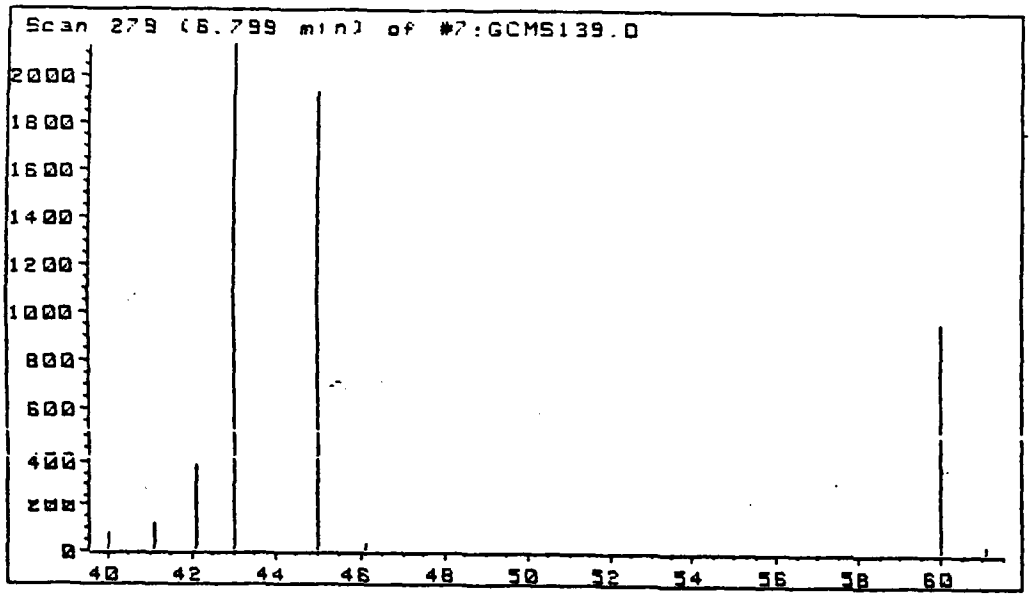

Figure 35. Typical Mass Spectrum of Chromatographic Peak at ca 6.8 Minutes, PEG 5-3-0, 325°C

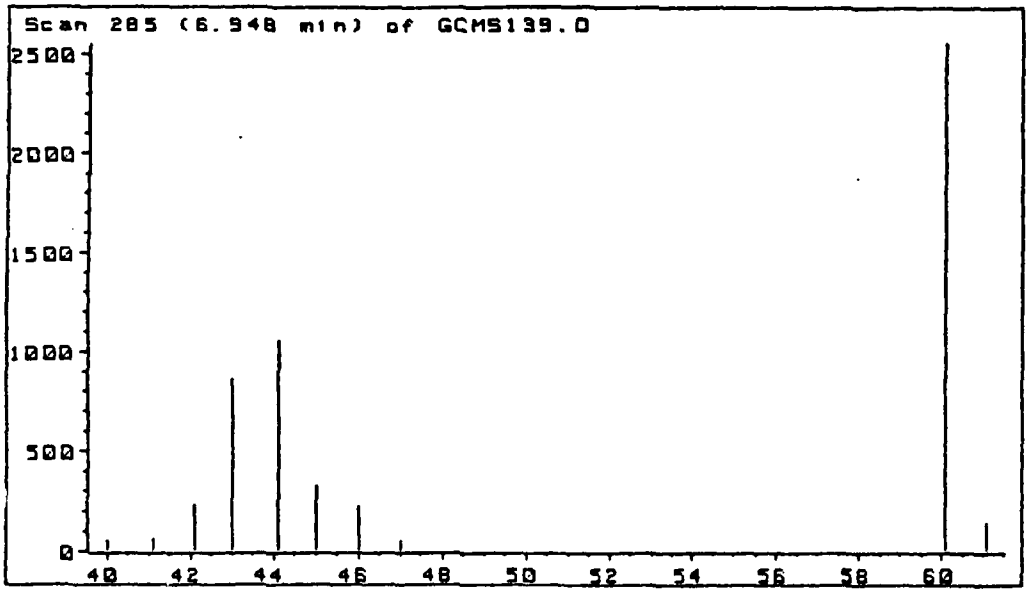

Figure 36. Typical Mass Spectrum of Chromatographic Peak at ca 6.9 Minutes, PEG 5-3-0, 325°C

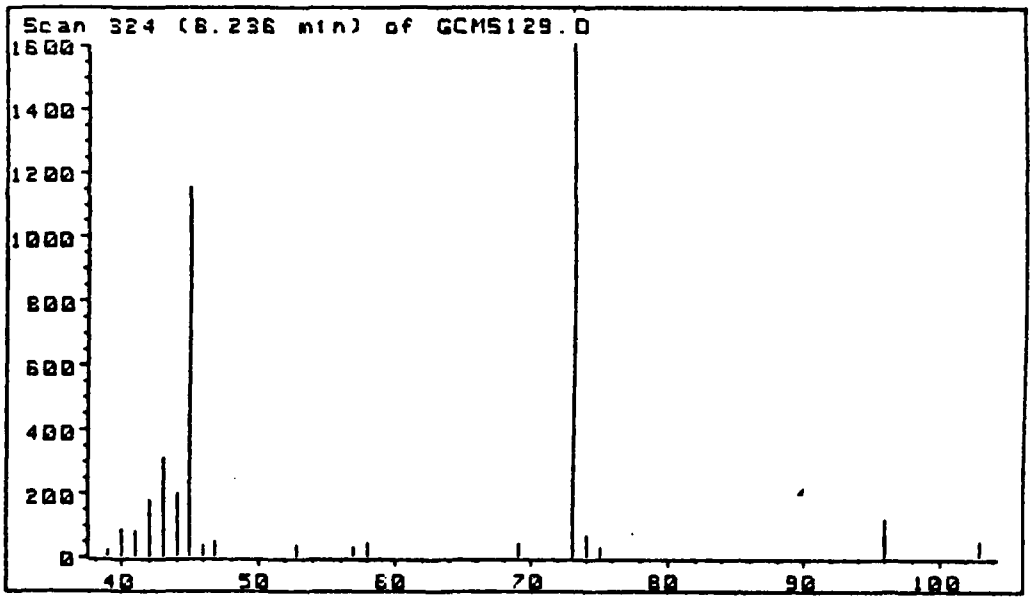

Figure 37. Typical Mass Spectrum of Chromatographic Peak at ca 6.2 Minutes, PEG 5-3-0, 325°C

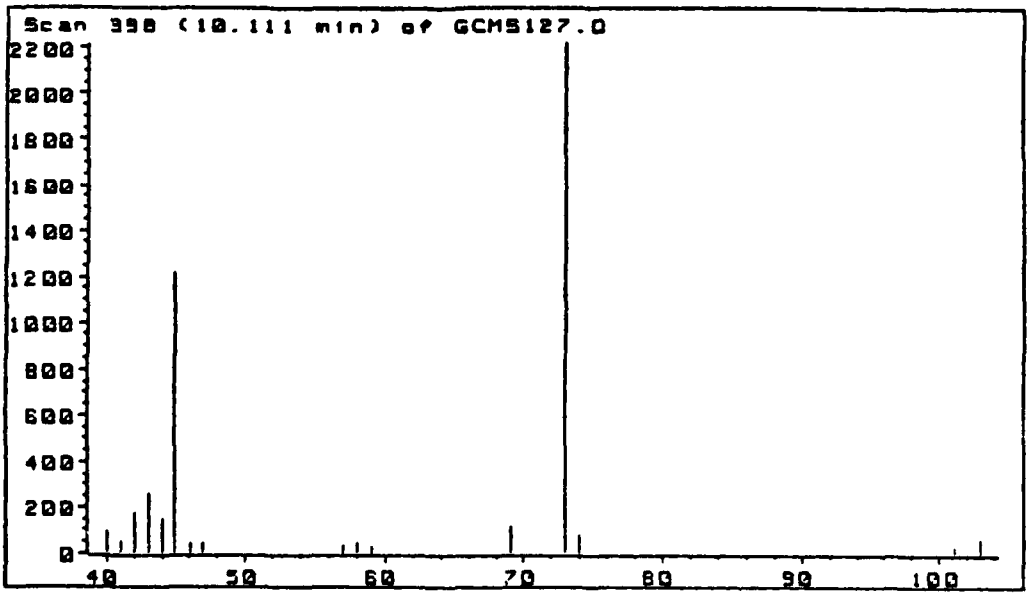

Figure 38. Typical Mass Spectrum of Chromatographic Peak at ca 10.1 Minutes, PEG 5-3-0, 325°C

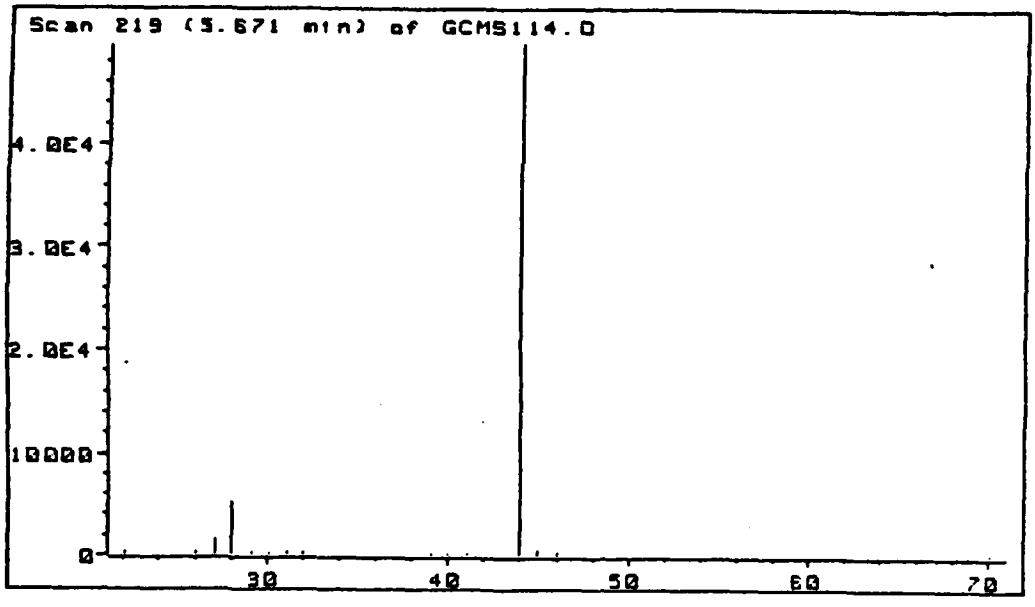

Figure 39. Typical Mass Spectrum of Chromatographic Peak at ca 5.7 Minutes, PEG 5-3-0, 600°C

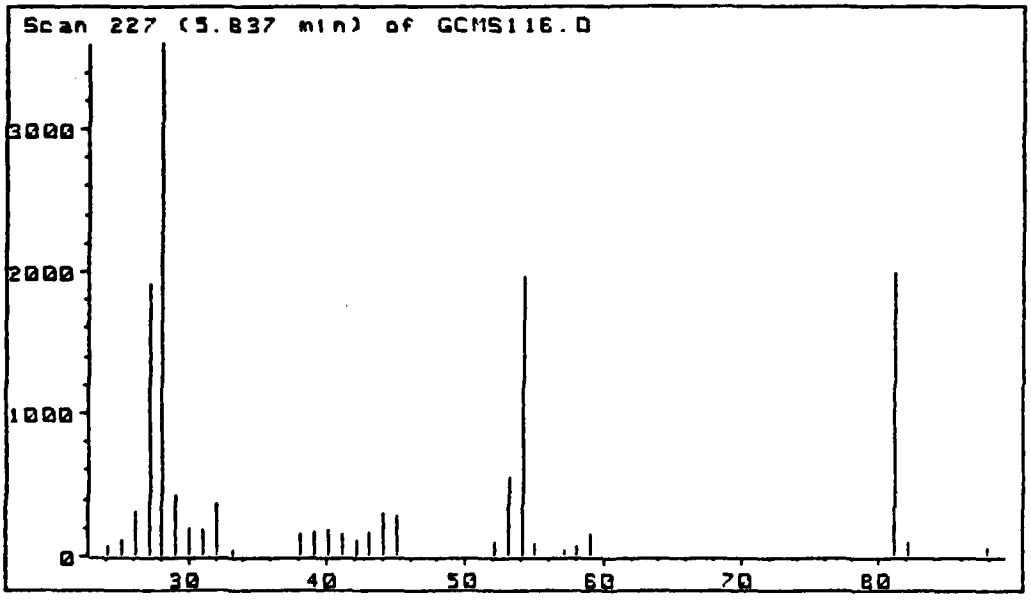

Figure 40. Typical Mass Spectrum of Chromatographic Peak at ca 5.8 Minutes, PEG 5-3-0, 600°C

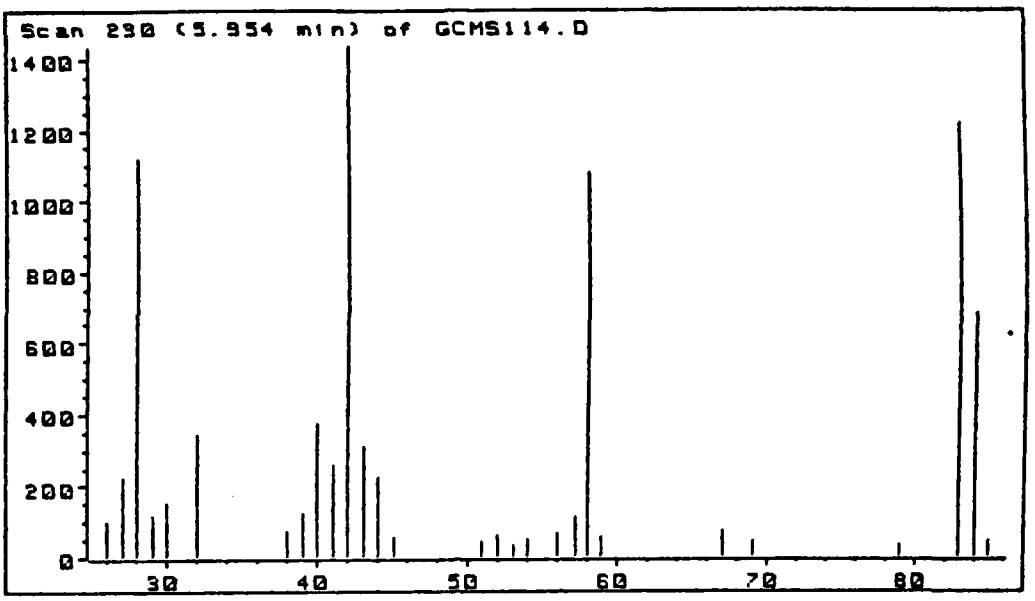

Figure 41. Typical Mass Spectrum of Chromatographic Peak at ca 6.0 Minutes, PEG 5-3-0, 600°C

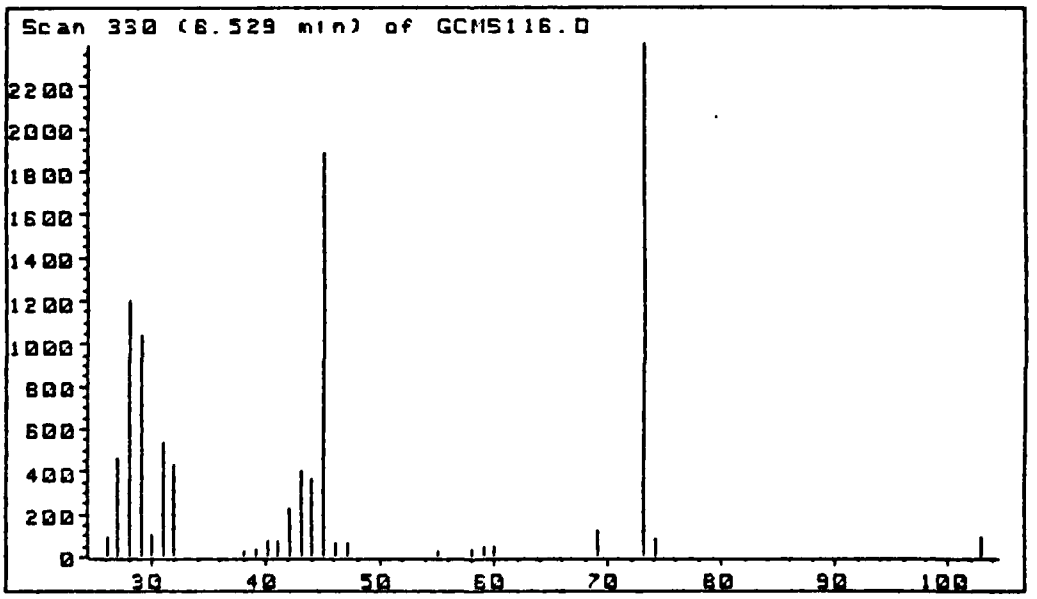

Figure 42. Typical Mass Spectrum of Chromatographic Peak at ca 6.5 Minutes, PEG 5-3-0, 600°C

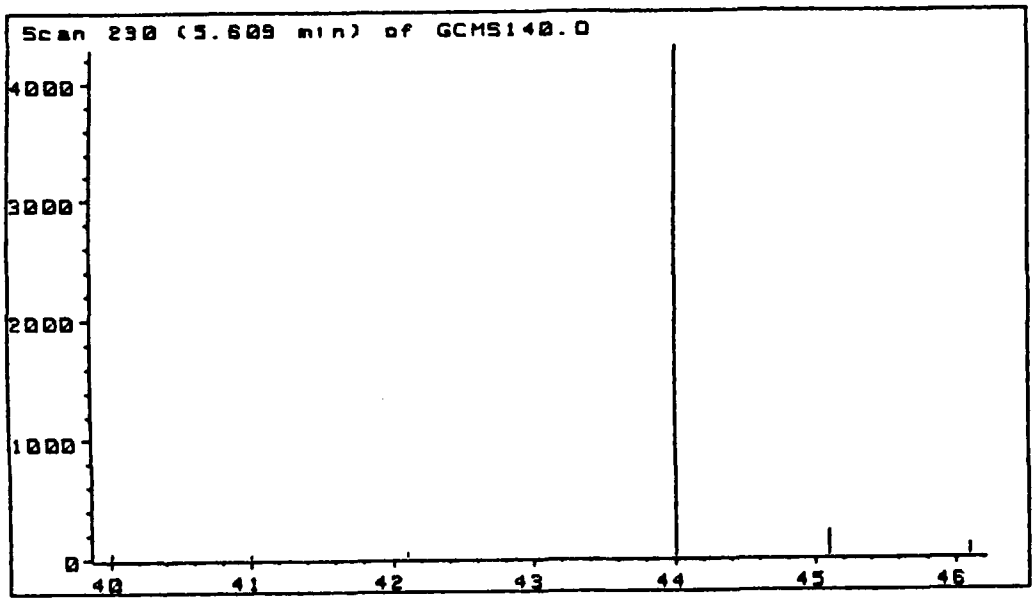

Figure 43. Typical Mass Spectrum of Chromatographic Peak at ca 5.6 Minutes, PEG 5-3-0, 800°C

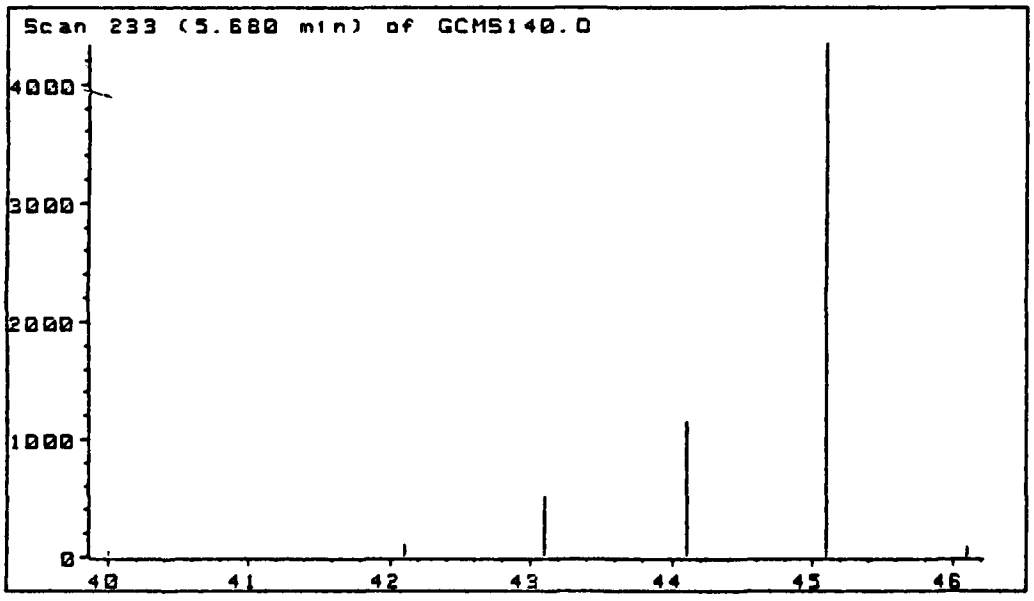

Figure 44. Typical Mass Spectrum of Chromatographic Peak at ca 5.7 Minutes, PEG 5-3-0, 800°C

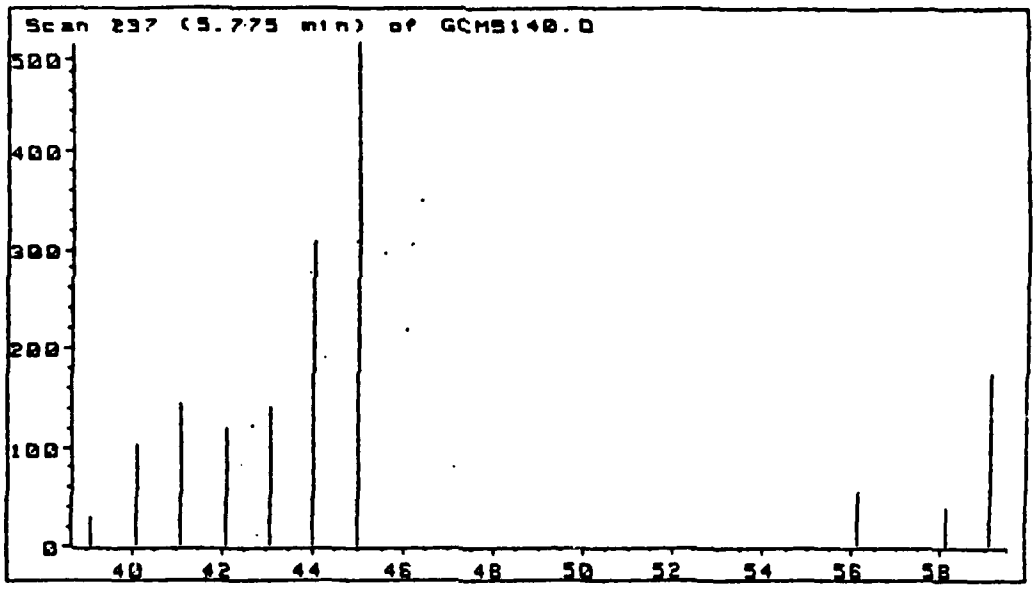

Figure 45. Typical Mass Spectrum of First Chromatographic Peak at ca 5.8 Minutes, PEG 5-3-0, 800°C

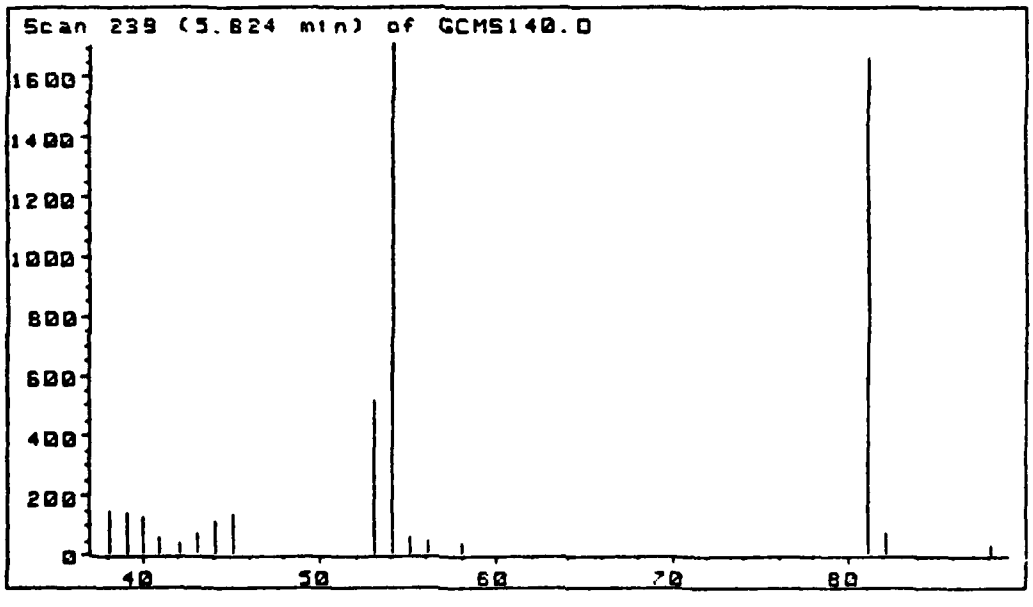

Figure 46. Typical Mass Spectrum of Second Chromatographic Peak at ca 5.8 Minutes, PEG 5-3-0, 800°C

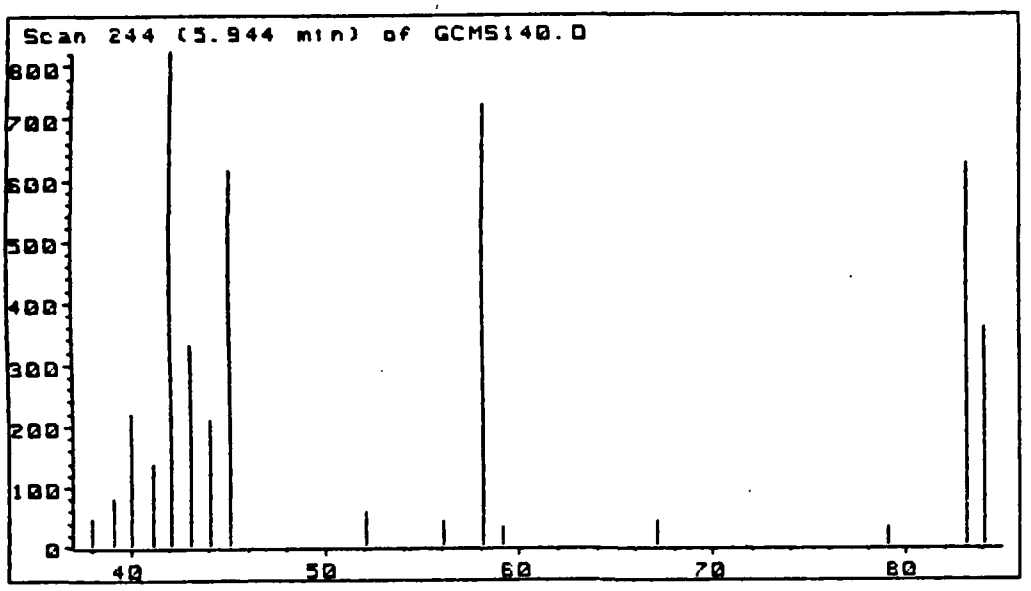

Figure 47. Typical Mass Spectrum of Chromatographic Peak at ca 5.9 Minutes, PEG 5-3-0, 800°C

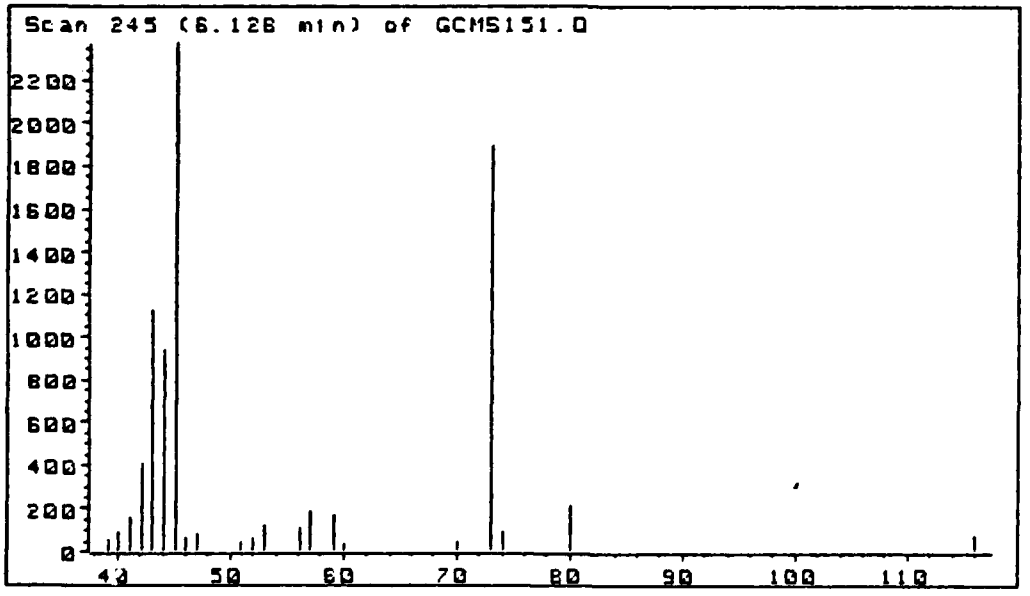

Figure 48. Typical Mass Spectrum of Chromatographic Peak at ca 6.1 Minutes, PEG 5-3-0, 800°C

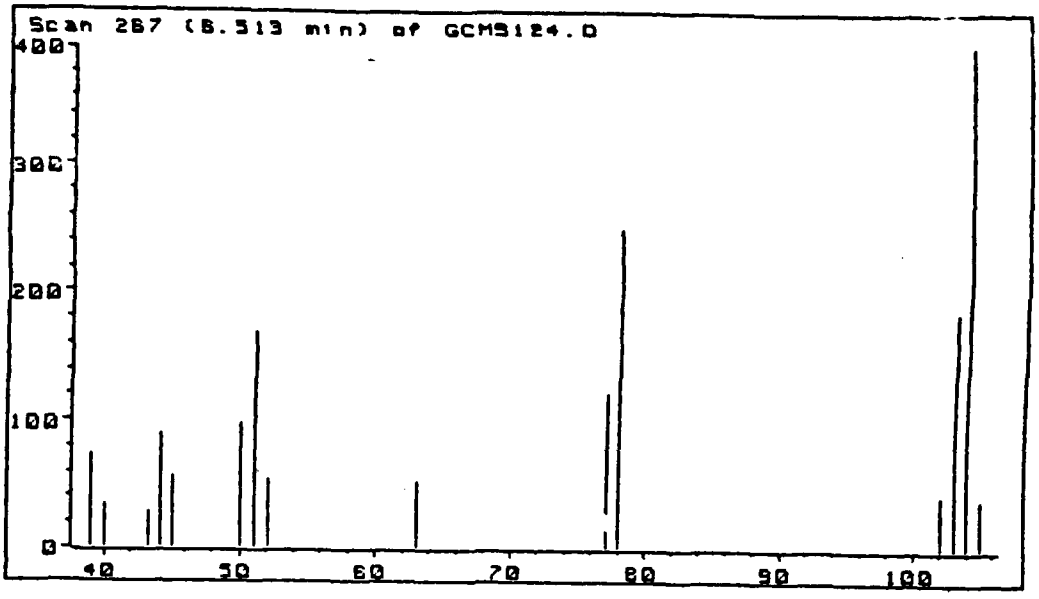

Figure 49. Typical Mass Spectrum of Chromatographic Peak at ca 6.5 Minutes, PEG 5-3-0, 800°C

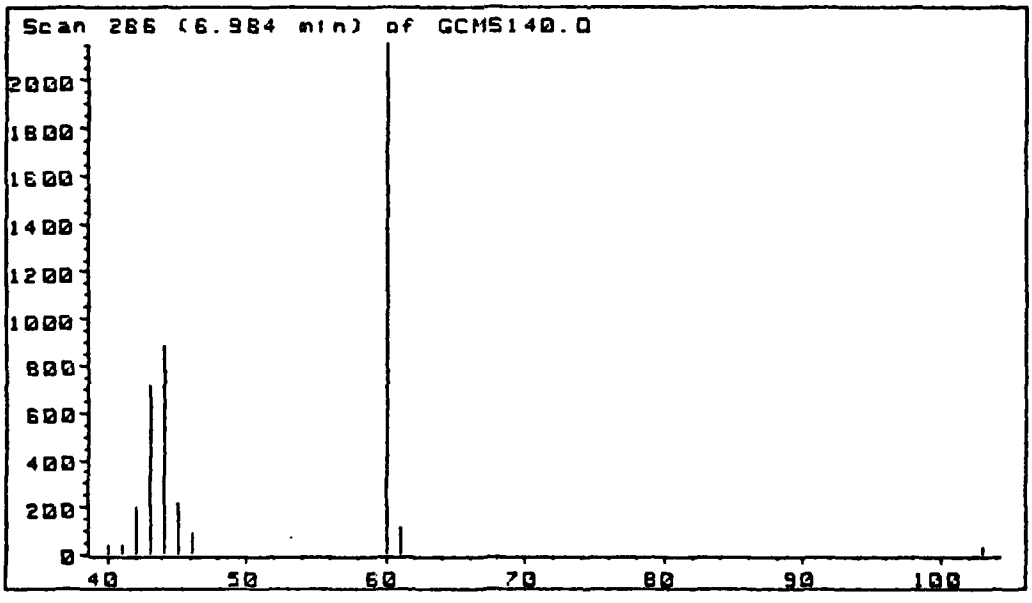

Figure 50. Typical Mass Spectrum of Chromatographic Peak at ca 7.0 Minutes, PEG 5-3-0, 800°C

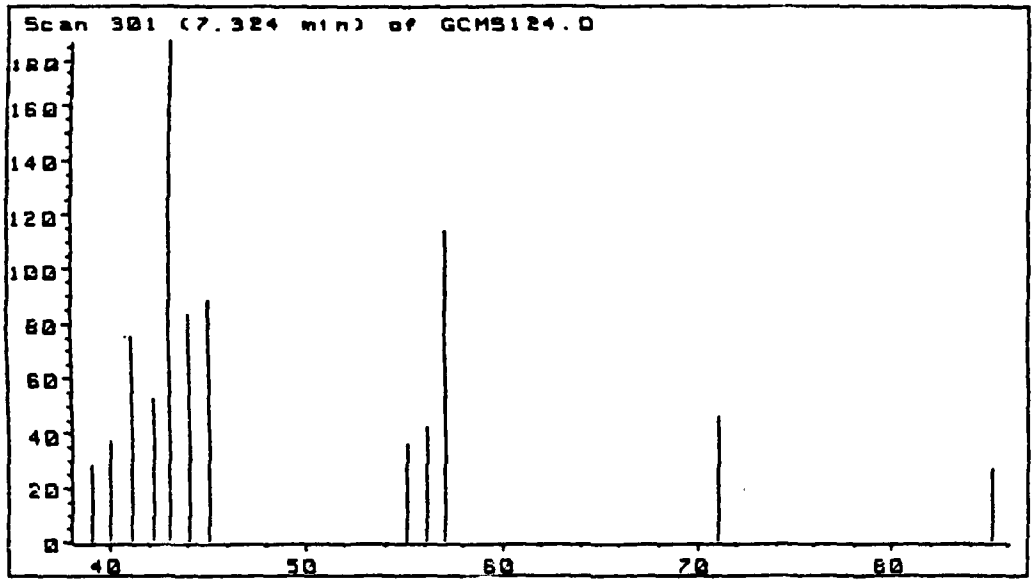

Figure 51. Typical Mass Spectrum of Chromatographic Peak at ca 7.3 Minutes, PEG 5-3-0, 800°C

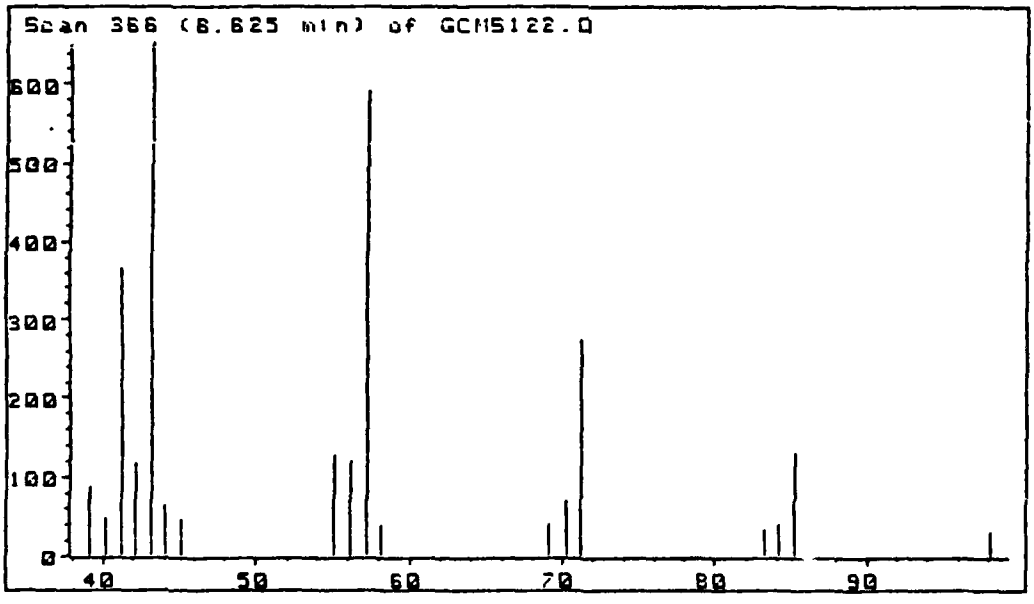

Figure 52. Typical Mass Spectrum of Chromatographic Peak at ca 6.6 Minutes, PEG 5-3-0, 800°C

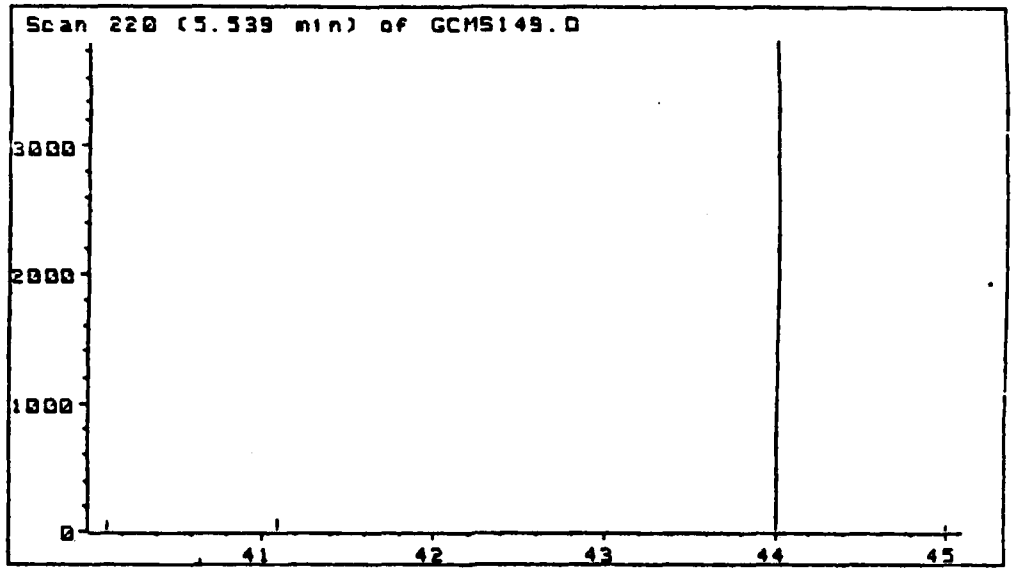

Figure 53. Typical Mass Spectrum of Chromatographic Peak at ca 5.5 Minutes, GAP 5-3-15, 325°C

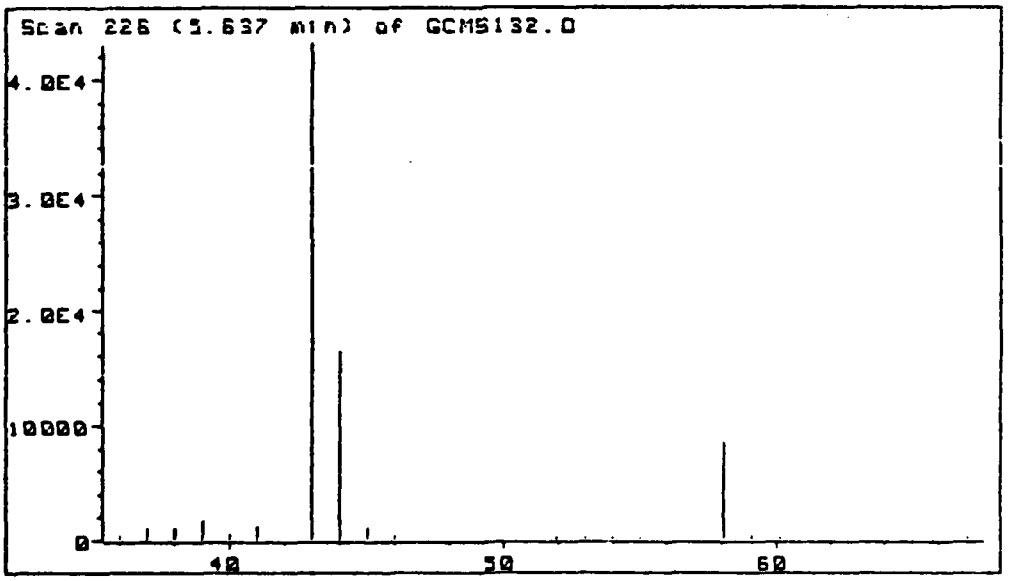

Figure 54. Typical Mass Spectrum of Chromatographic Peak at ca 5.6 Minutes, GAP 5-3-15, 325°C

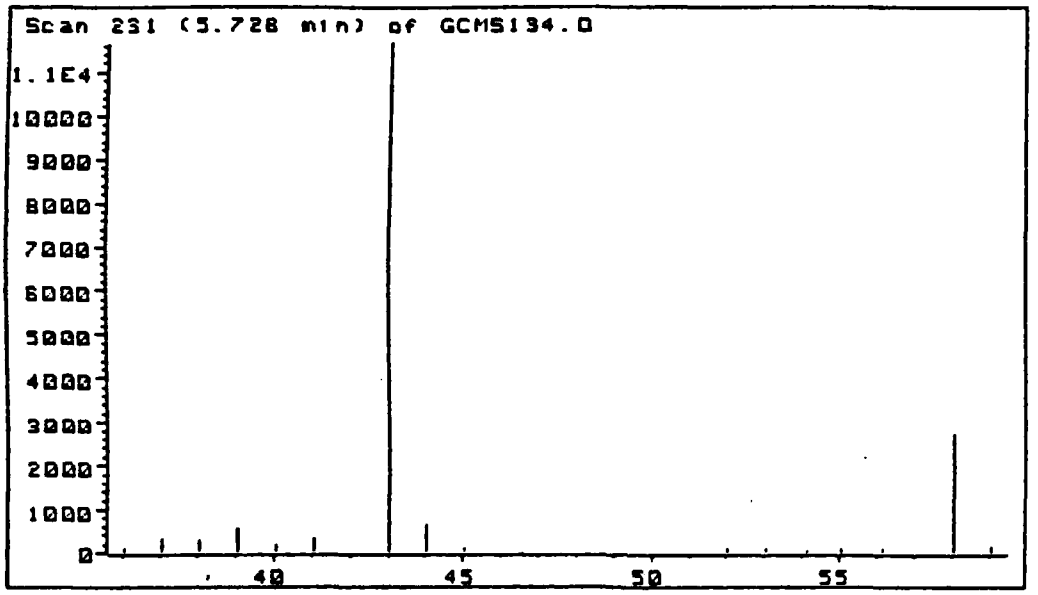

Figure 55. Typical Mass Spectrum of Chromatographic Peak at ca 5.7 Minutes, GAP 5-3-15, 325°C

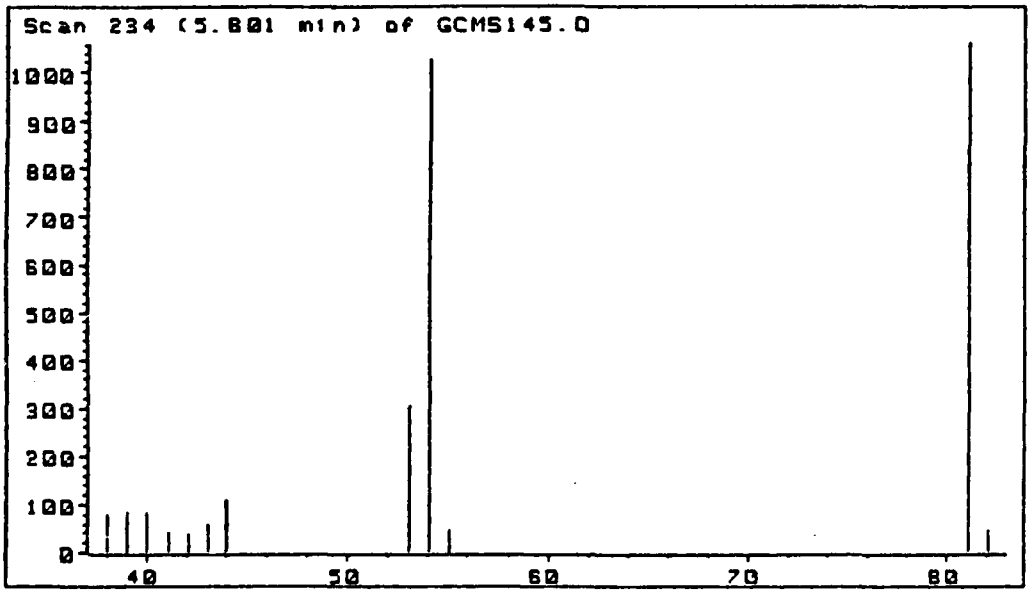

Figure 56. Typical Mass Spectrum of Chromatographic Peak at ca 5.8 Minutes, GAP 5-3-15, 325°C

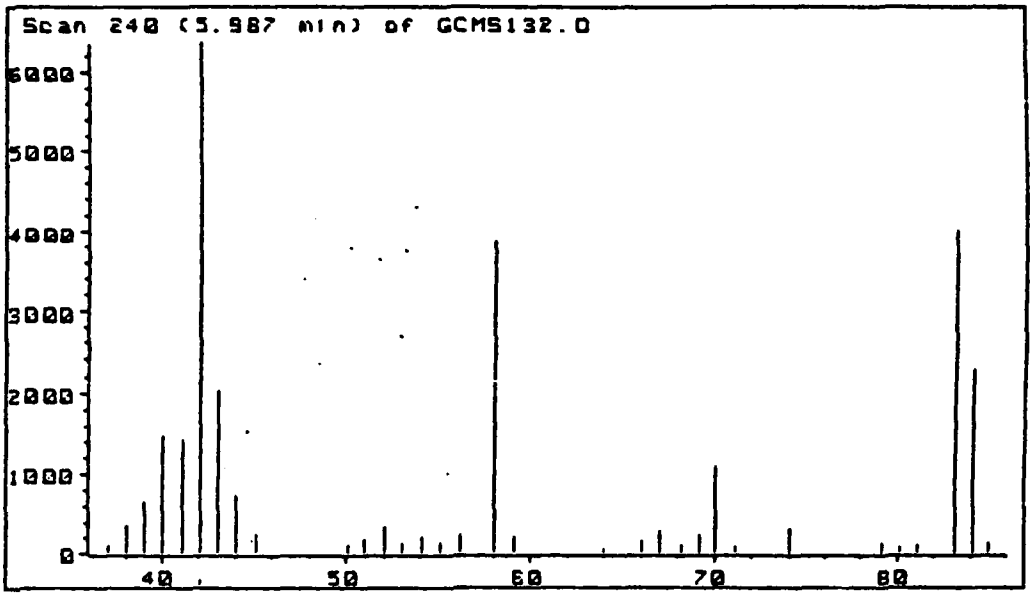

Figure 57. Typical Mass Spectrum of Chromatographic Peak at ca 6.0 Minutes, GAP 5-3-15, 325°C

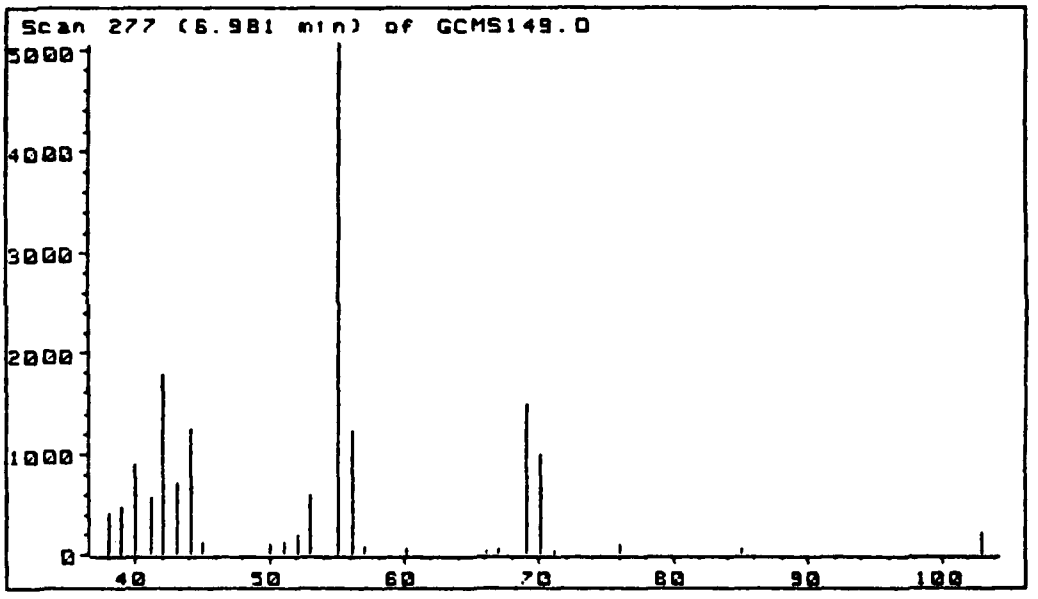

Figure 58. Typical Mass Spectrum of Chromatographic Peak at ca 7.0 Minutes, GAP 5-3-15, 325°C

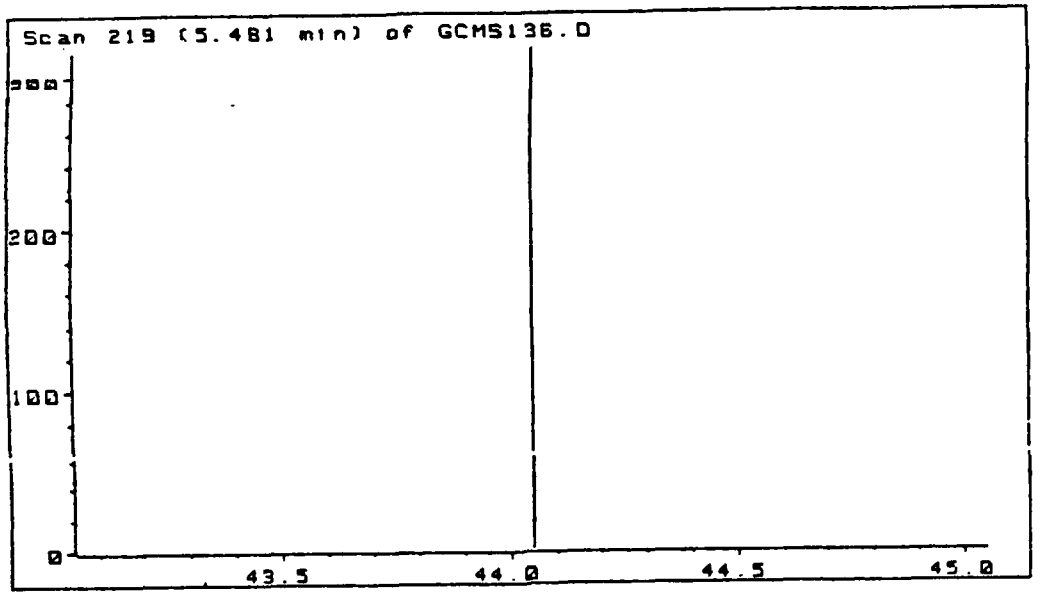

Figure 59. Typical Mass Spectrum of Chromatographic Peak at ca 5.5 Minutes, GAP 5-3-15, 800°C

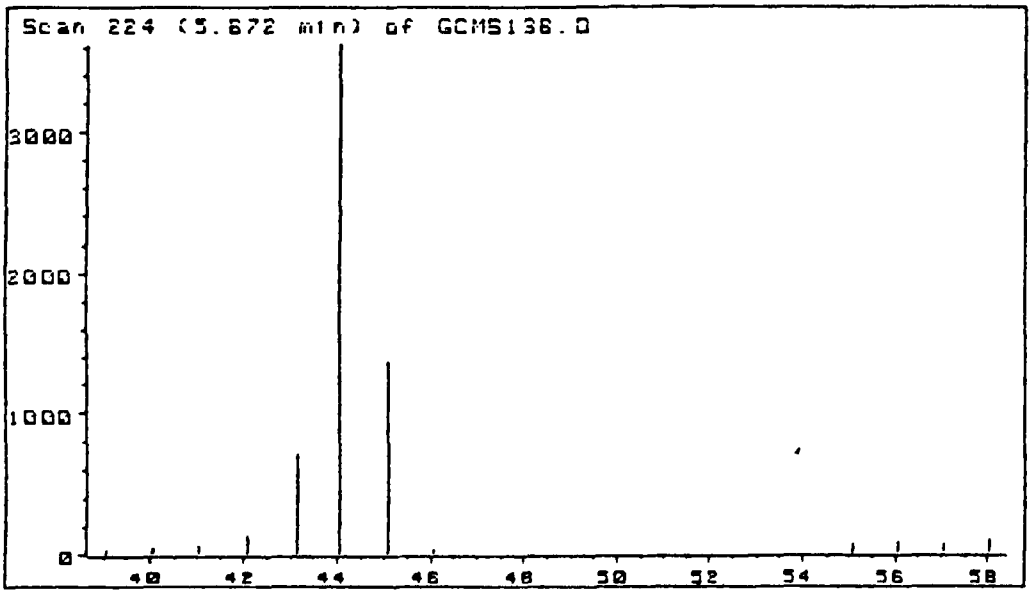

Figure 60. Typical Mass Spectrum of Chromatographic Peak at ca 5.7 Minutes, GAP 5-3-15, 800°C

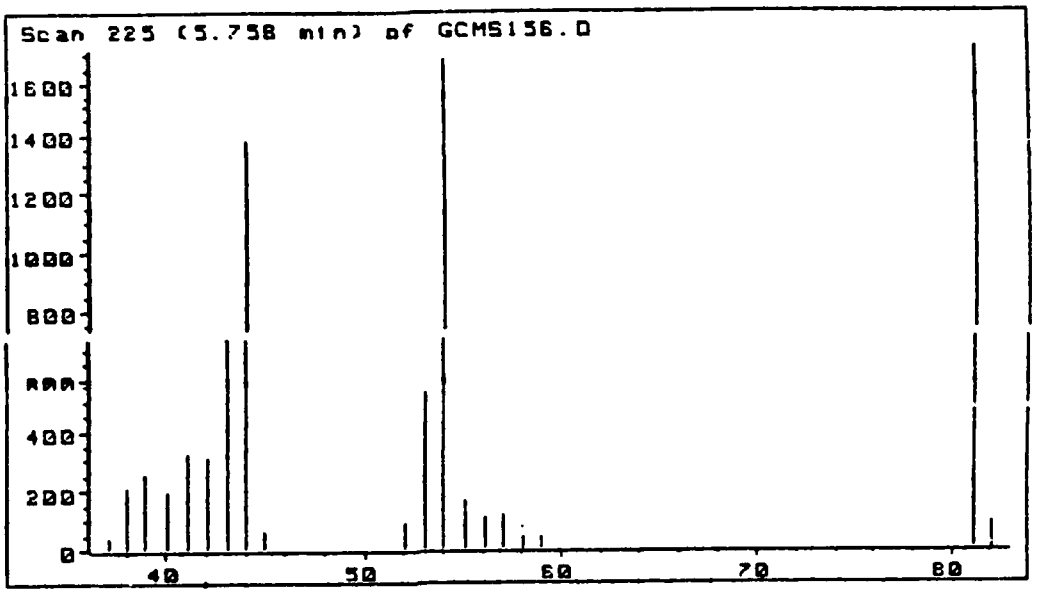

Figure 61. Typical Mass Spectrum of Chromatographic Peak at ca 5.8 Minutes, GAP 5-3-15, 800°C

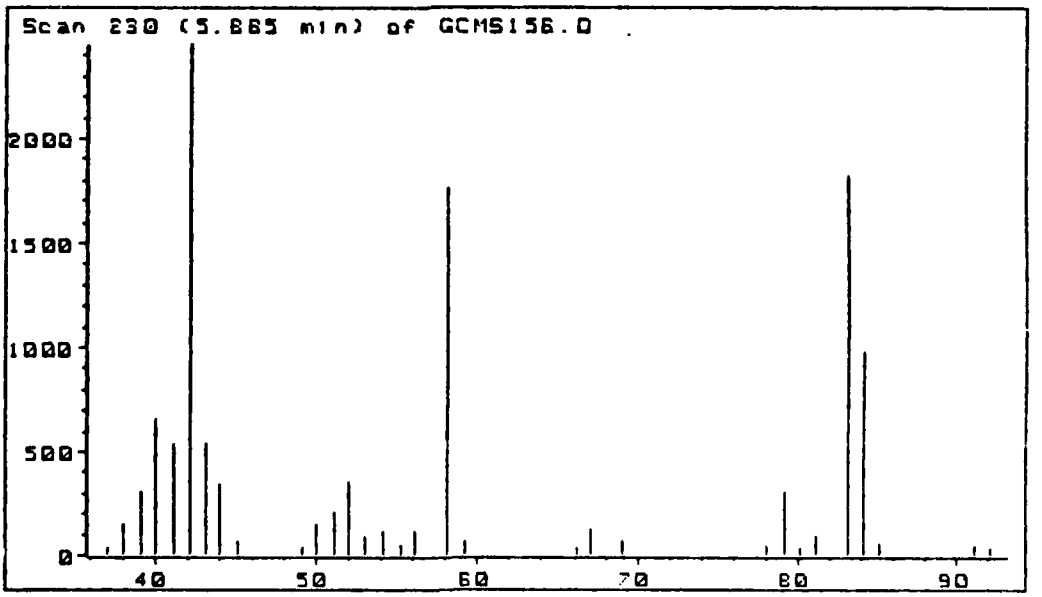

Figure 62. Typical Mass Spectrum of Chromatographic Peak at ca 5.9 Minutes, GAP 5-3-15, 800°C

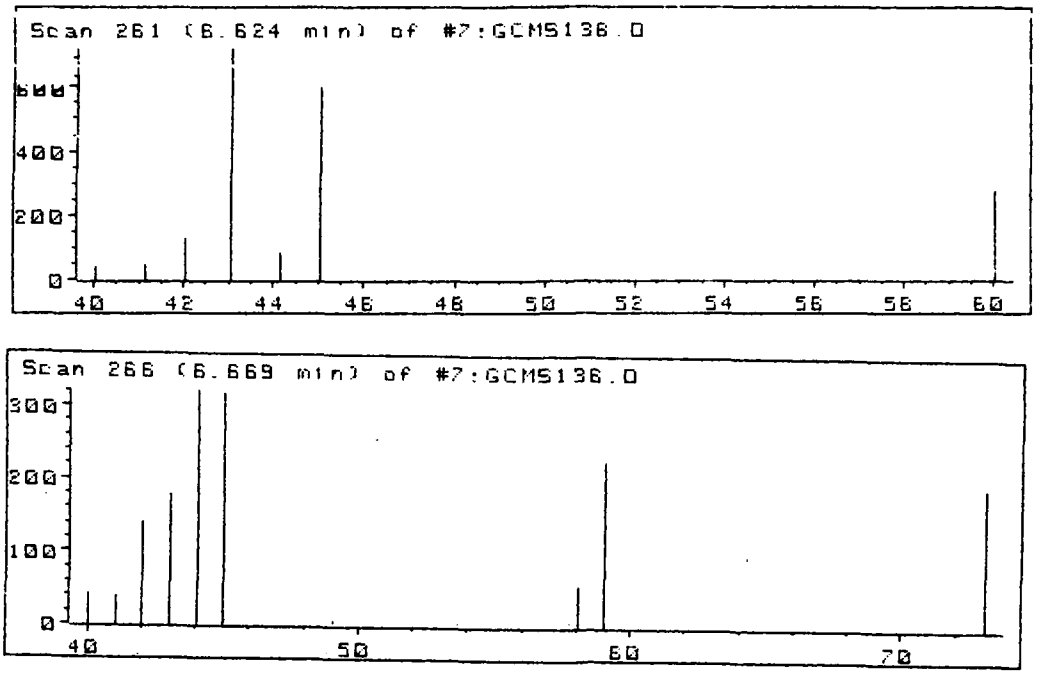

Figure 63. Typical Mass Spectra of Chromatographic Peak at ca 6.6 Minutes, GAP 5-3-15, 800°C

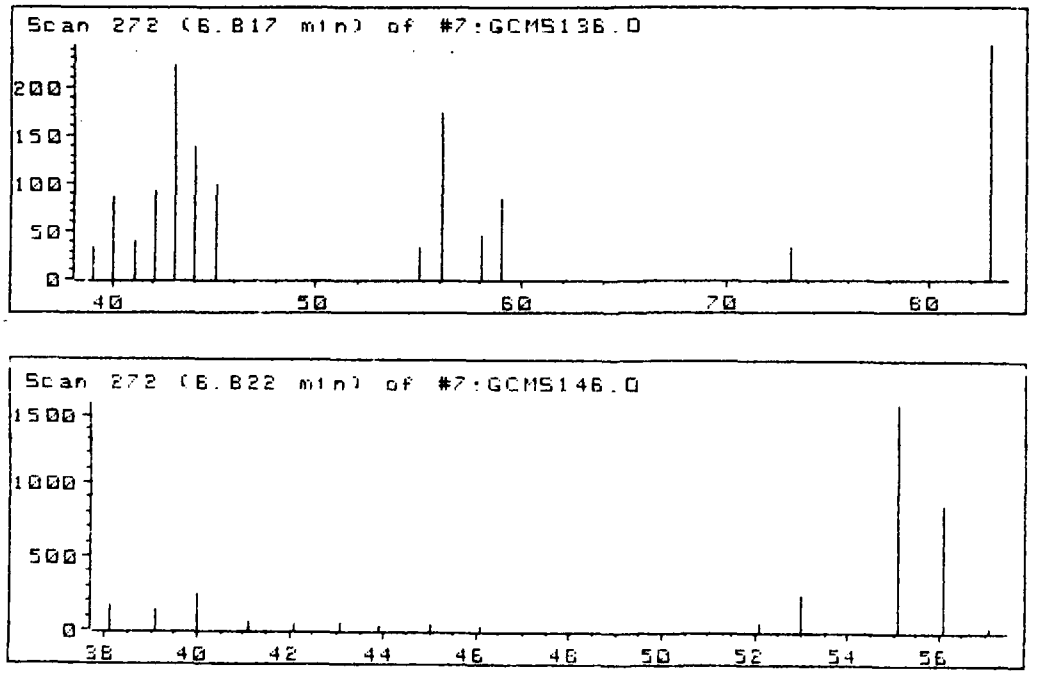

Figure 64. Typical Mass Spectra of Chromatographic Peak at ca 6.8 Minutes, GAP 5-3-15, 800°C

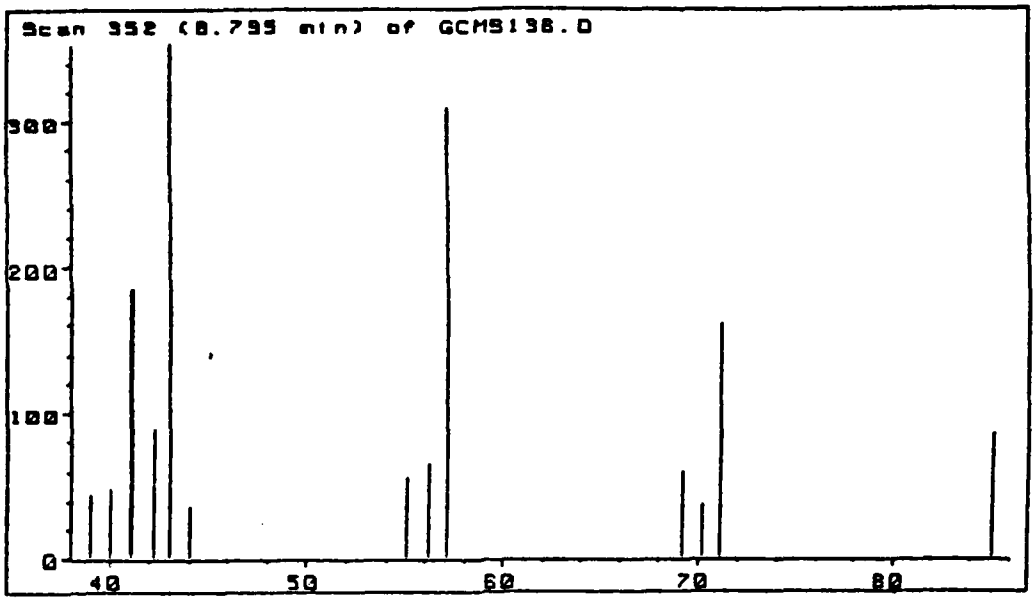

Figure 65. Typical Mass Spectrum of Chromatographic Peak at ca 8.8 Minutes, GAP 5-3-15, 800°C

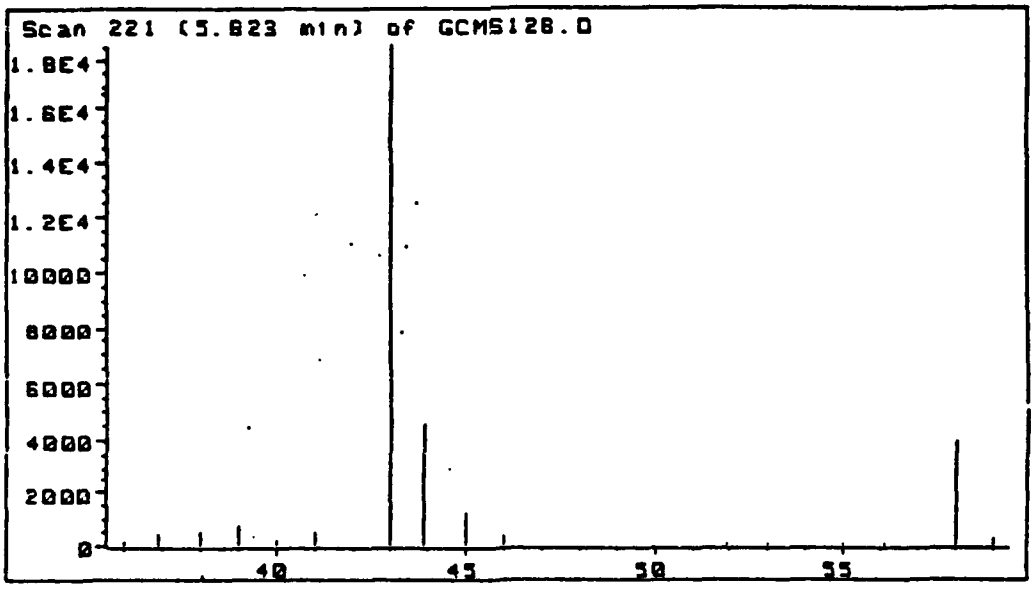

Figure 66. Typical Mass Spectrum of Chromatographic Peak at ca 5.6 Minutes, PEG 5-3-15, 325°C

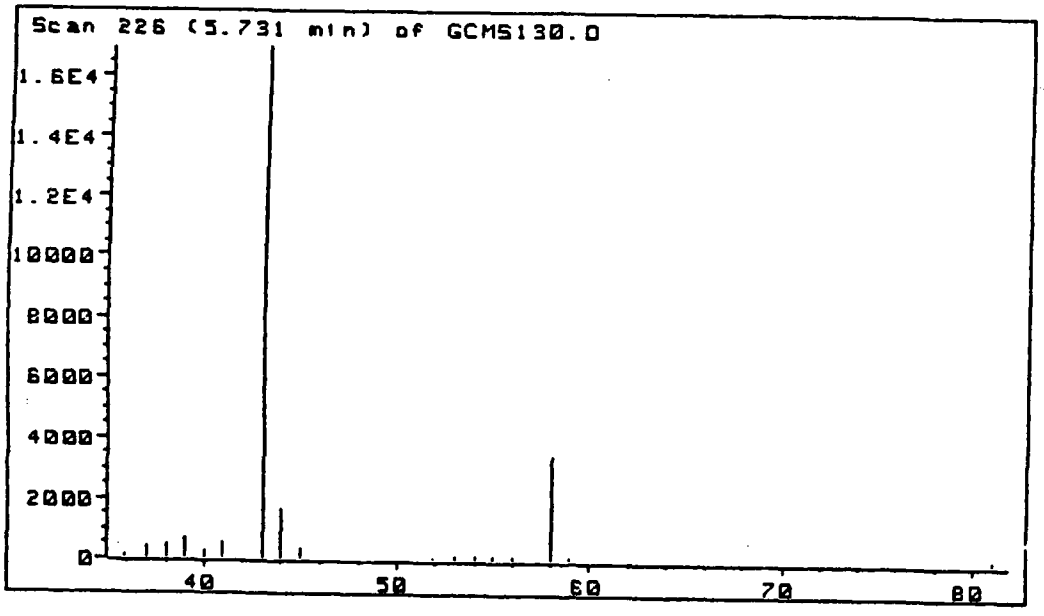

Figure 67. Typical Mass Spectrum of Chromatographic Peak at ca 5.7 Minutes, PEG 5-3-15, 325°C

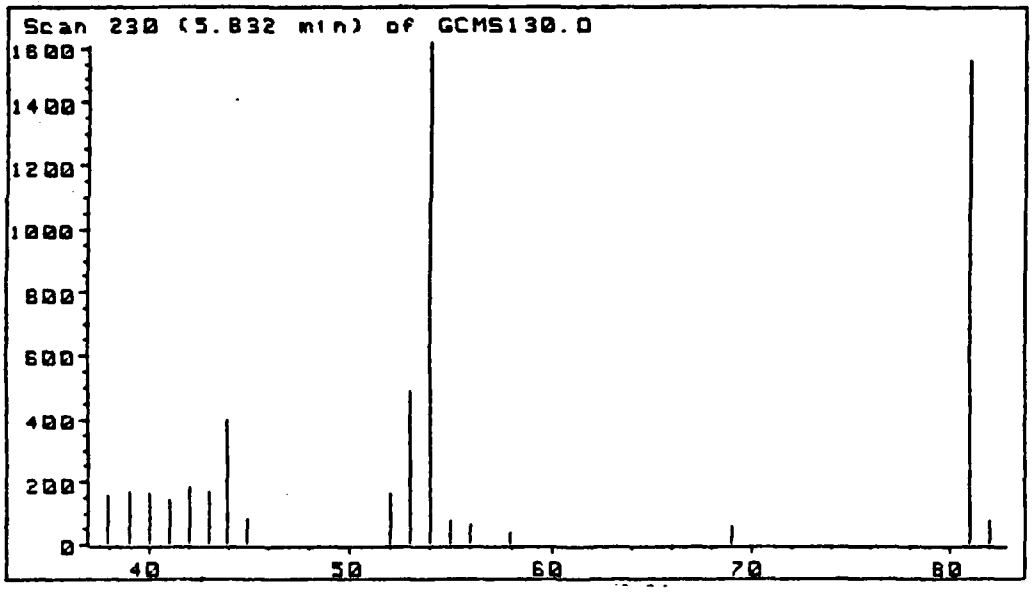

Figure 68. Typical Mass Spectrum of Chromatographic Peak at ca 5.8 Minutes, PEG 5-3-15, 325°C

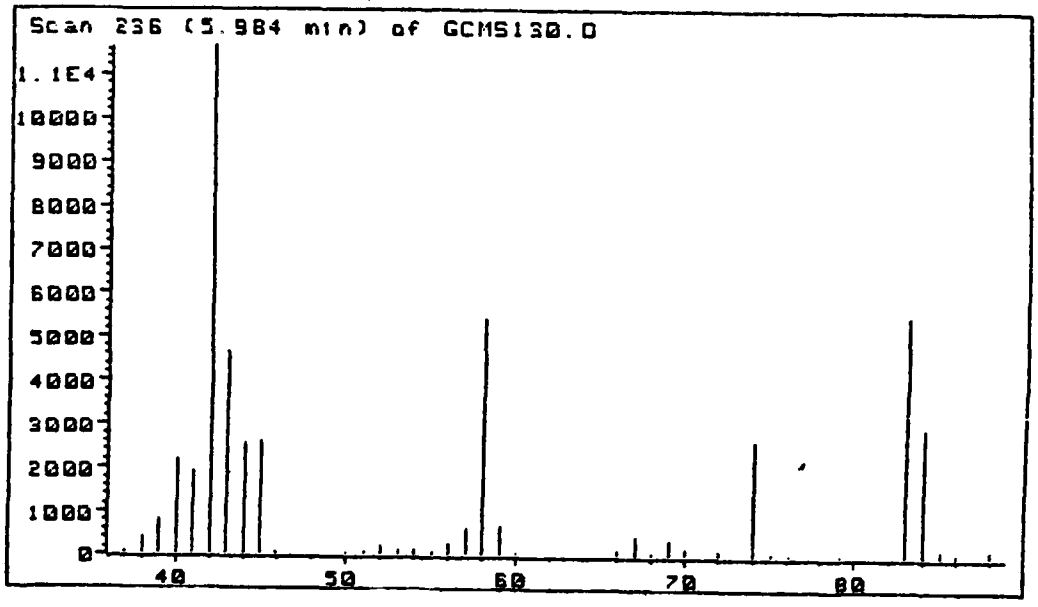

Figure 69. Typical Mass Spectrum of Chromatographic Peak at ca 6.0 Minutes, PEG 5-3-15, 325°C

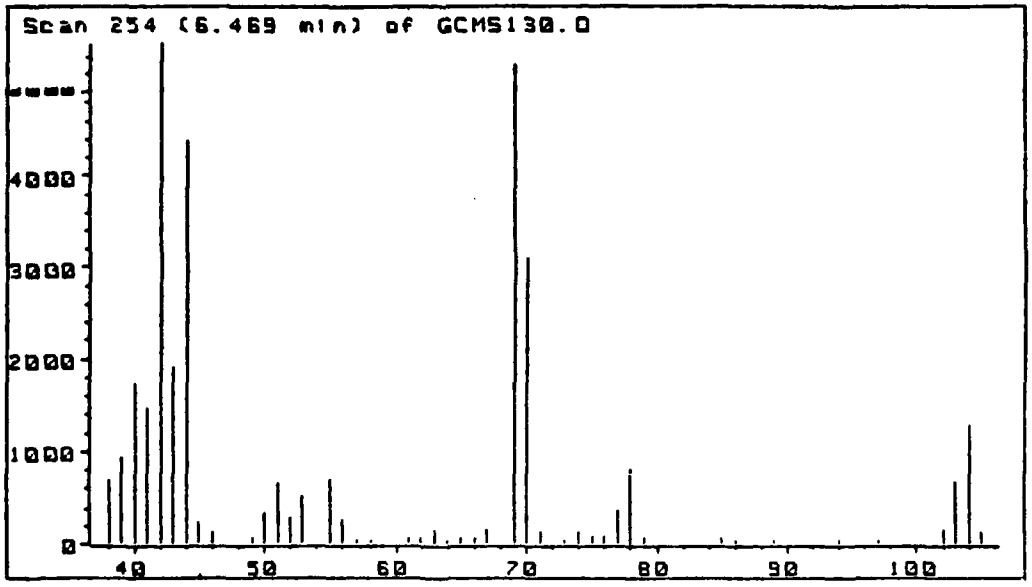

Figure 70. Typical Mass Spectrum of Chromatographic Peak at ca 6.5 Minutes, PEG 5-3-15, 325°C

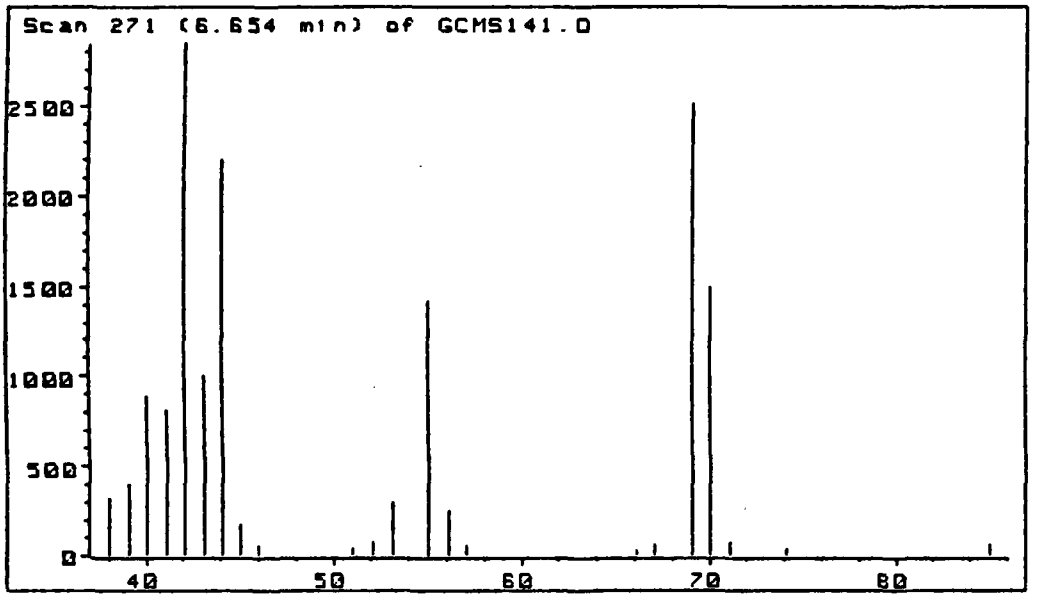

Figure 71. Typical Mass Spectrum of Chromatographic Peak at ca 6.7 Minutes, PEG 5-3-15, 325°C

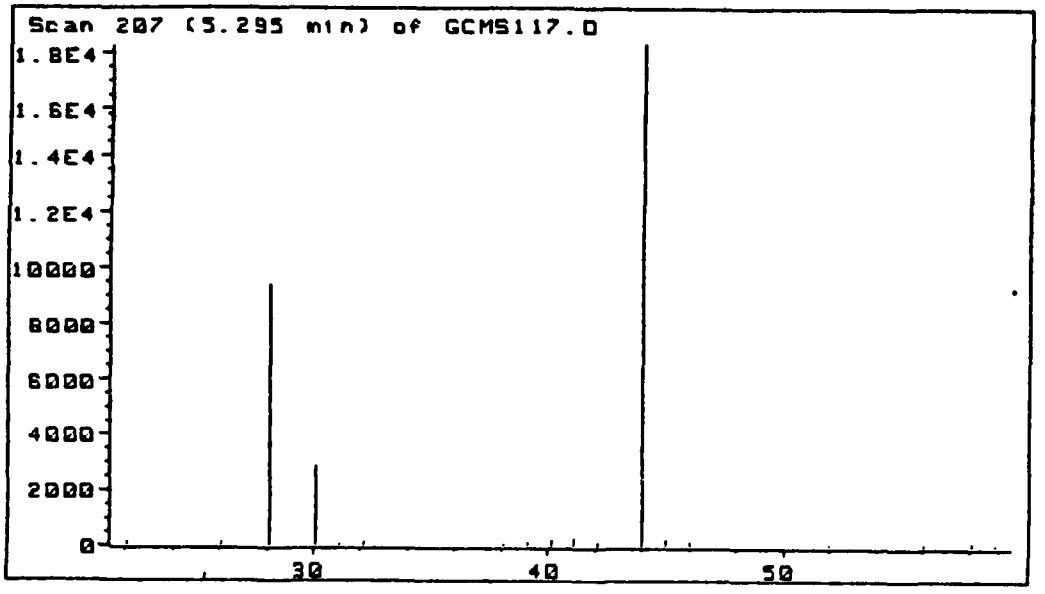

Figure 72. Typical Mass Spectrum of Chromatographic Peak at ca 5.3 Minutes, PEG 5-3-15, 600°C

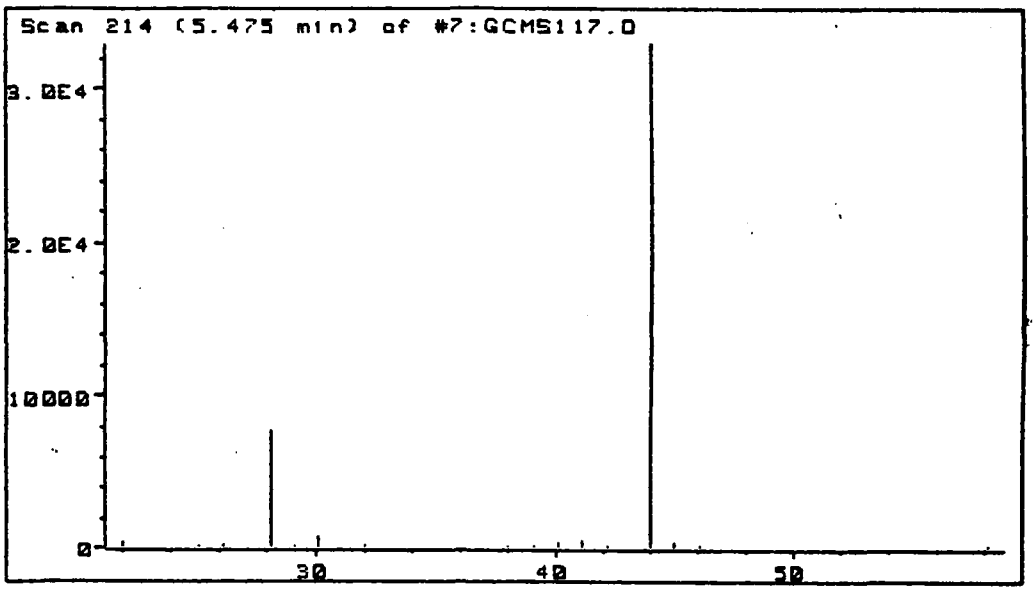

Figure 73. Typical Mass Spectrum of Chromatographic Peak at ca 5.5 Minutes, PEG 5-3-15, 600°C

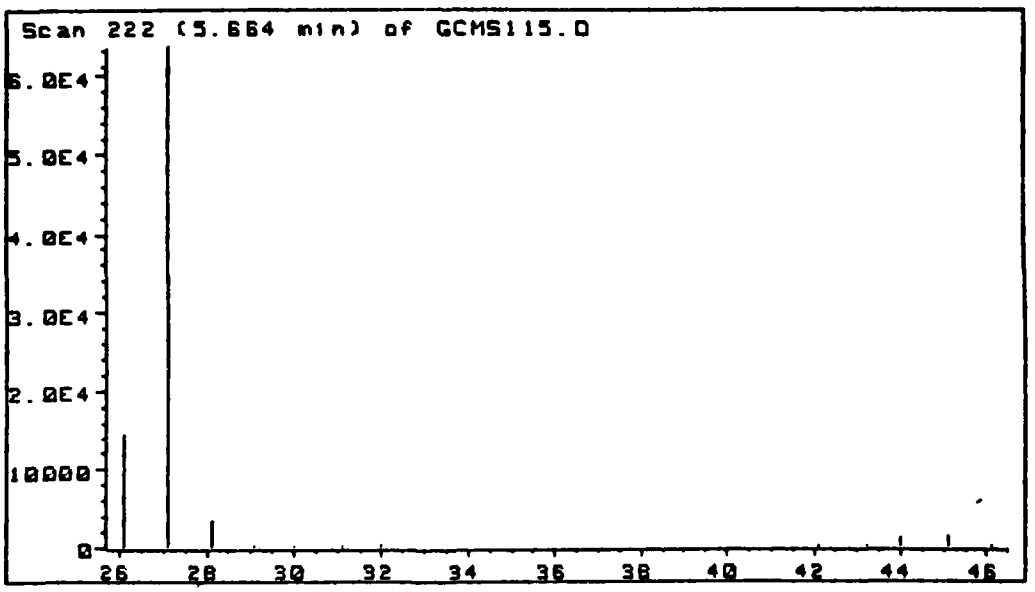

Figure 74. Typical Mass Spectrum of Chromatographic Peak at ca 5.6 Minutes, PEG 5-3-15, 600°C

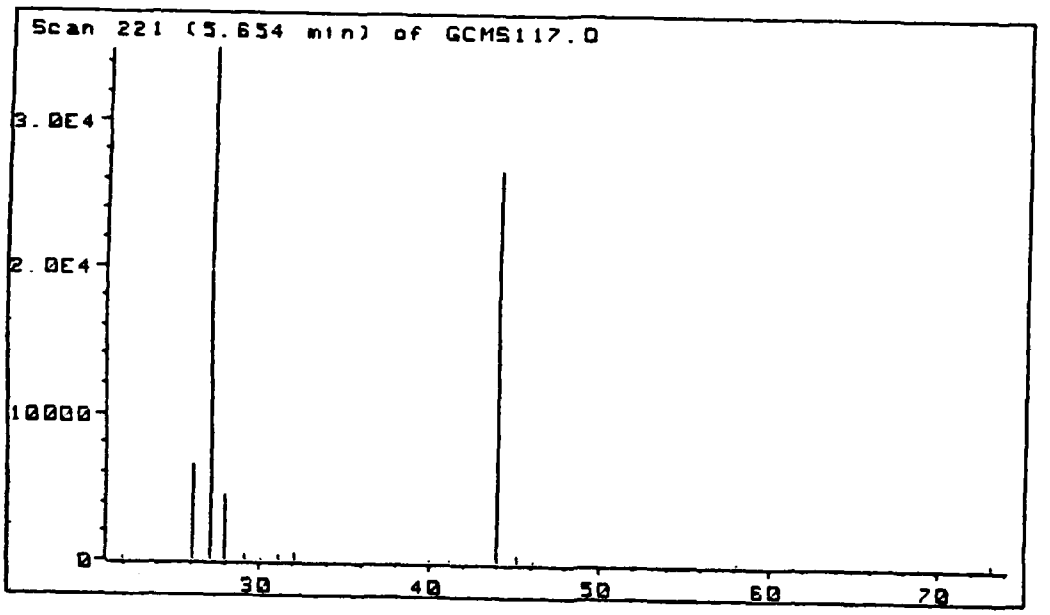

Figure 75. Typical Mass Spectrum of Chromatographic Peak at ca 5.7 Minutes, PEG 5-3-15, 600°C

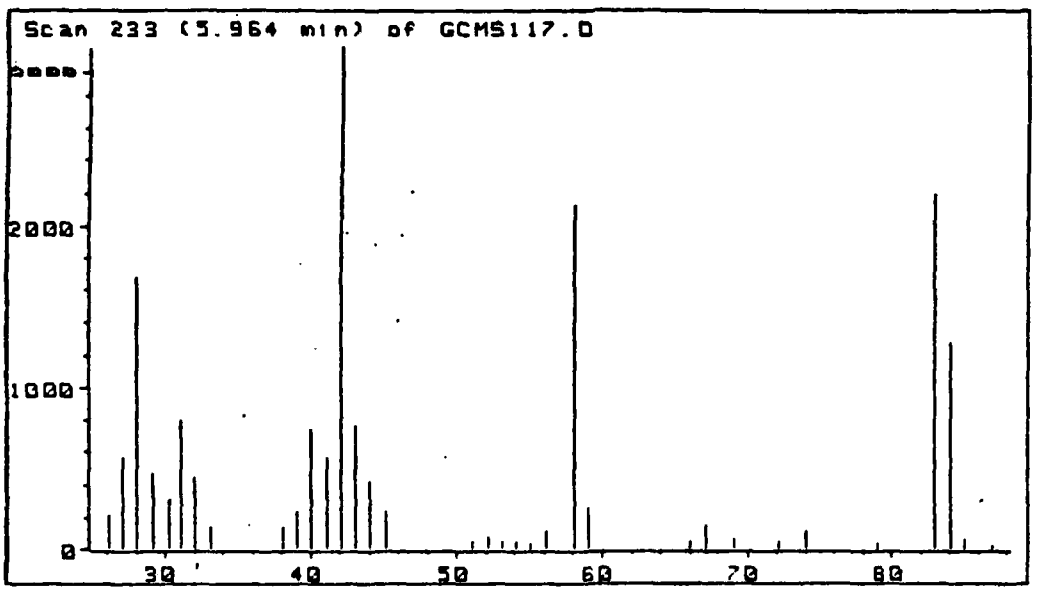

Figure 76. Typical Mass Spectrum of Chromatographic Peak at ca 6.0 Minutes, PEG 5-3-15, 600°C

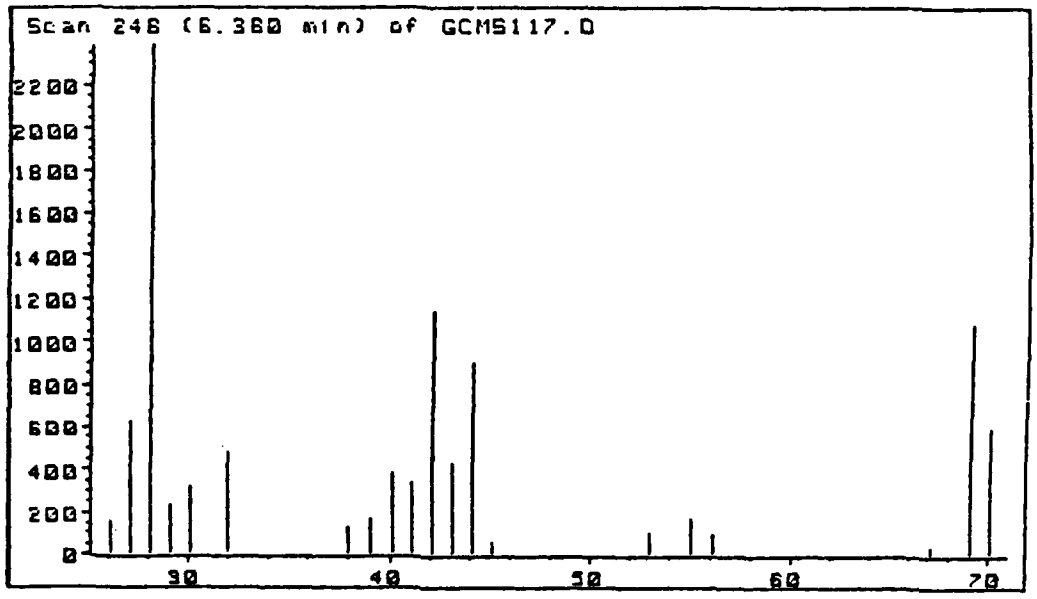

Figure 77. Typical Mass Spectrum of Chromatographic Peak at ca 6.4 Minutes, PEG 5-3-15, 600°C

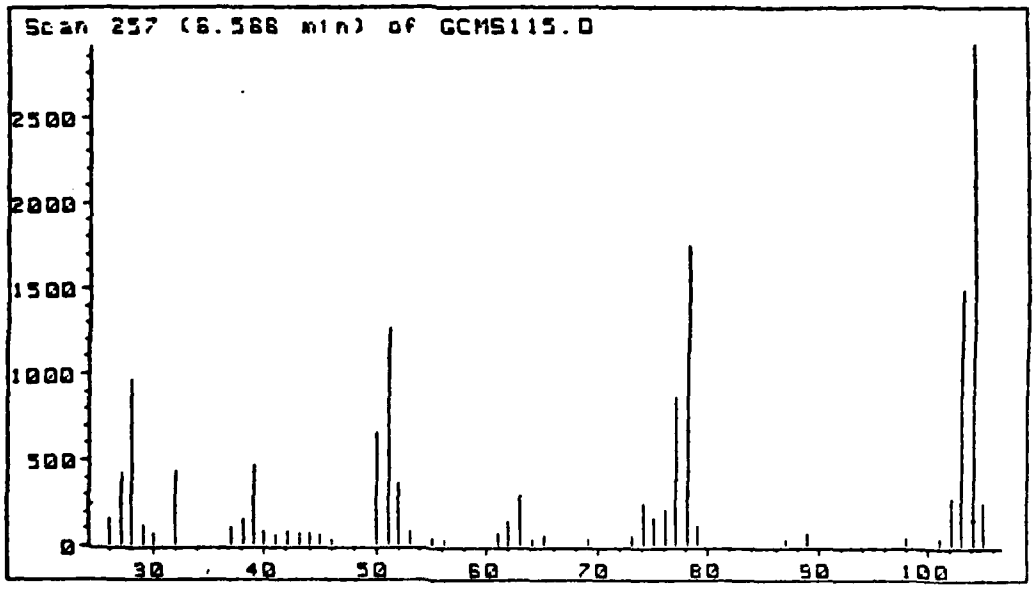

Figure 78. Typical Mass Spectrum of Chromatographic Peak at ca 6.6 Minutes, PEG 5-3-15, 600°C

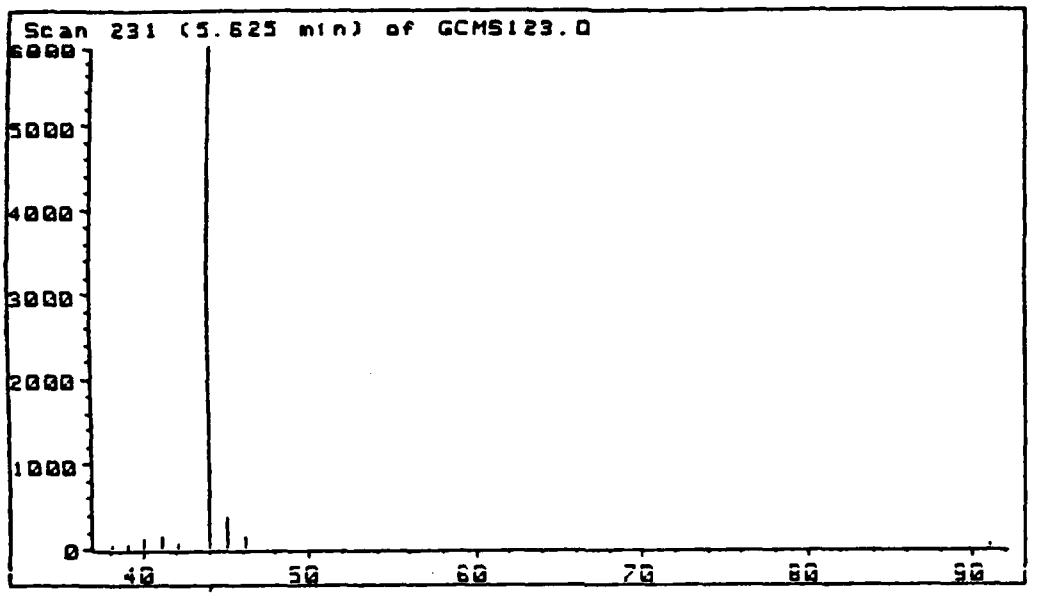

Figure 79. Typical Mass Spectrum of Chromatographic Peak at ca 5.6 Minutes, PEG 5-3-15, 800°C

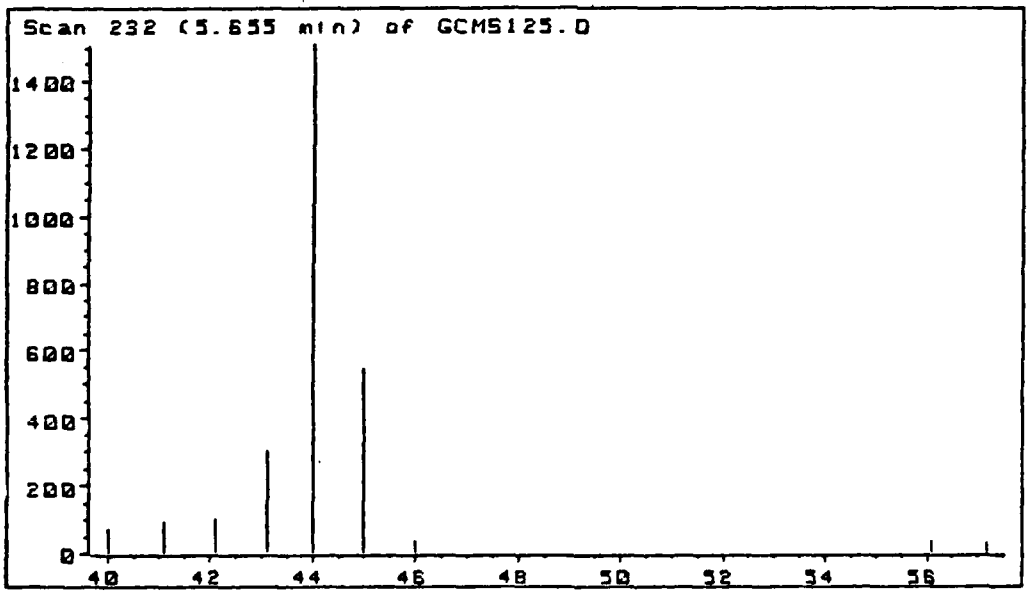

Figure 80. Typical Mass Spectrum of First Chromatographic Peak at ca 5.7 Minutes, PEG 5-3-15, 800°C

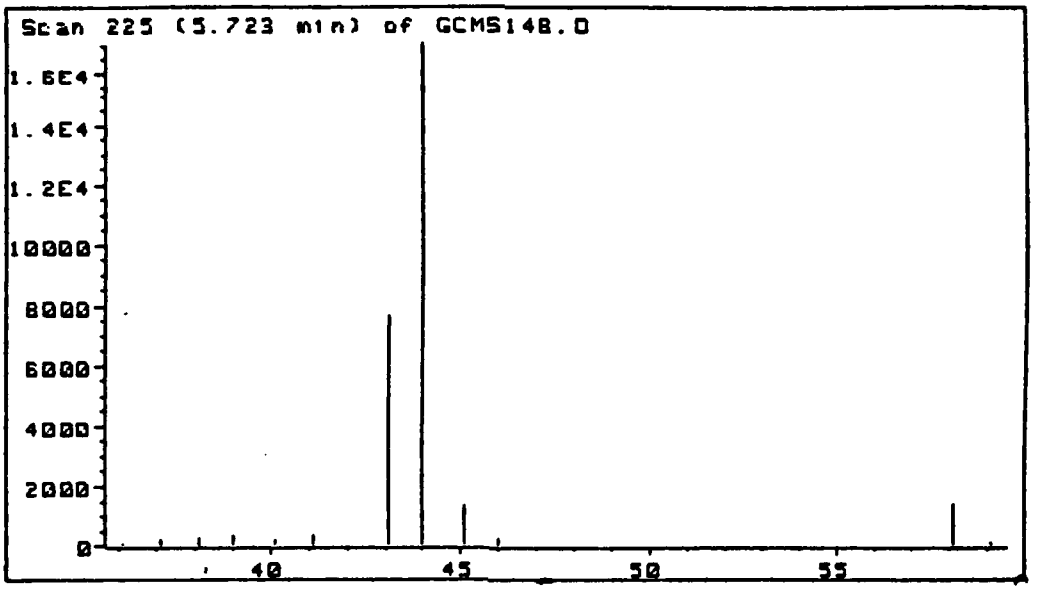

Figure 81. Typical Mass Spectrum of Second Chromatographic Peak at ca 5.7 Minutes, PEG 5-3-15, 800°C

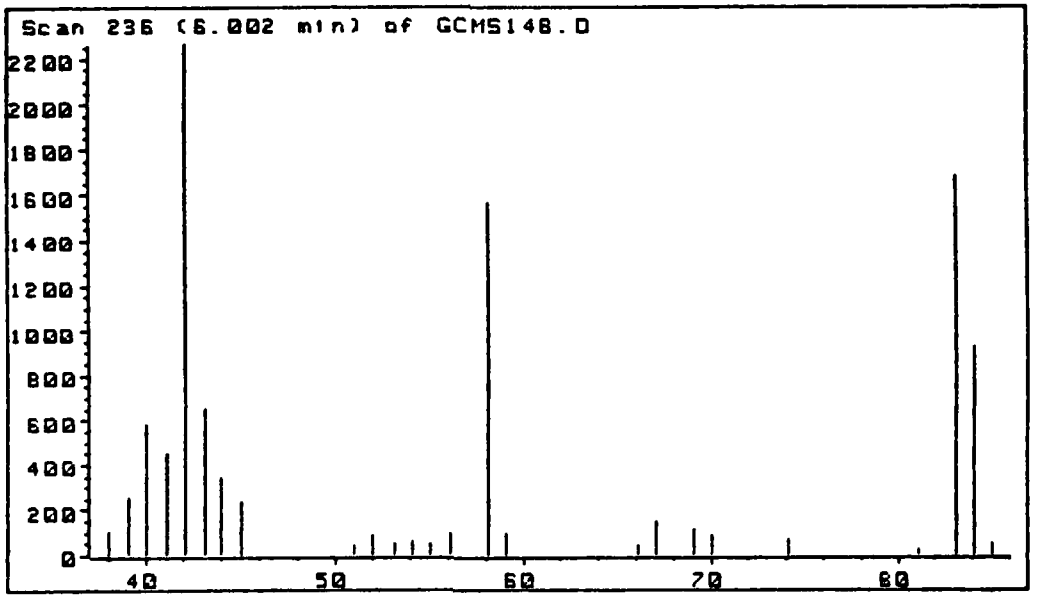

Figure 82. Typical Mass Spectrum of Chromatographic Peak at ca 6.0 Minutes, PEG 5-3-15, 800°C

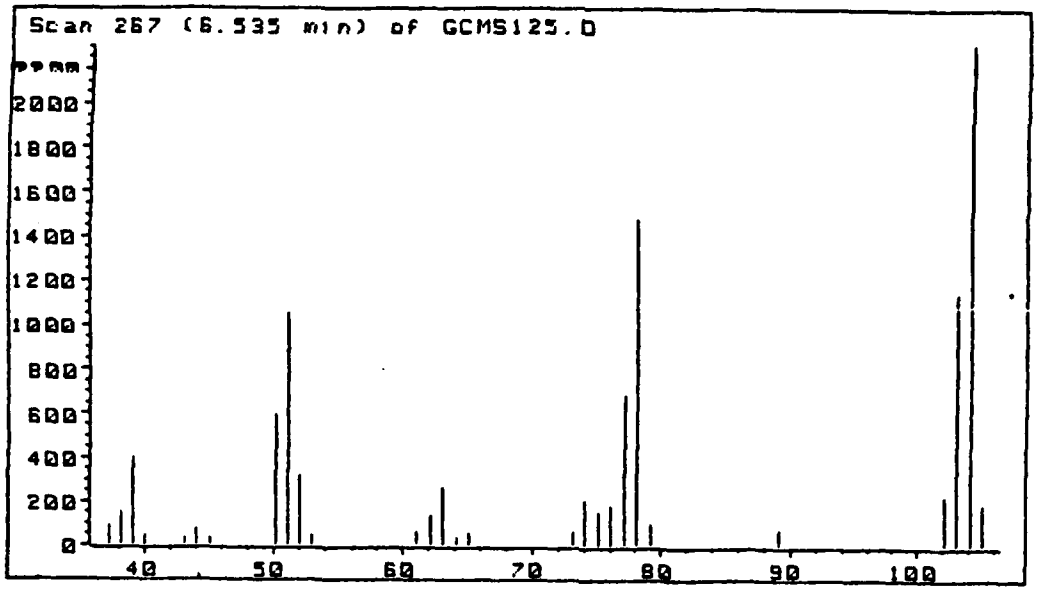

Figure 83. Typical Mass Spectrum of Chromatographic Peak at ca 6.5 Minutes, PEG 5-3-15, 800°C

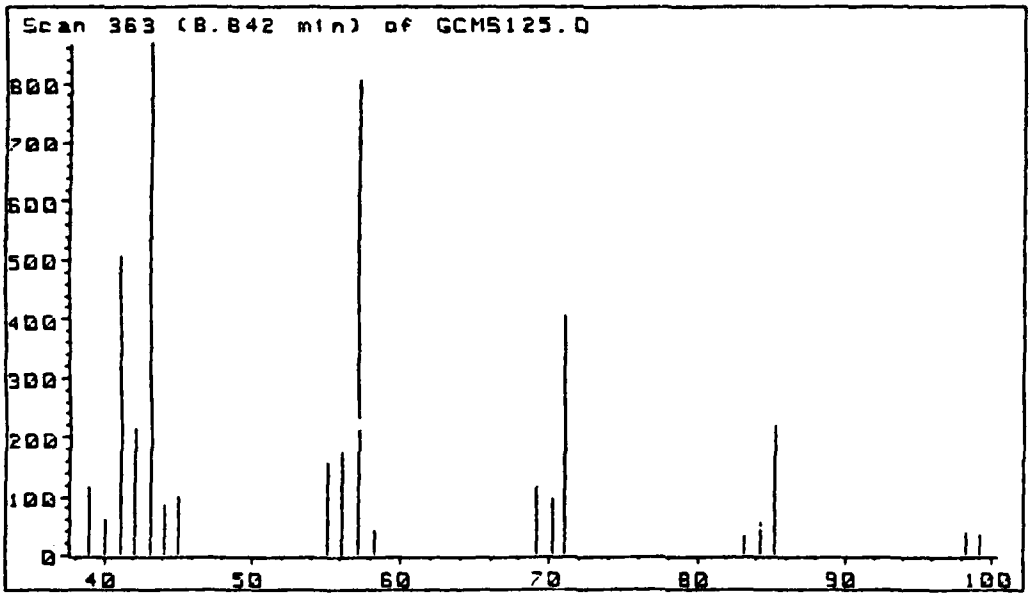

Figure 84. Typical Mass Spectrum of Chromatographic Peak at ca 8.8 Minutes, PEG 5-3-15, 800°C

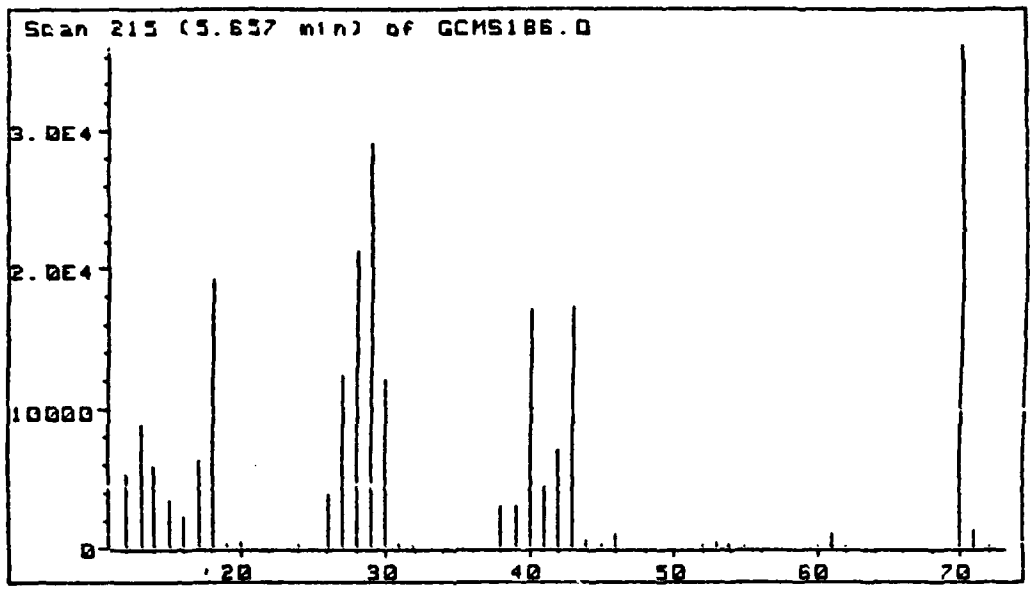

Figure 85. Typical Mass Spectrum of Chromatographic Peak at ca 5.7 Minutes, HMX, 325°C

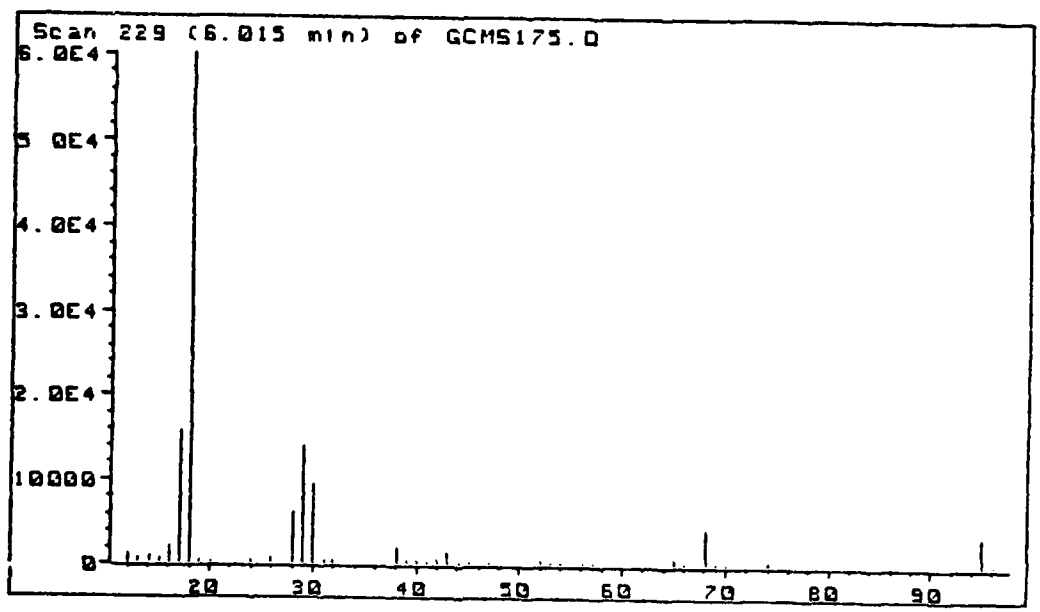

Figure 86. Typical Mass Spectrum of Chromatographic Peak at ca 6.0 Minutes, HMX, 325°C

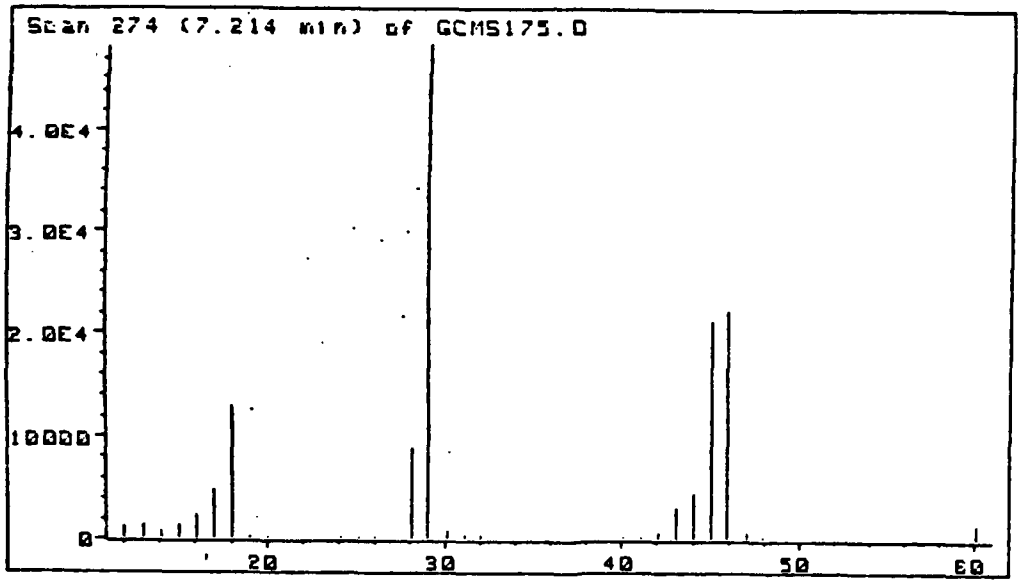

Figure 87. Typical Mass Spectrum of Chromatographic Peak at ca 7.2 Minutes, HMX, 325°C

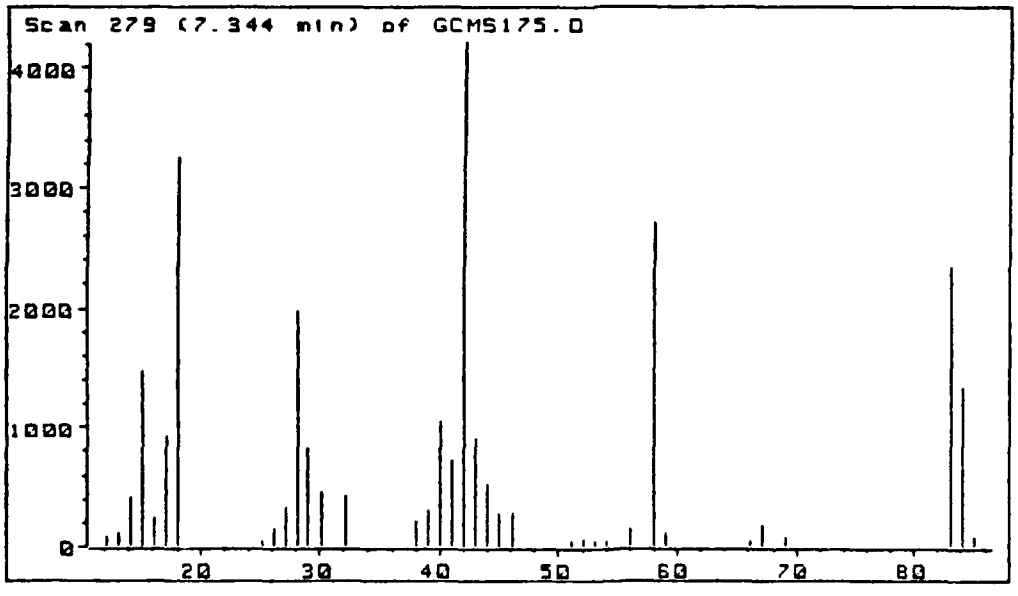

Figure 88. Typical Mass Spectrum of Chromatographic Peak at ca 7.3 Minutes, HMX, 325°C

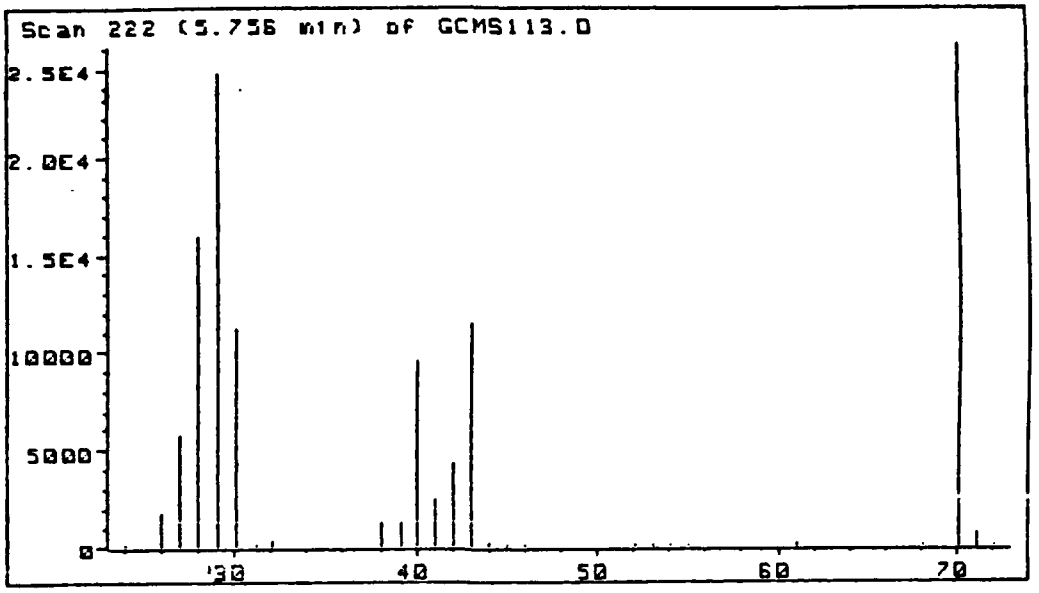

Figure 89. Typical Mass Spectrum of Chromatographic Peak at ca 5.8 Minutes, HMX, 400°C

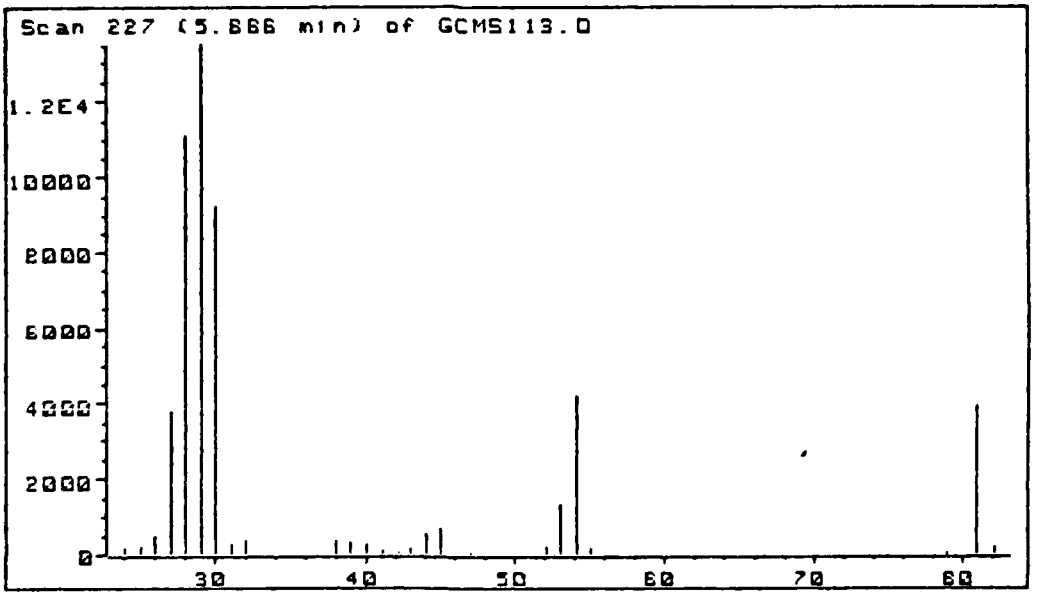

Figure 90. Typical Mass Spectrum of Chromatographic Peak at ca 5.7 Minutes, HMX, 400°C

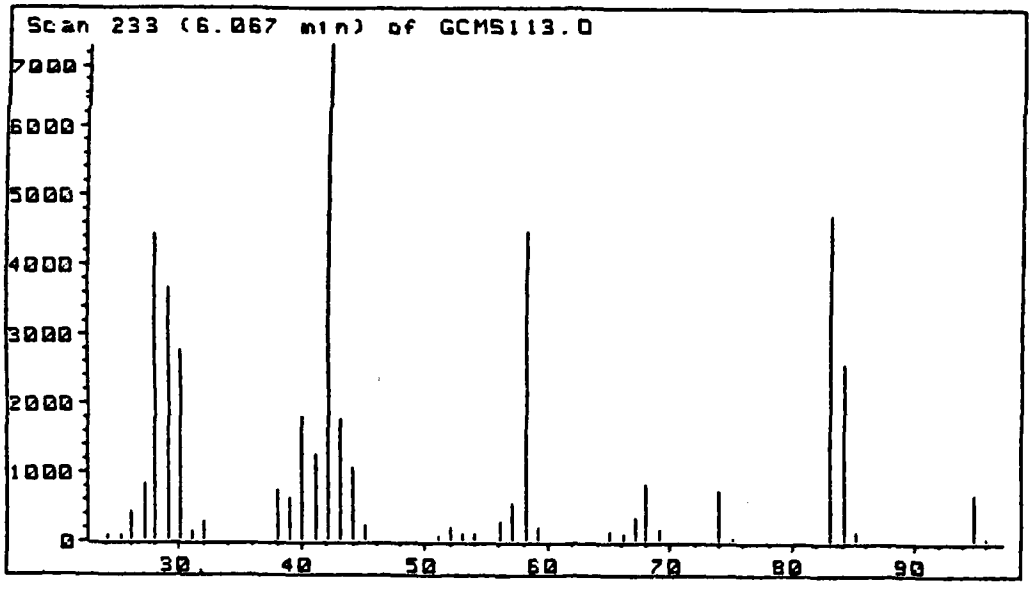

Figure 91. Typical Mass Spectrum of Chromatographic Peak at ca 6.1 Minutes, HMX, 400°C

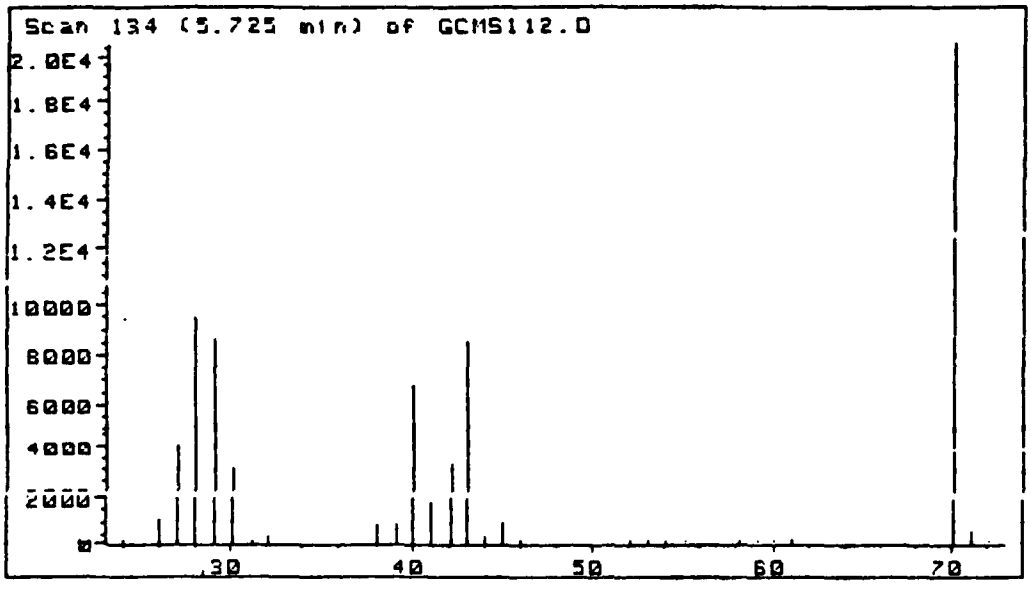

Figure 92. Typical Mass Spectrum of Chromatographic Peak at ca 5.7 Minutes, HMX, 600°C

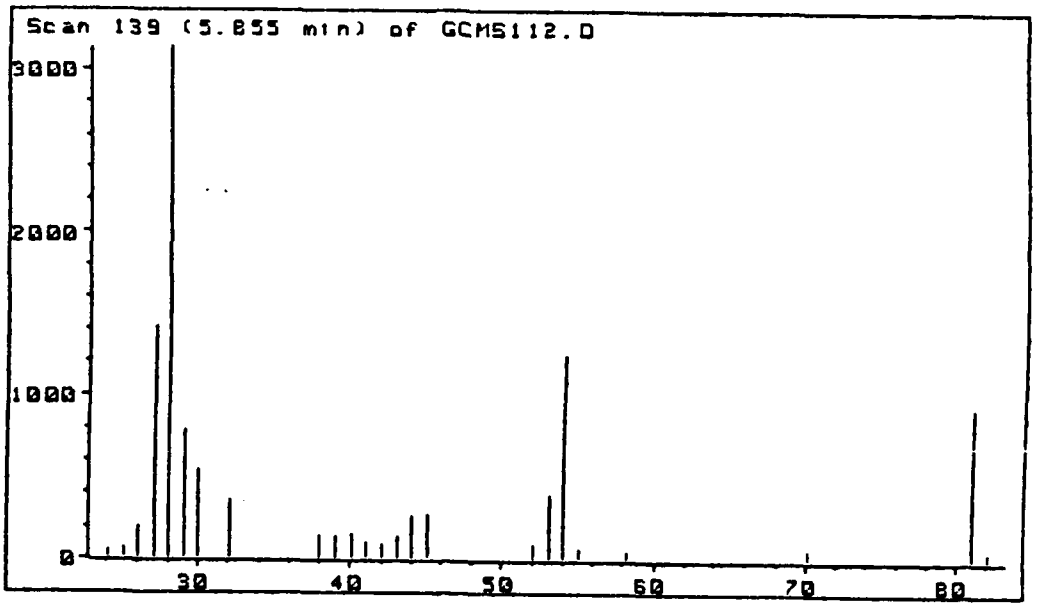

Figure 93. Typical Mass Spectrum of Chromatographic Peak at ca 5.9 Minutes, HMX, 600°C

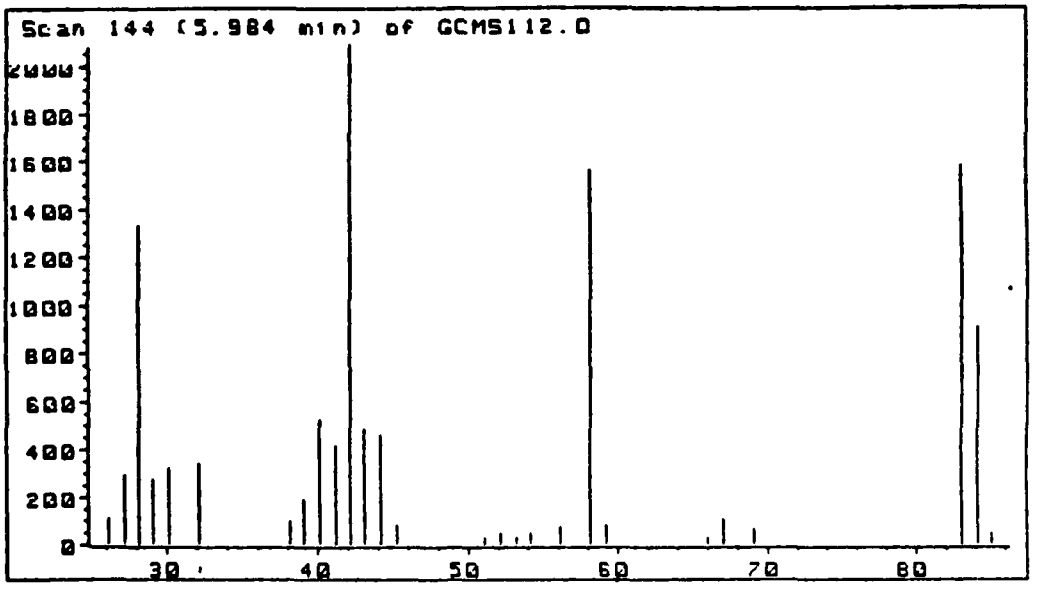

Figure 94. Typical Mass Spectrum of Chromatographic Peak at ca 6.0 Minutes, HMX, 600°C

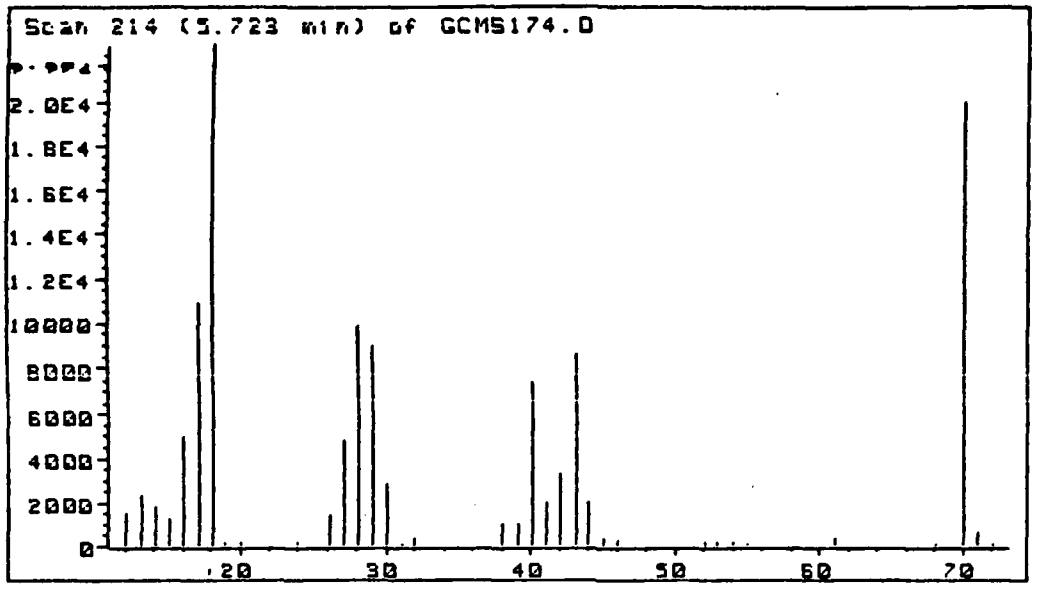

Figure 95. Typical Mass Spectrum of Chromatographic Peak at ca 5.7 Minutes, HMX, 800°C

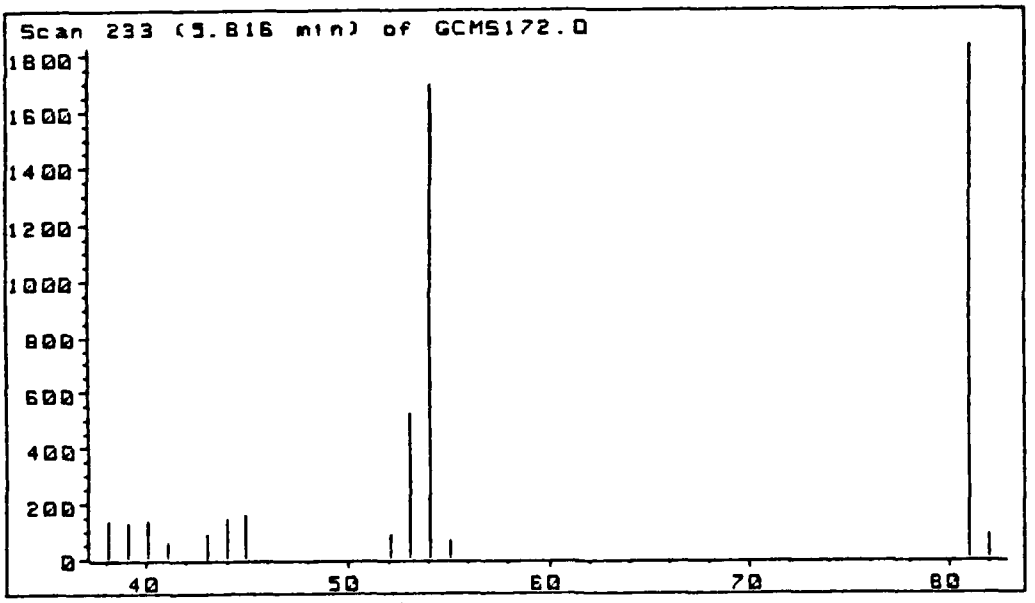

Figure 96. Typical Mass Spectrum of Chromatographic Peak at ca 5.8 Minutes, HMX, 800°C

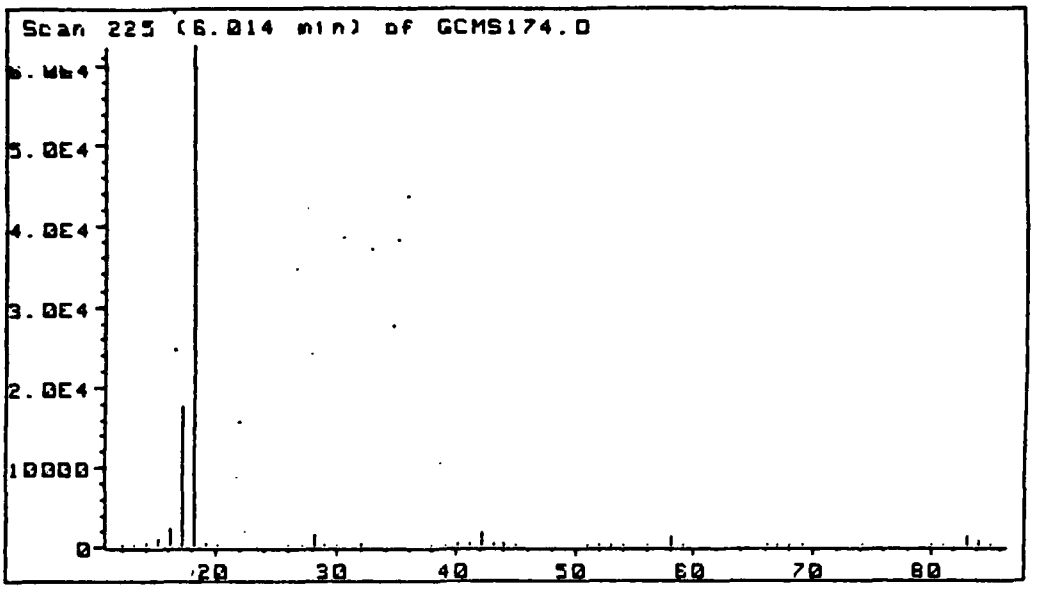

Figure 97. Typical Mass Spectrum of Chromatographic Peak at ca 6.0 Minutes, HMX, 800°C

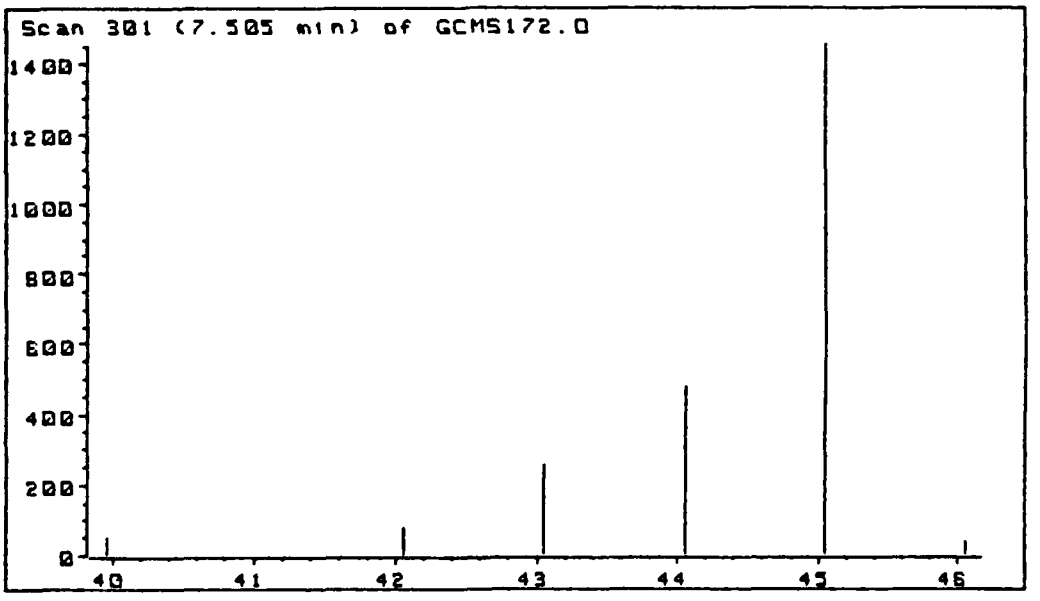

Figure 98. Typical Mass Spectrum of Chromatographic Peak at ca 7.5 Minutes, HMX, 800°C

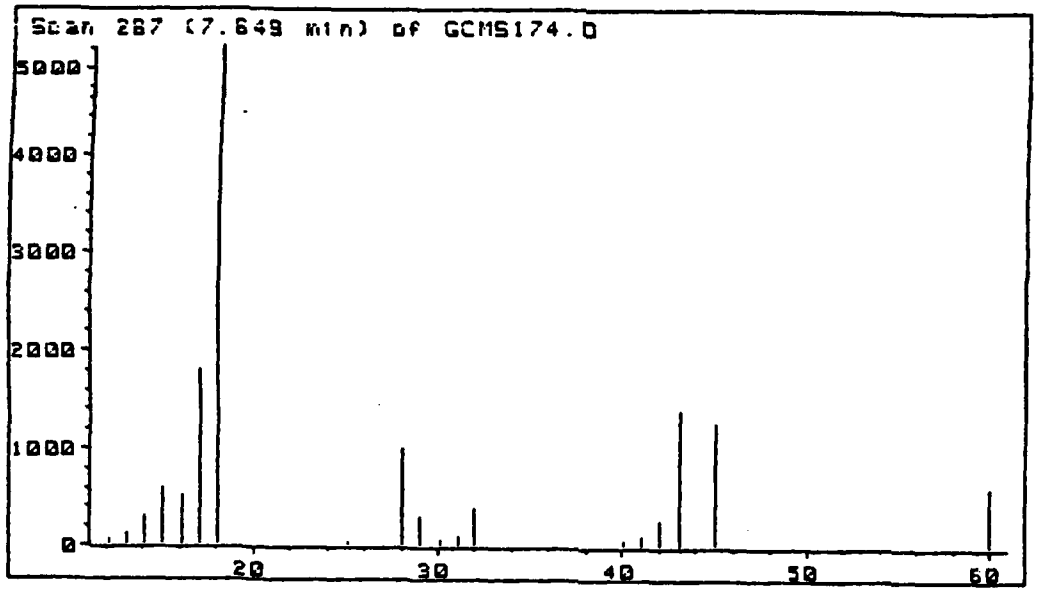

Figure 99. Typical Mass Spectrum of Chromatographic Peak at ca 7.6 Minutes, HMX, 800°C

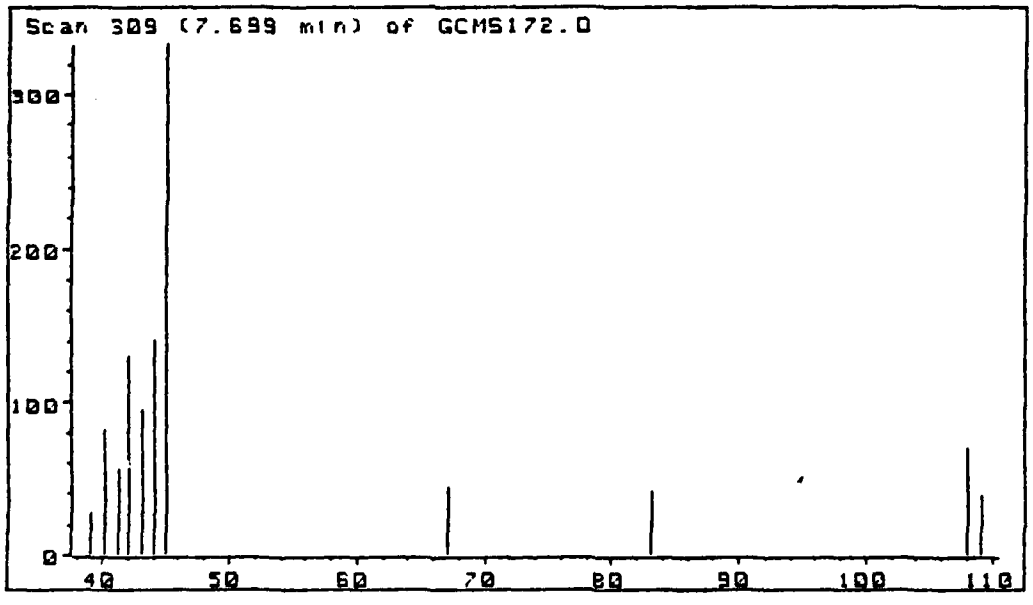

Figure 100. Typical Mass Spectrum of Chromatographic Peak at ca 7.7 Minutes, HMX, 800°C

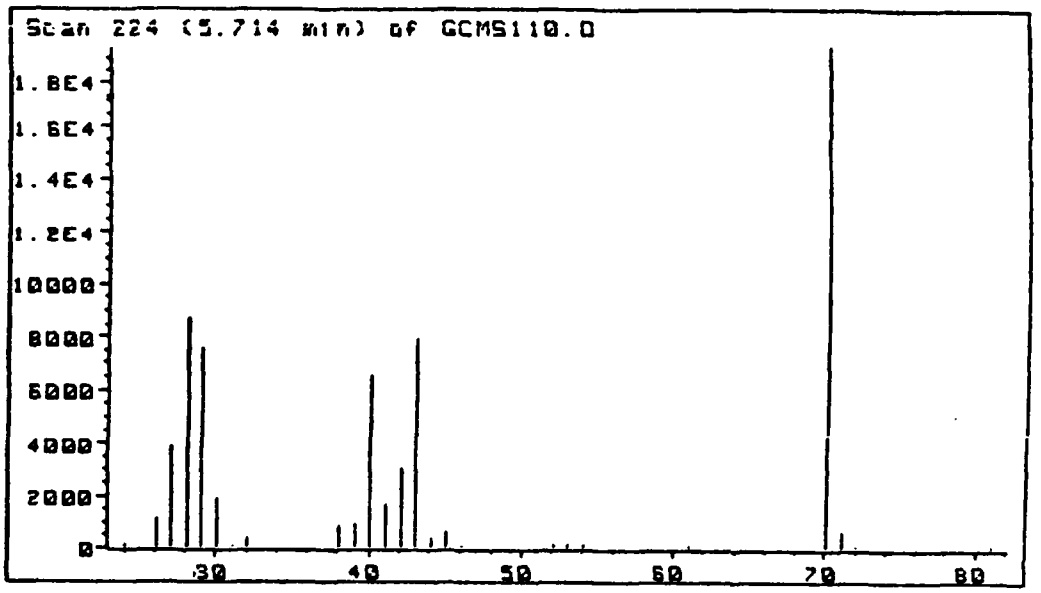

Figure 101. Typical Mass Spectrum of Chromatographic Peak at ca 5.7 Minutes, RDX, 600°C

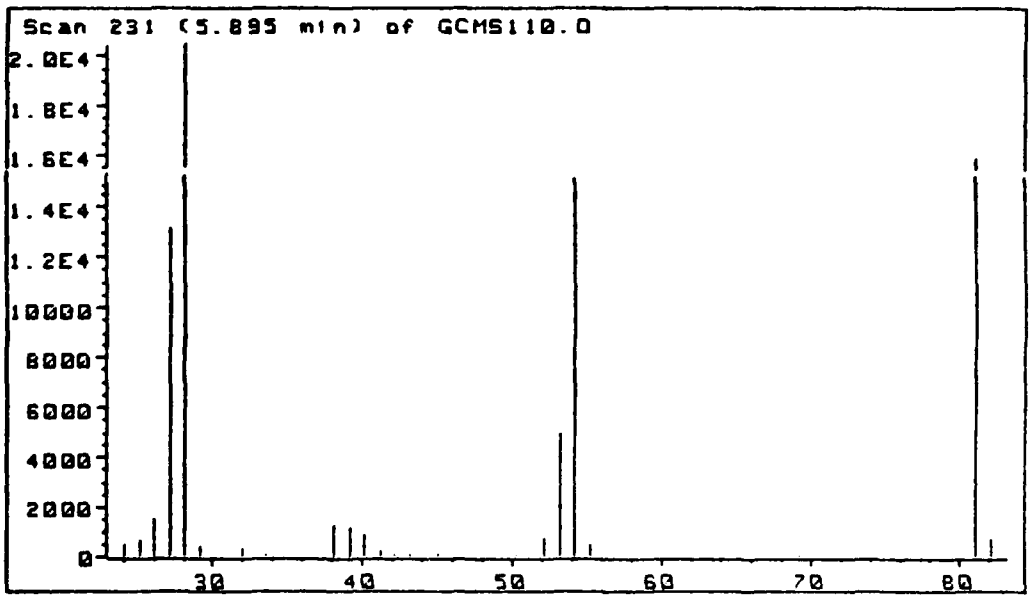

Figure 102. Typical Mass Spectrum of Chromatographic Peak at ca 5.9 Minutes, RDX, 600°C

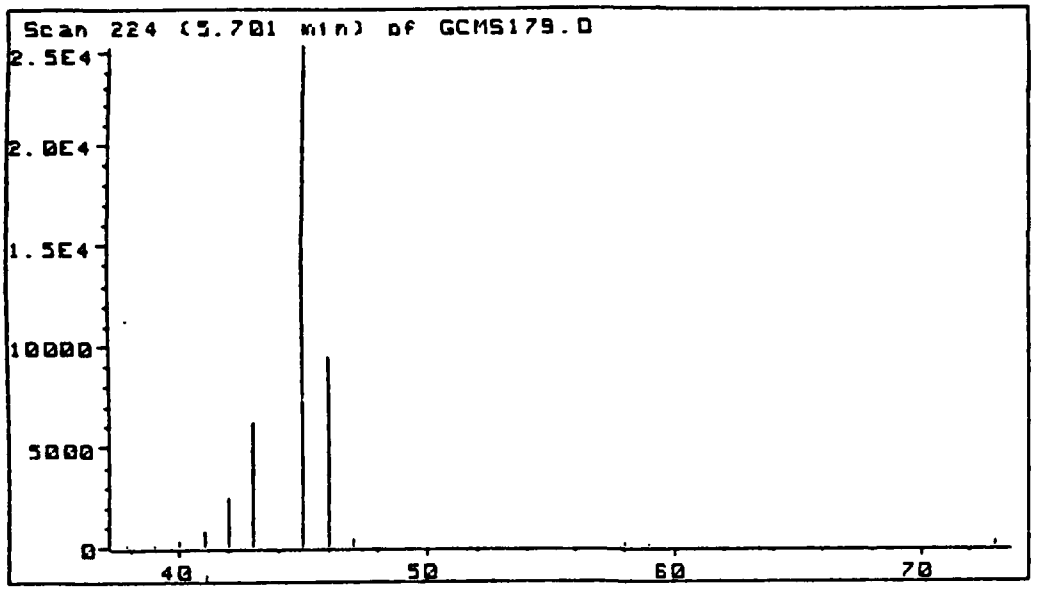

Figure 103. Typical Mass Spectrum of Chromatographic Peak at ca 5.7 Minutes, PEG, 325°C

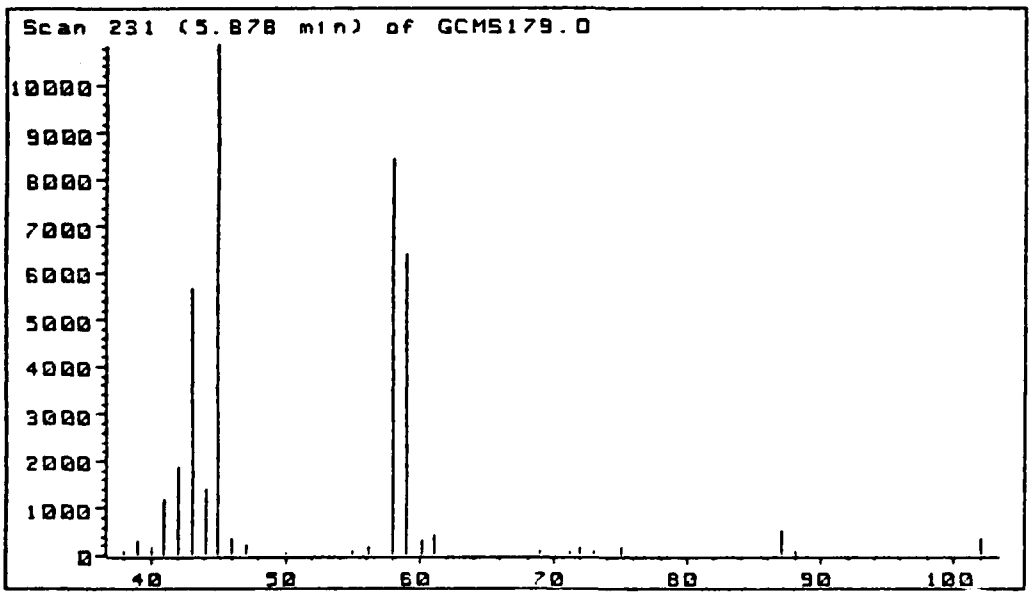

Figure 104. Typical Mass Spectrum of Chromatographic Peak at ca 5.9 Minutes, PEG, 325°C

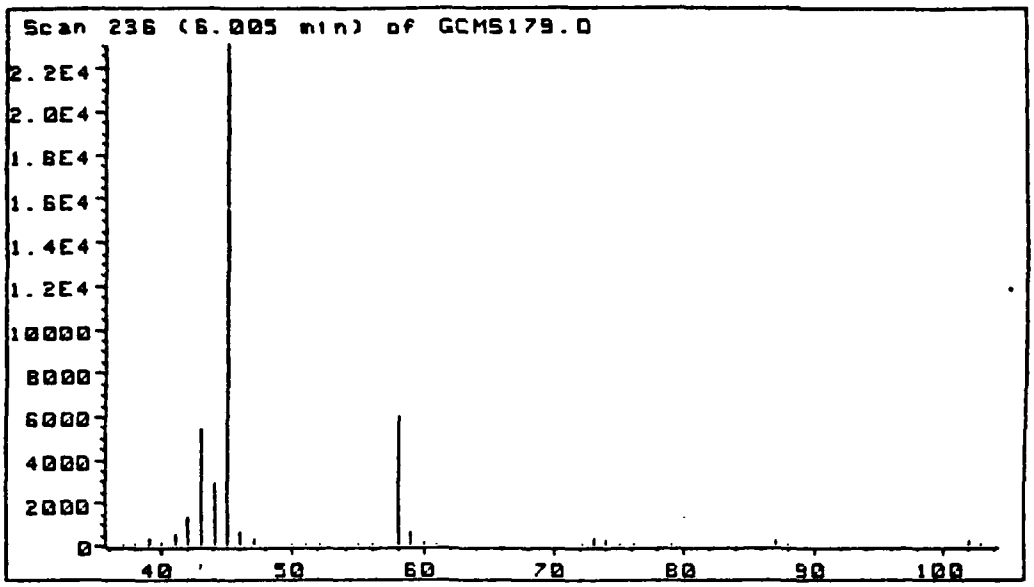

Figure 105. Typical Mass Spectrum of Chromatographic Peak at ca 6.0 Minutes, PEG, 325°C

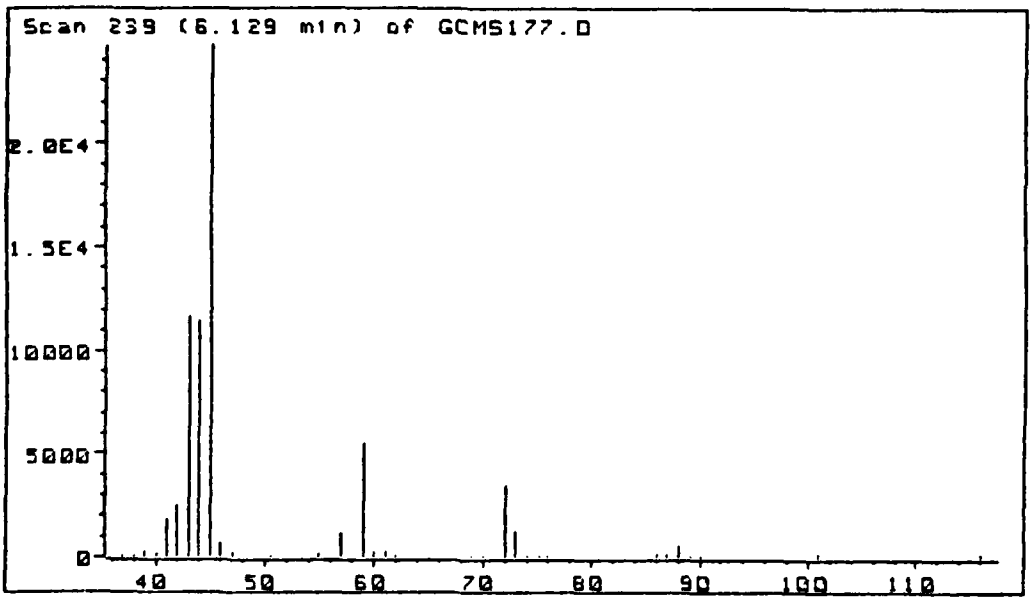

Figure 106. Typical Mass Spectrum of Chromatographic Peak at ca 6.1 Minutes, PEG, 325°C

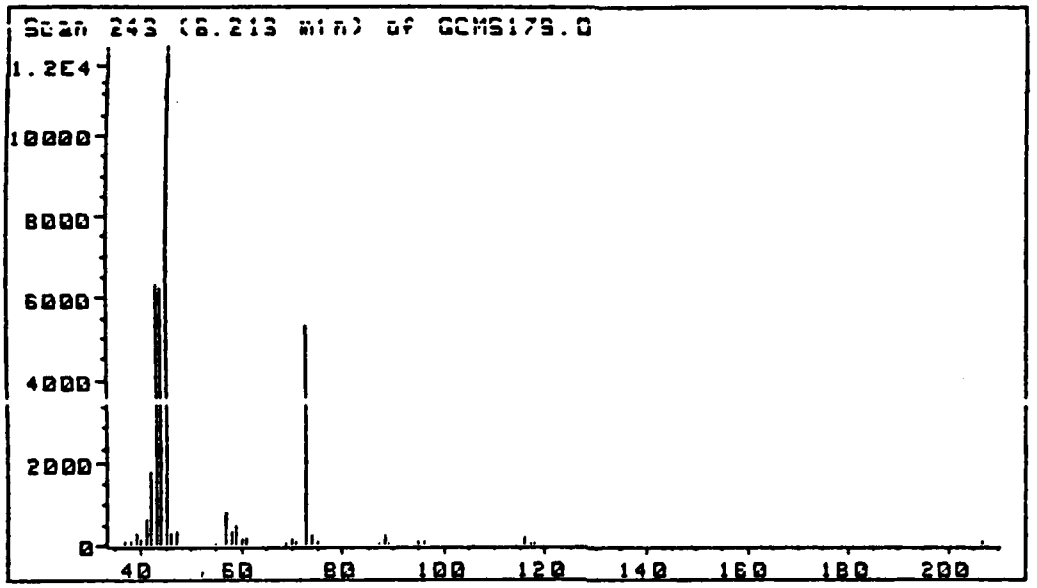

Figure 107. Typical Mass Spectrum of Chromatographic Peak at ca 6.2 Minutes, PEG, 325°C

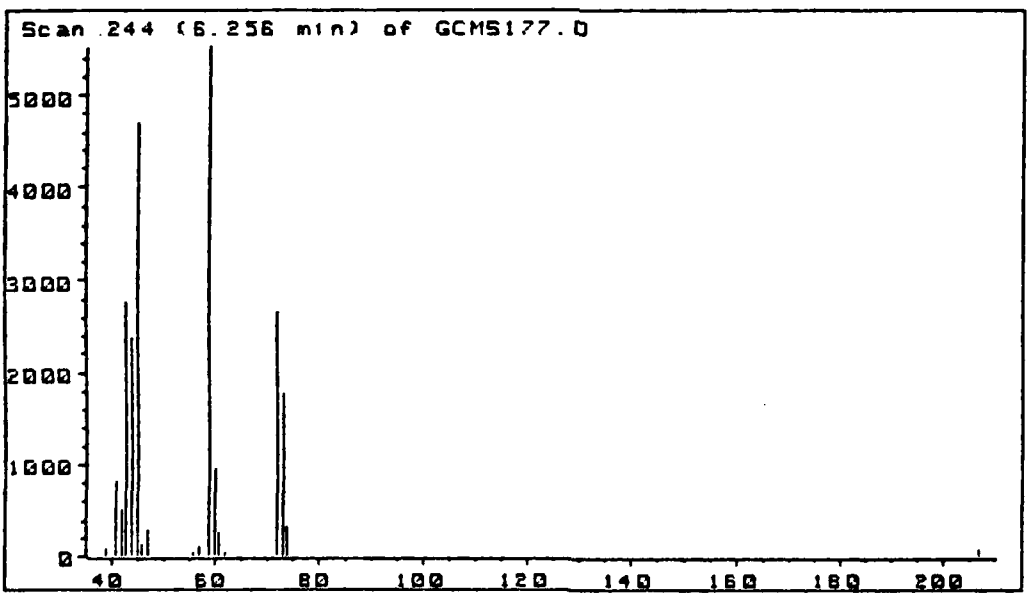

Figure 108. Typical Mass Spectrum of Chromatographic Peak at ca 6.3 Minutes, PEG, 325°C

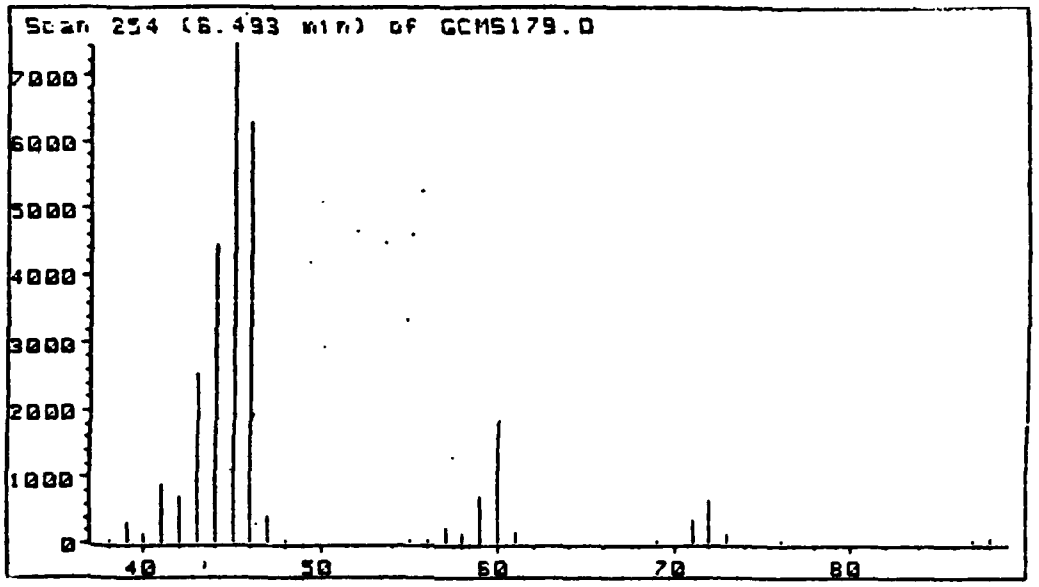

Figure 109. Typical Mass Spectrum of Chromatographic Peak at ca 6.5 Minutes, PEG, 325°C

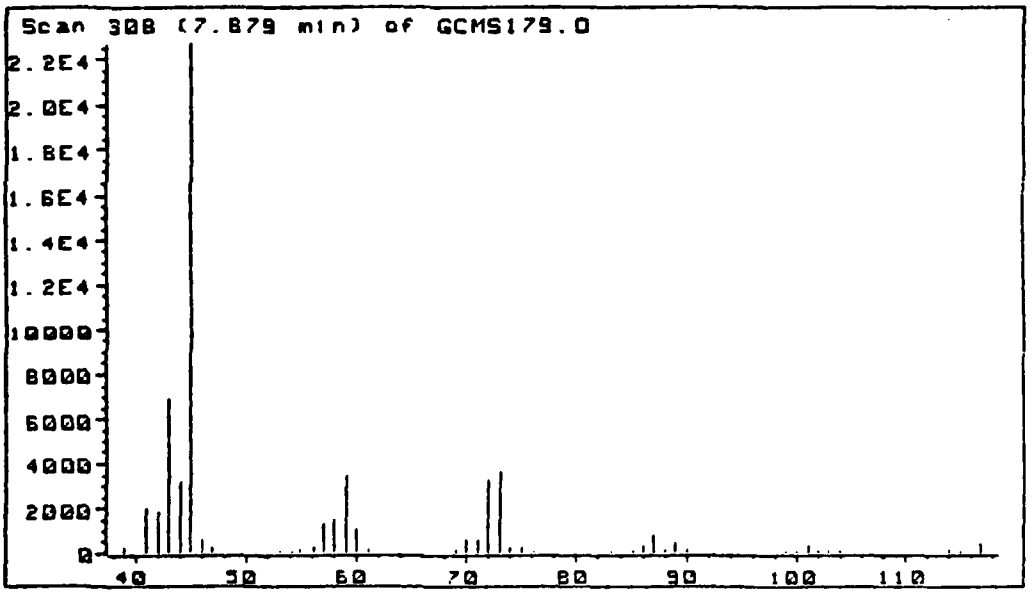

Figure 110. Typical Mass Spectrum of Chromatographic Peak at ca 7.9 Minutes, PEG, 325°C

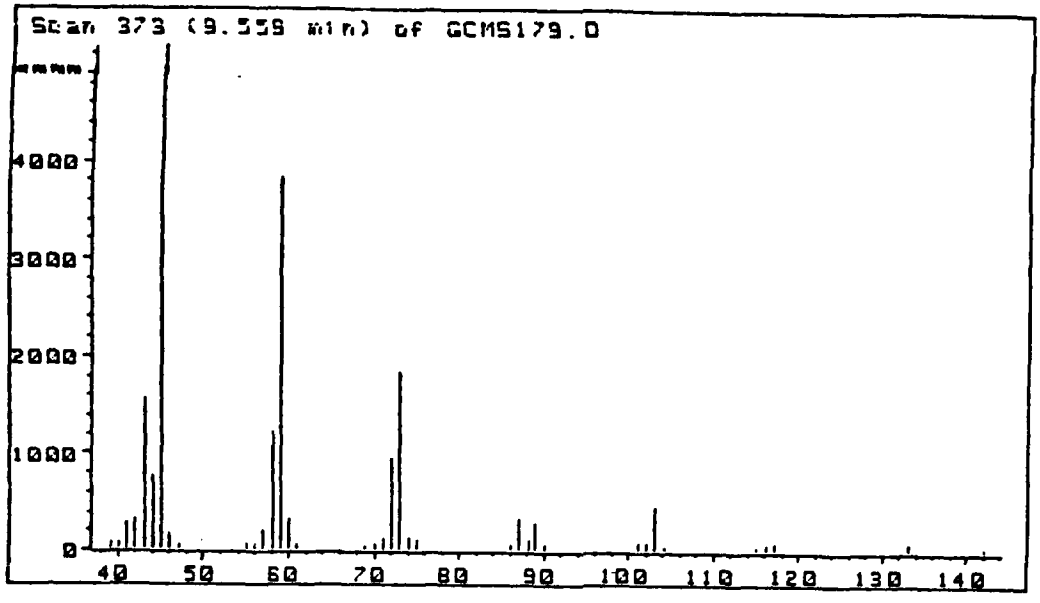

Figure 111. Typical Mass Spectrum of Chromatographic Peak at ca 9.6 Minutes, PEG, 325°C

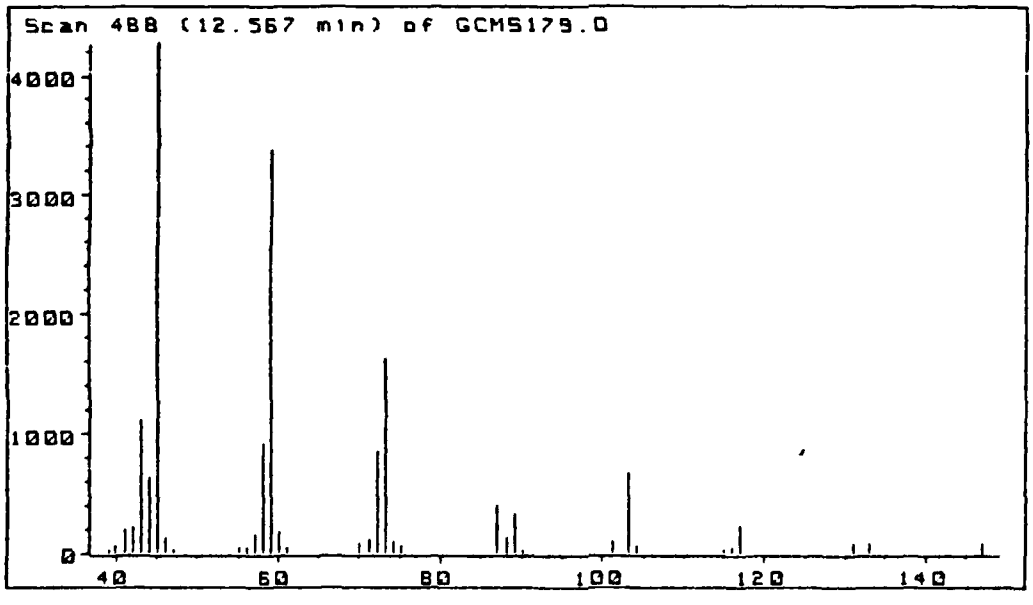

Figure 112. Typical Mass Spectrum of Chromatographic Peak at ca 12.6 Minutes, PEG, 325°C

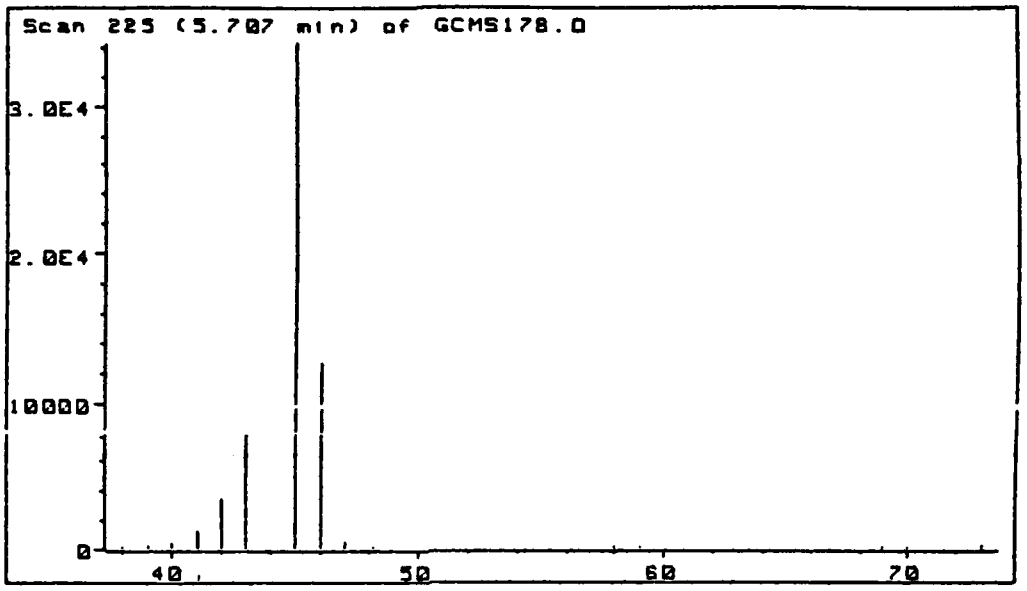

Figure 113. Typical Mass Spectrum of Chromatographic Peak at ca 5.7 Minutes, PEG, 800°C

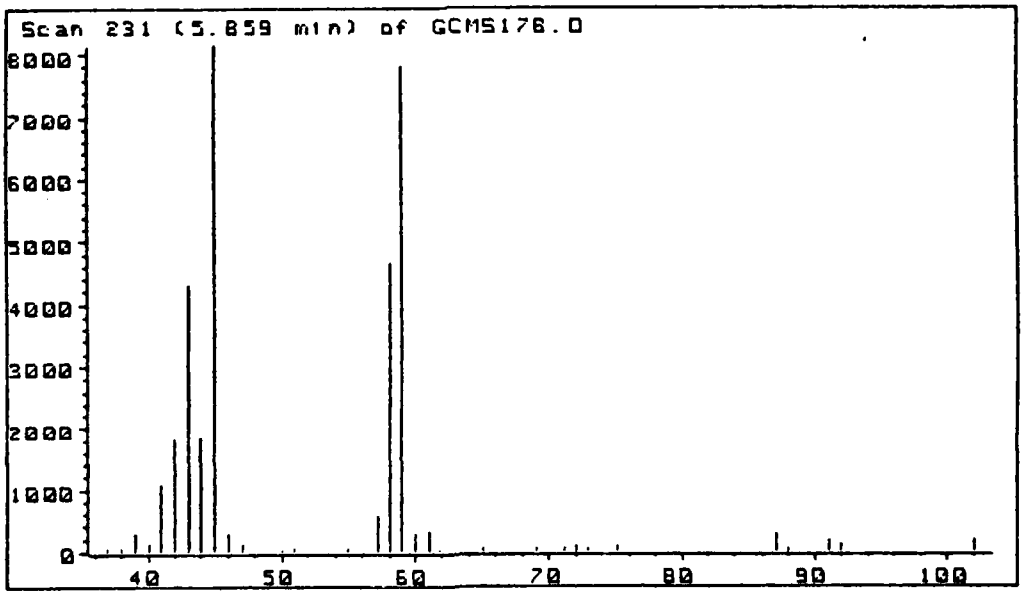

Figure 114. Typical Mass Spectrum of Chromatographic Peak at ca 5.86 Minutes, PEG, 800°C

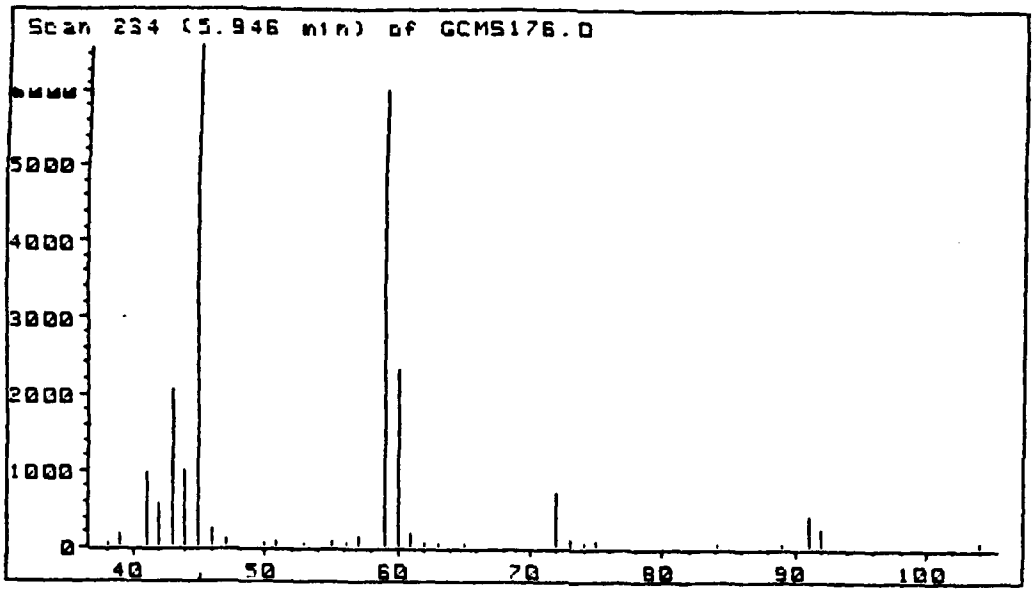

Figure 115. Typical Mass Spectrum of Chromatographic Peak at ca 5.95 Minutes, PEG, 800°C

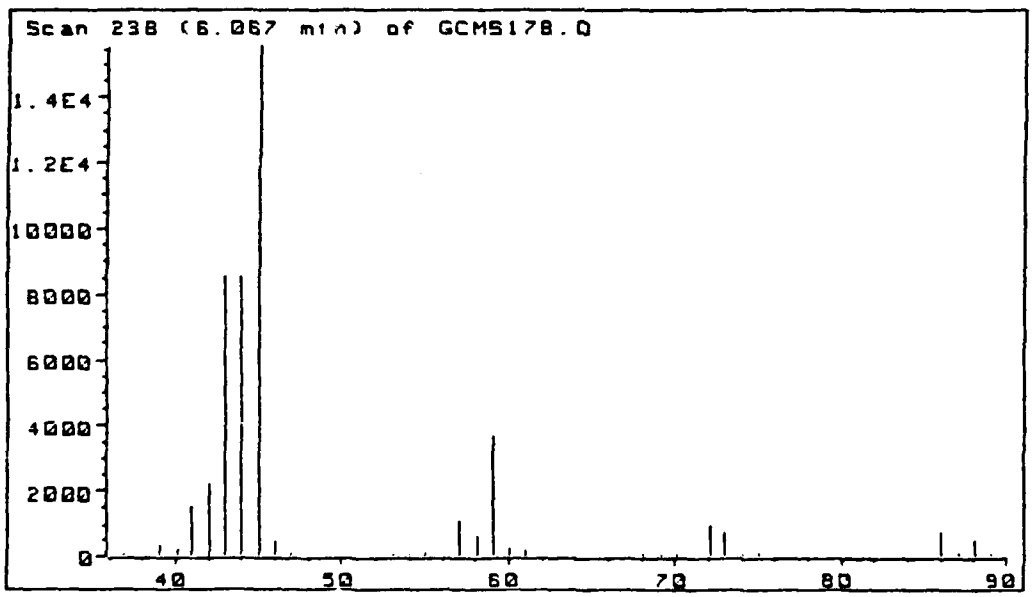

Figure 116. Typical Mass Spectrum of Chromatographic Peak at ca 6.0 Minutes, PEG, 800°C

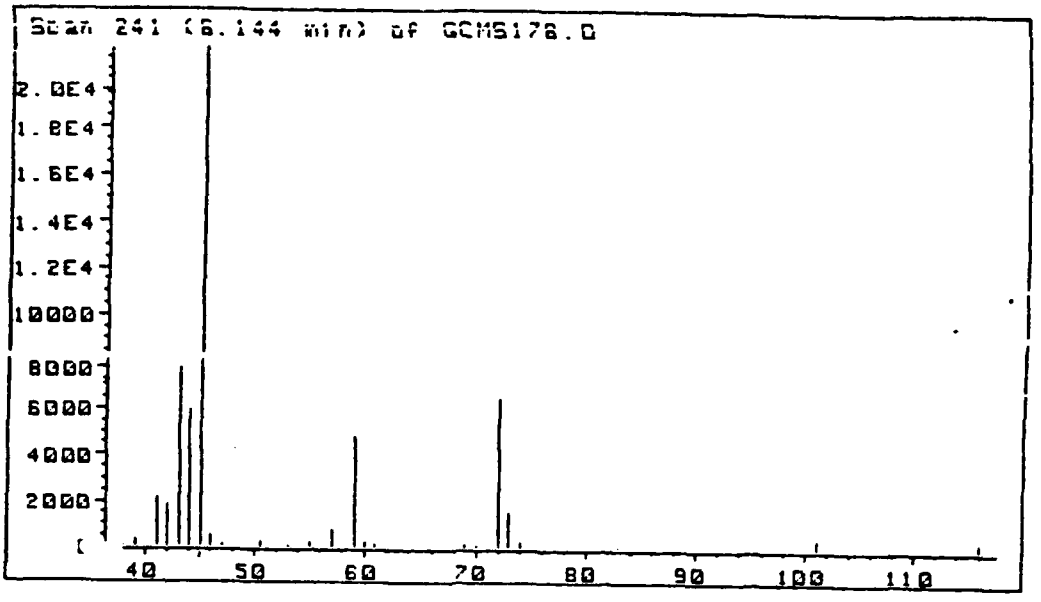

Figure 117. Typical Mass Spectrum of Chromatographic Peak at ca 6.1 Minutes, PEG, 800°C

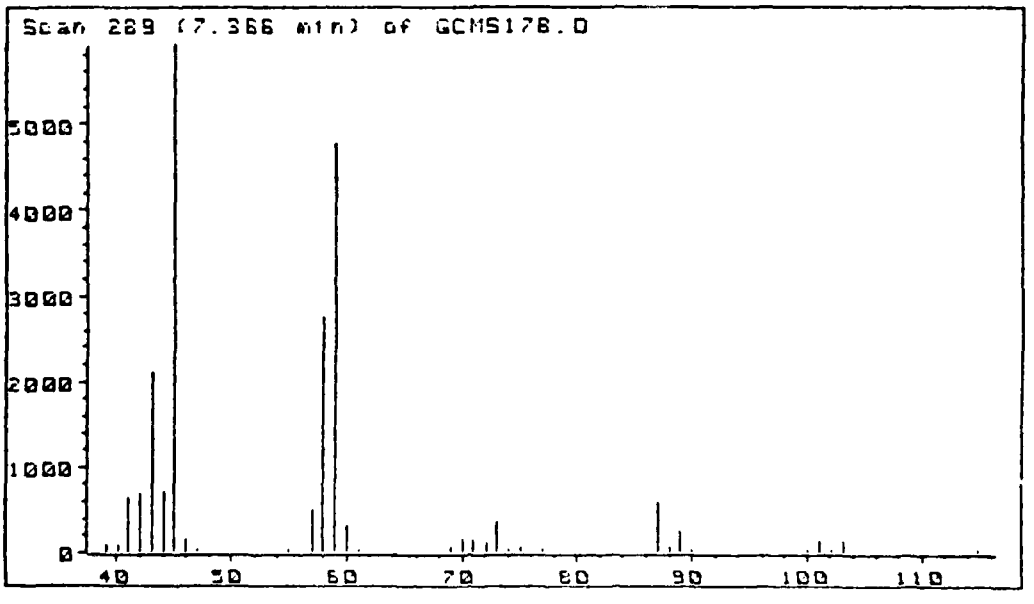

Figure 118. Typical Mass Spectrum of Chromatographic Peak at ca 7.4 Minutes, PEG, 800°C

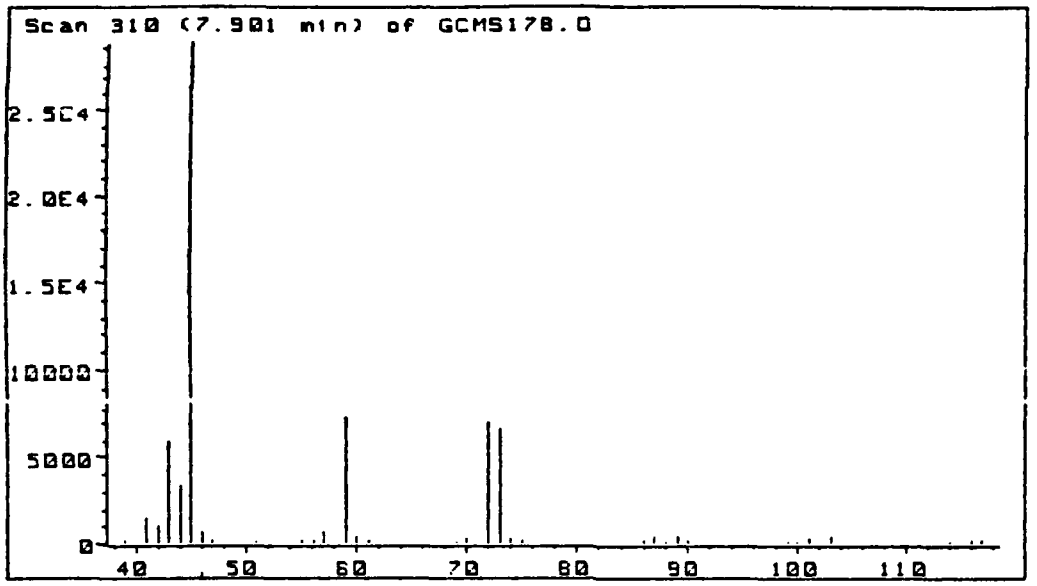

Figure 119. Typical Mass Spectrum of Chromatographic Peak at ca 7.9 Minutes, PEG, 800°C

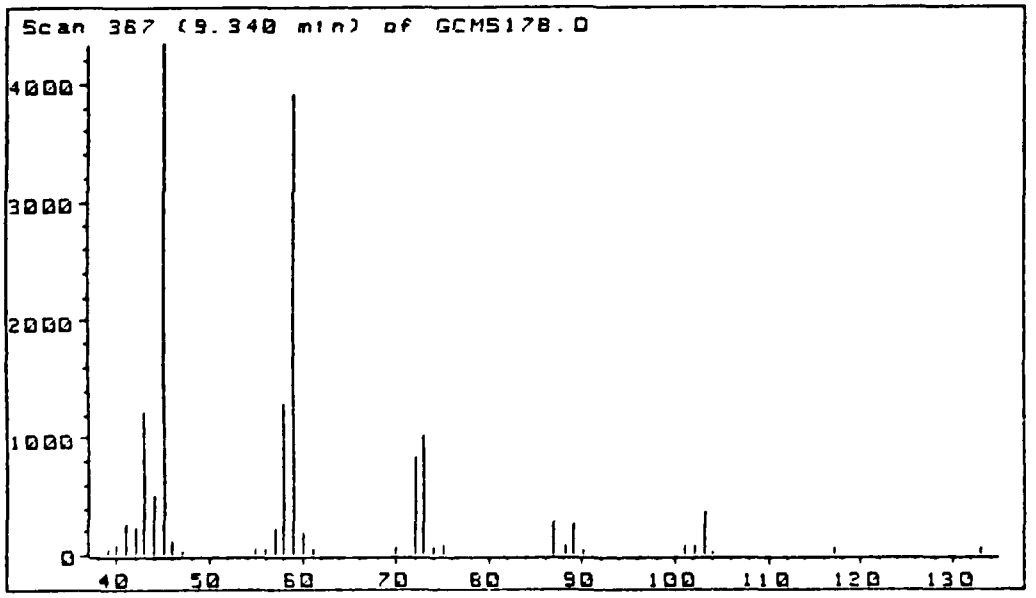

Figure 120. Typical Mass Spectrum of Chromatographic Peak at ca 9.3 Minutes, PEG, 800°C

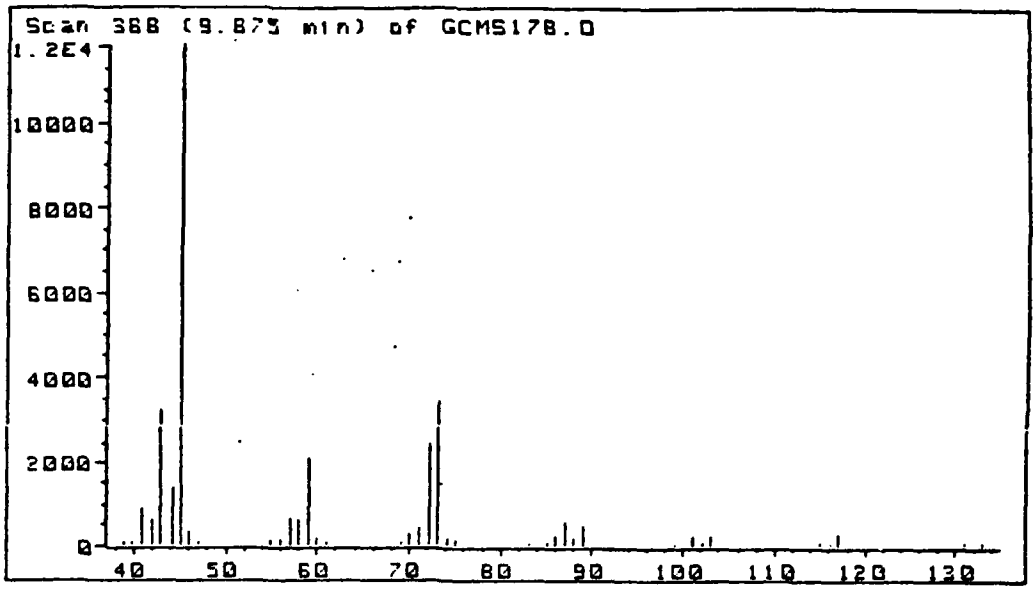

Figure 121. Typical Mass Spectrum of Chromatographic Peak at ca 9.9 Minutes, PEG, 800°C

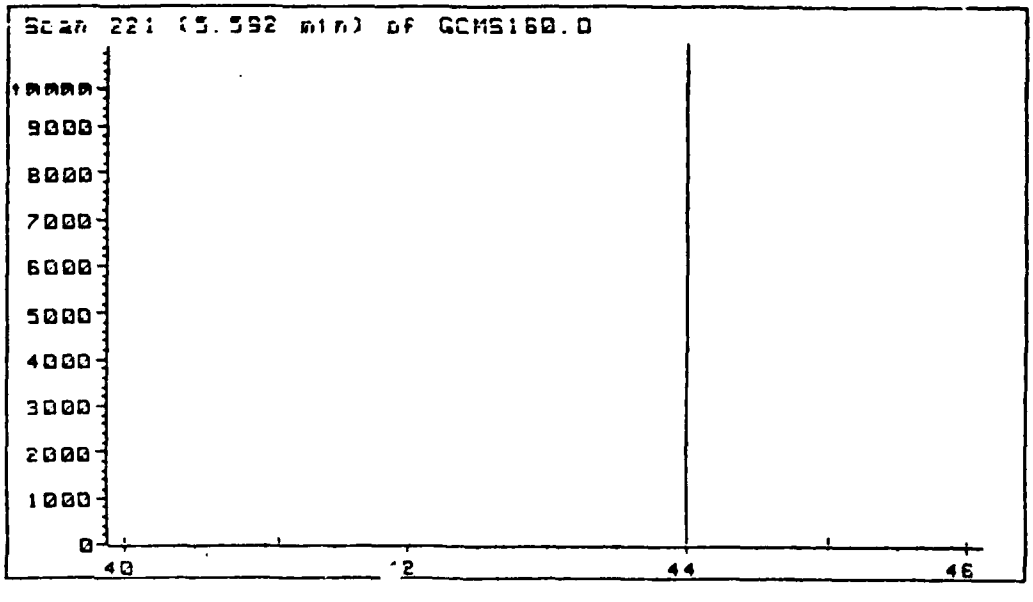

Figure 122. Typical Mass Spectrum of Chromatographic Peak at ca 5.6 Minutes, TAGN, 325°C

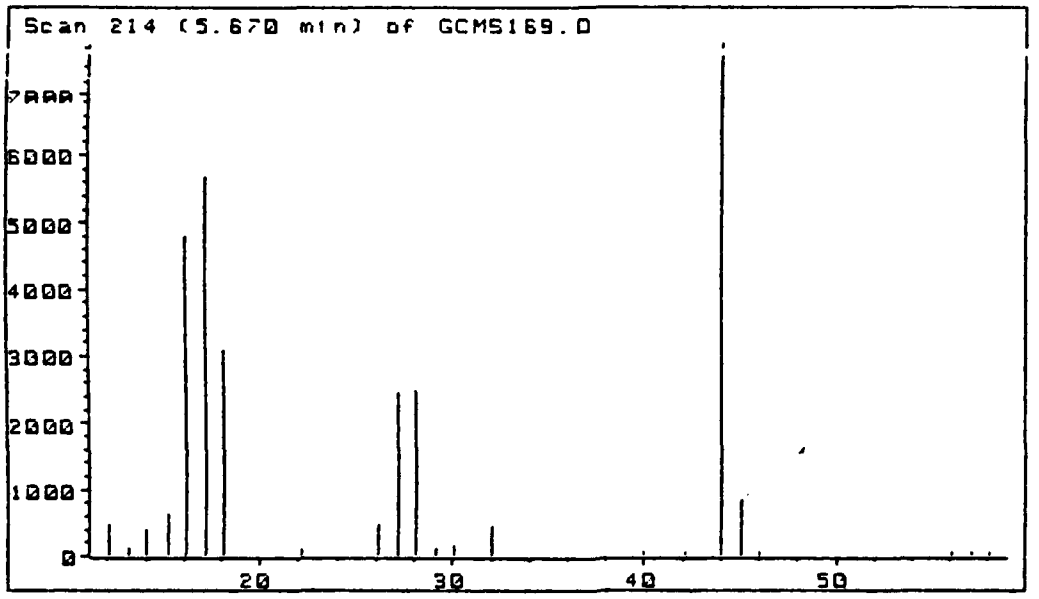

Figure 123. Typical Mass Spectrum of Chromatographic Peak at ca 5.7 Minutes, TAGN, 325°C

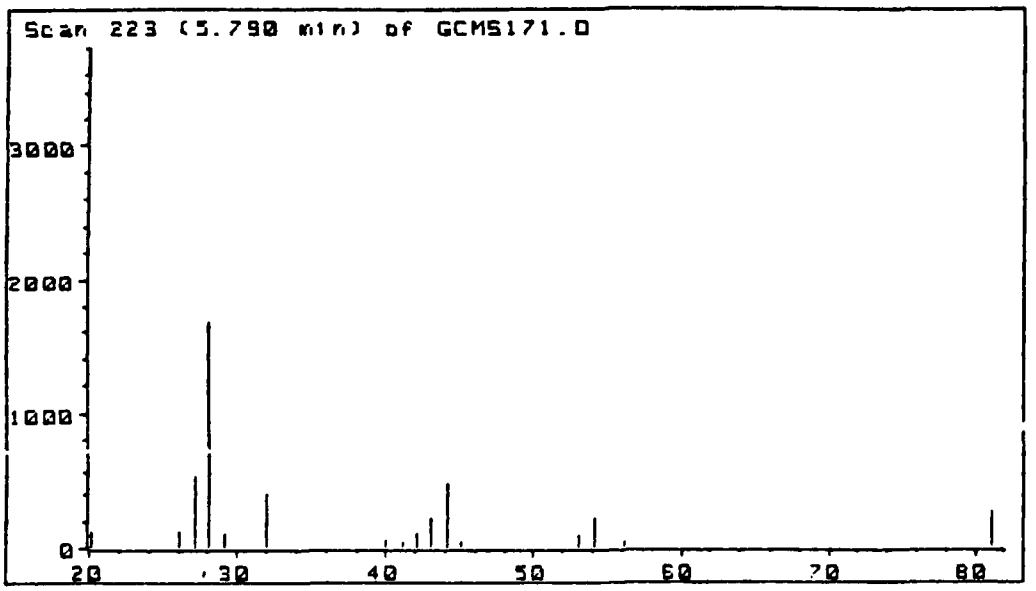

Figure 124. Typical Mass Spectrum of Chromatographic Peak at ca 5.8 Minutes, TAGN, 325°C

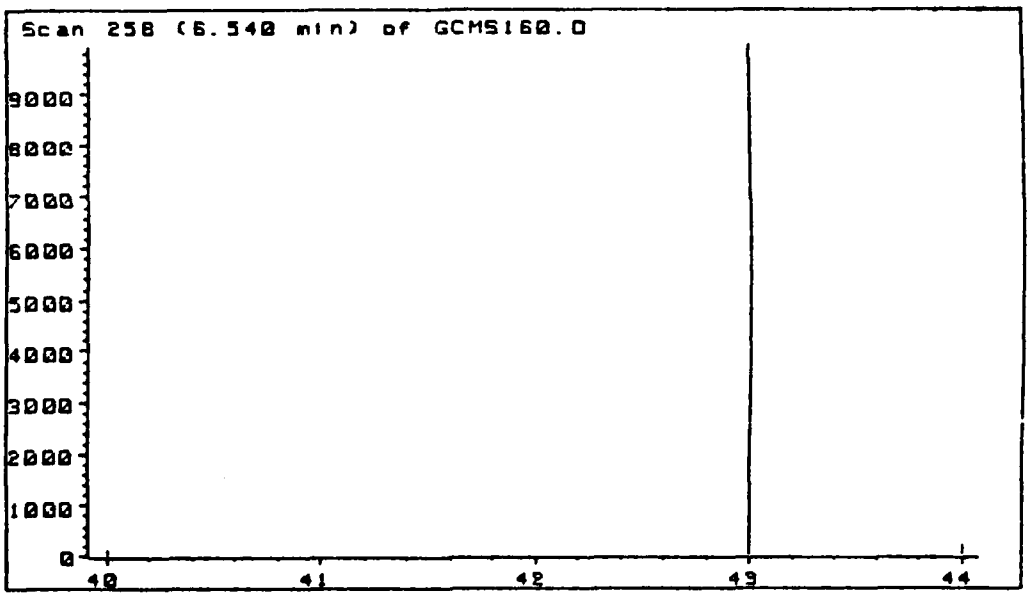

Figure 125. Typical Mass Spectrum of Chromatographic Peak at ca 6.5 Minutes, TAGN, 325°C

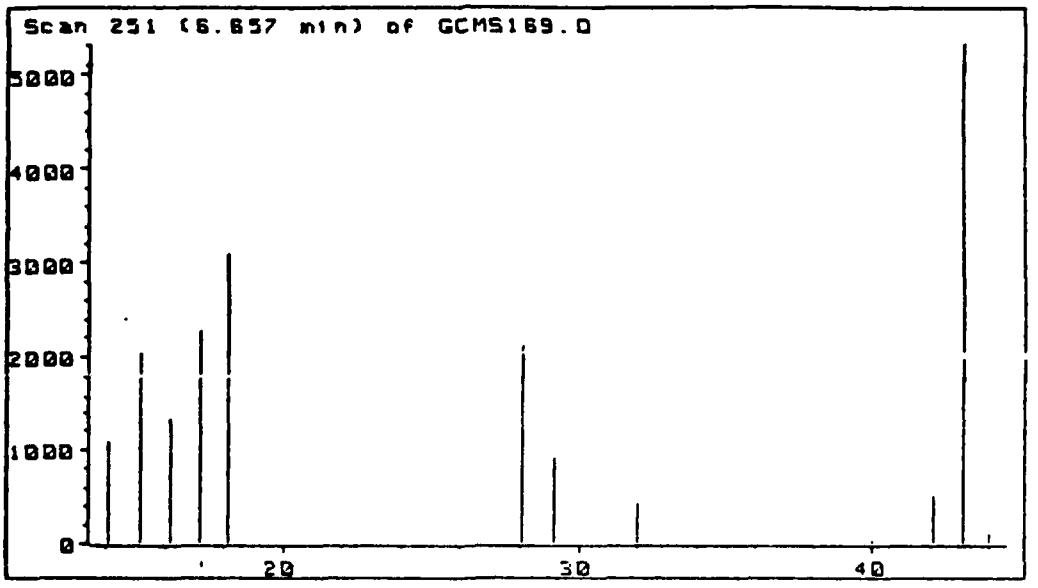

Figure 126. Typical Mass Spectrum of Chromatographic Peak at ca 6.7 Minutes, TAGN, 325°C

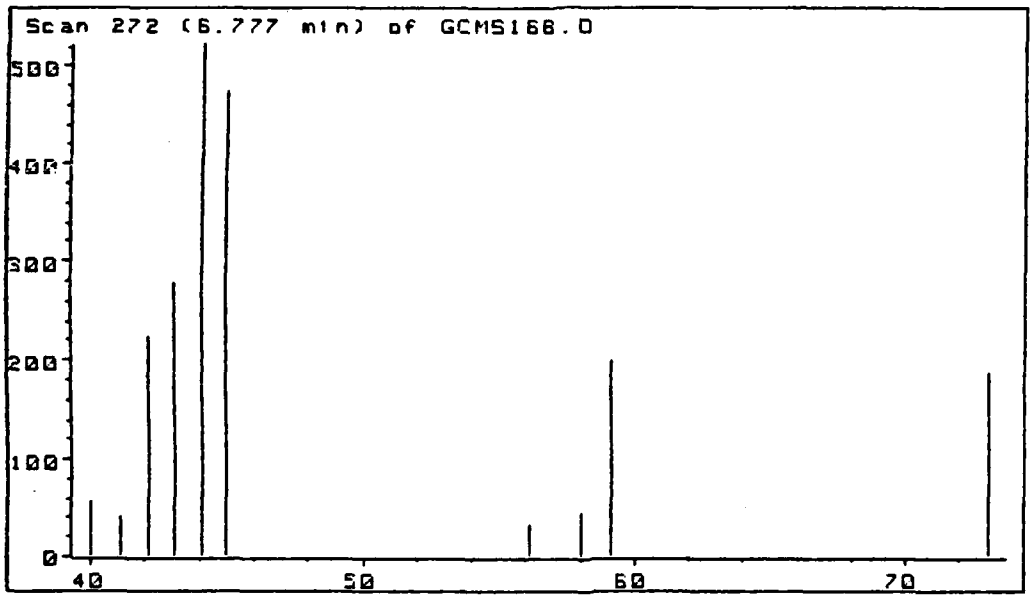

Figure 127. Typical Mass Spectrum of Chromatographic Peak at ca 6.8 Minutes, TAGN, 325°C

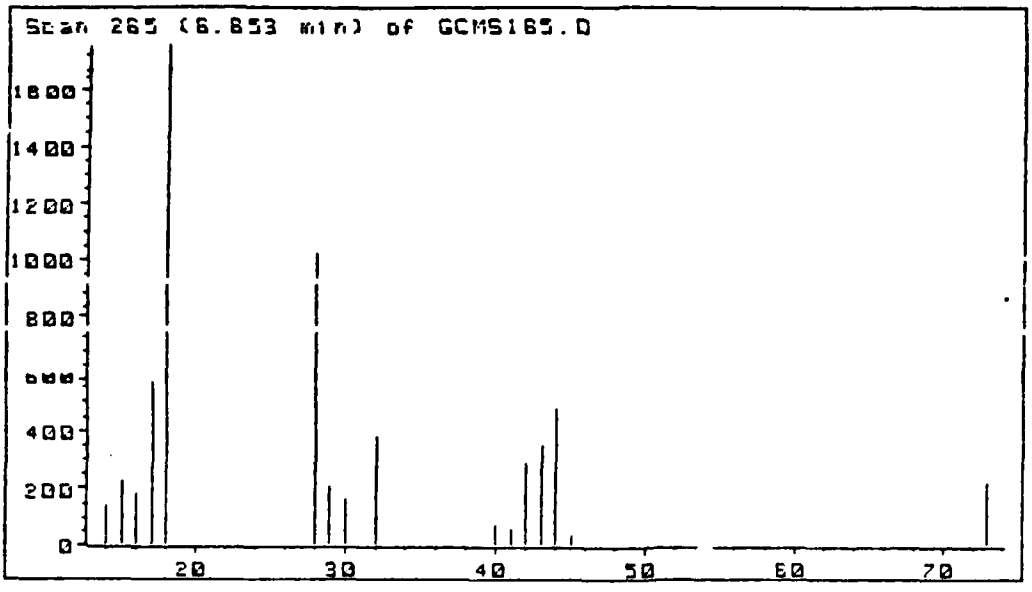

Figure 128. Typical Mass Spectrum of Chromatographic Peak at ca 6.85 Minutes, TAGN, 325°C

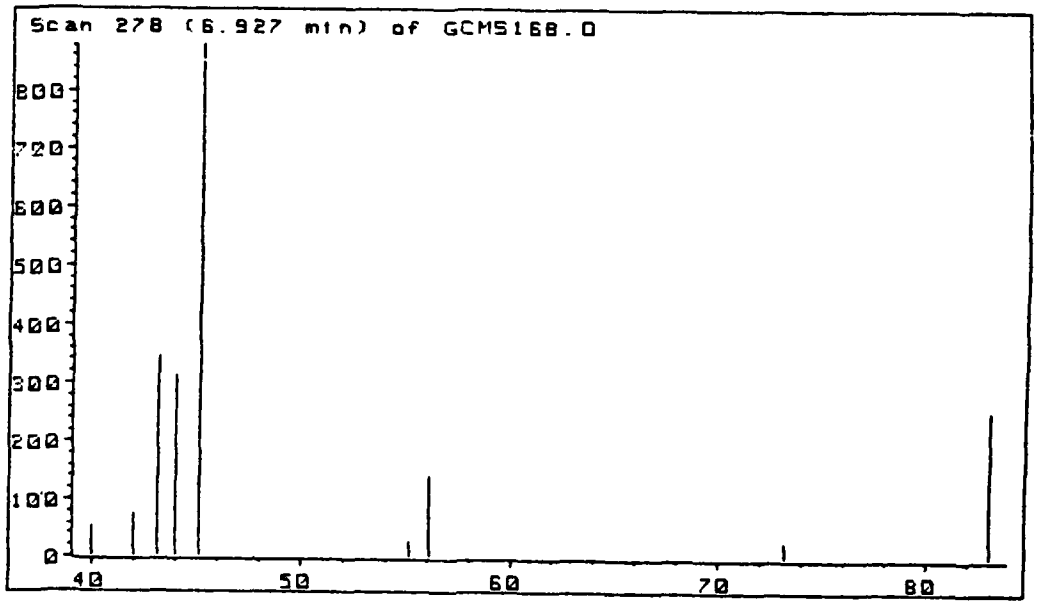

Figure 129. Typical Mass Spectrum of Chromatographic Peak at ca 6.93 Minutes, TAGN, 325°C

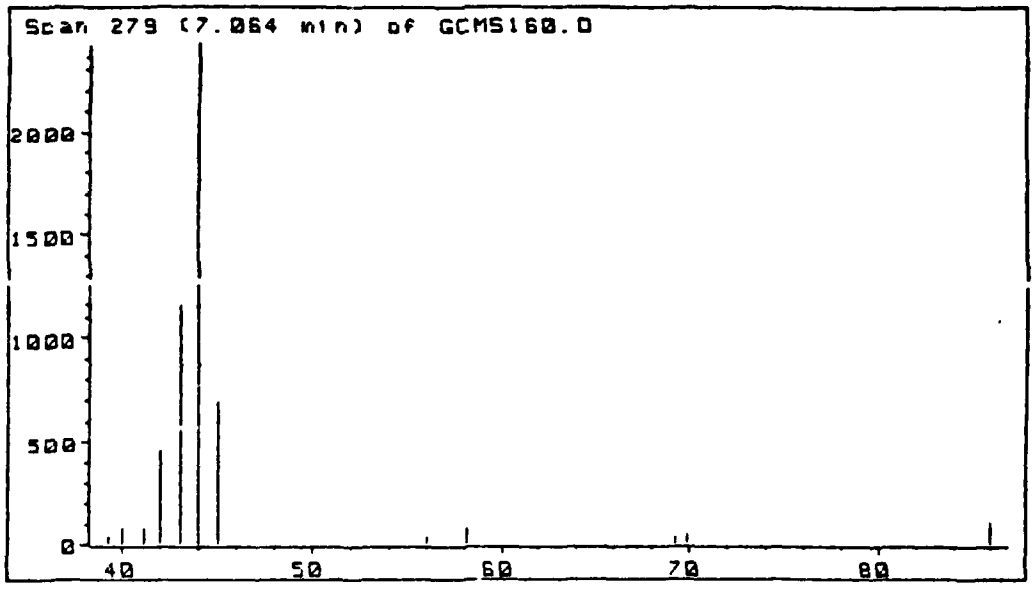

Figure 130. Typical Mass Spectrum of Chromatographic Peak at ca 7.1 Minutes, TAGN, 325°C

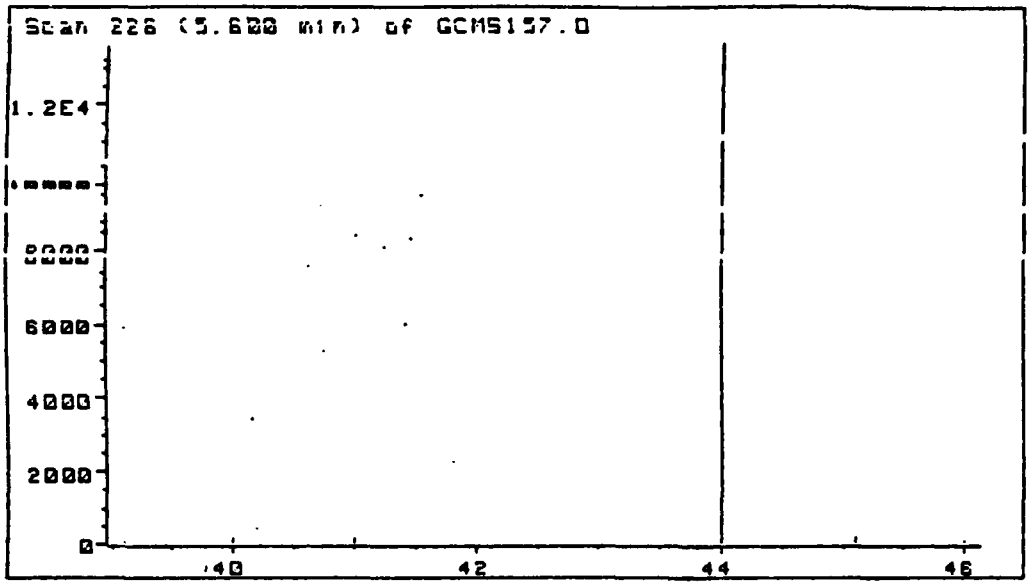

Figure 131. Typical Mass Spectrum of First Chromatographic Peak at ca 5.6 Minutes, TAGN, 800°C

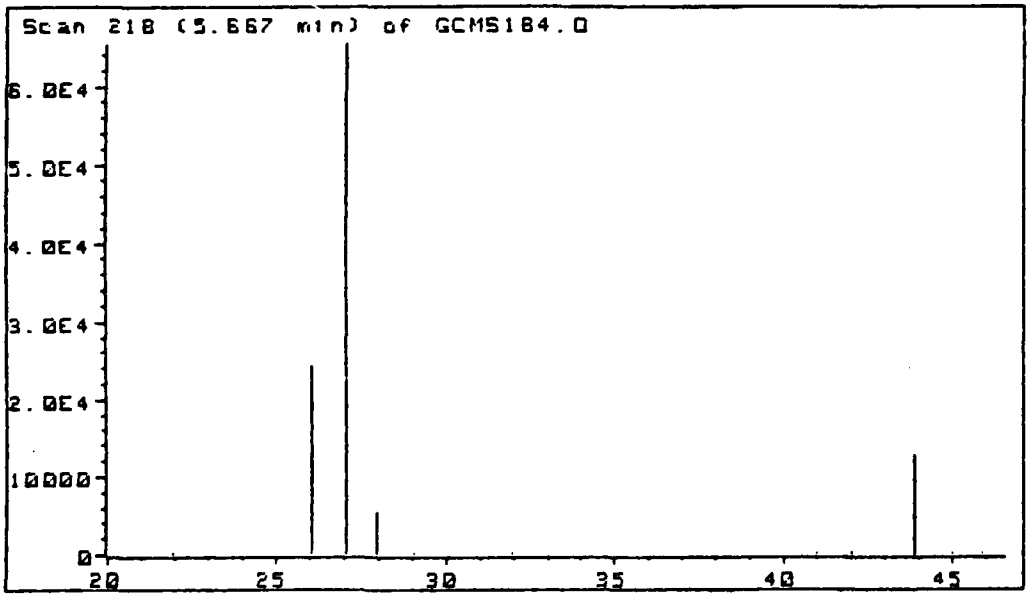

Figure 132. Typical Mass Spectrum of Second Chromatographic Peak at ca 5.7 Minutes, TAGN, 800°C

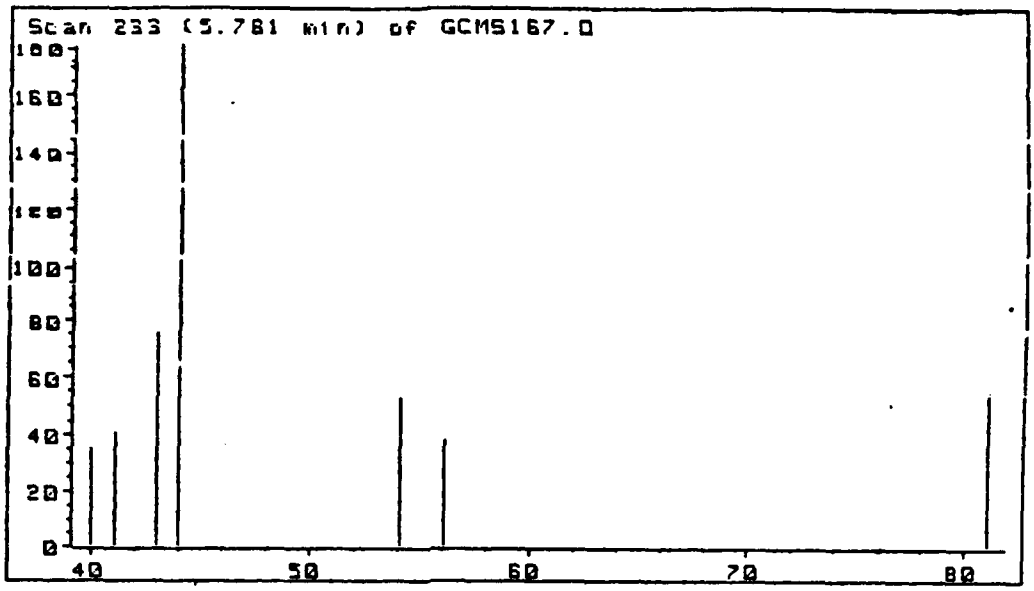

Figure 133. Typical Mass Spectrum of Chromatographic Peak at ca 5.8 Minutes, TAGN, 800°C

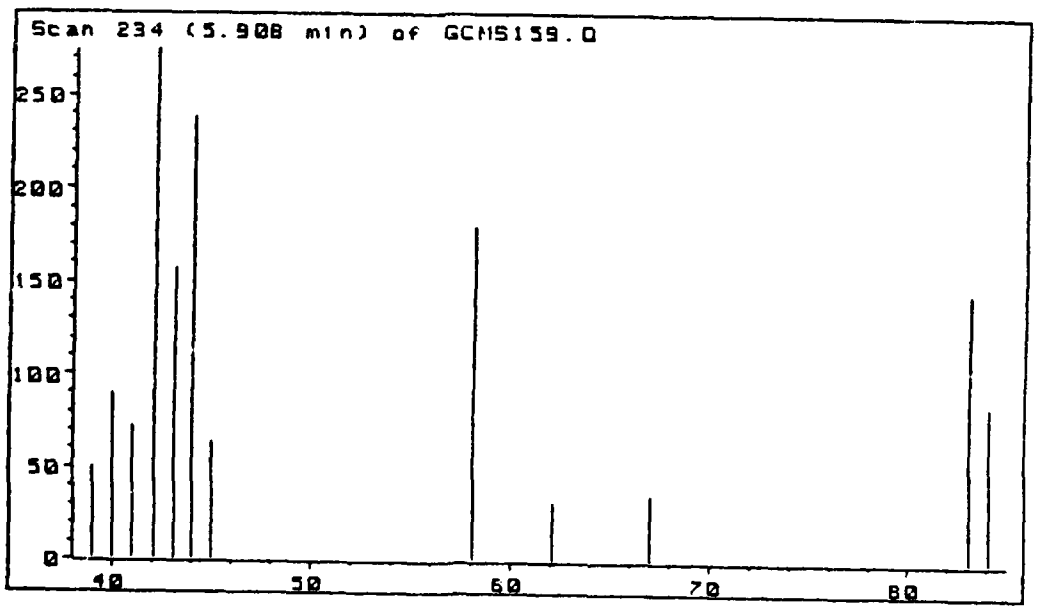

Figure 134. Typical Mass Spectrum of Chromatographic Peak at ca 5.9 Minutes, TAGN, 800°C

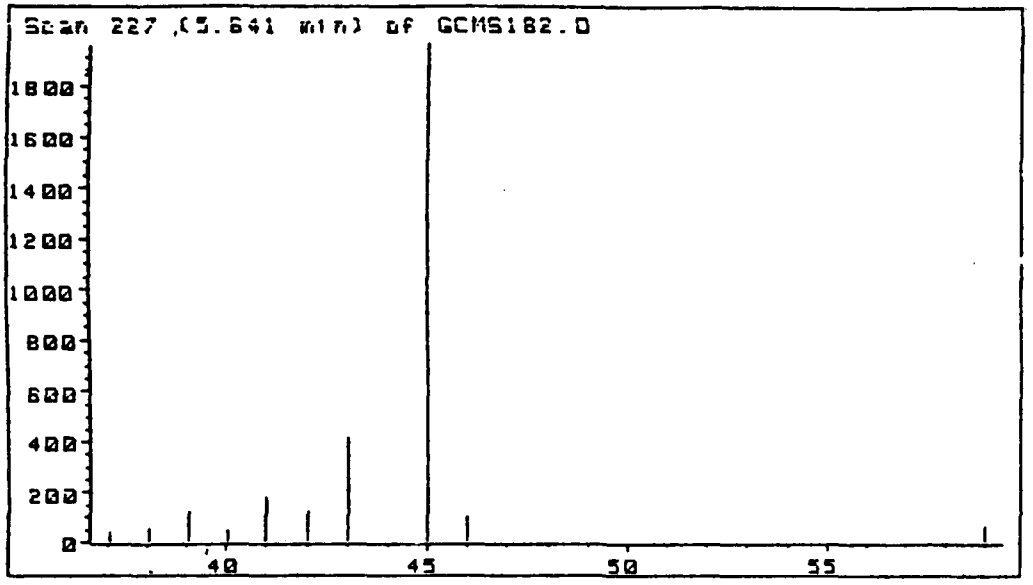

Figure 135. Typical Mass Spectrum of Chromatographic Peak at ca 5.6 Minutes, $K_2B_{10}H_{10}$, 325°C

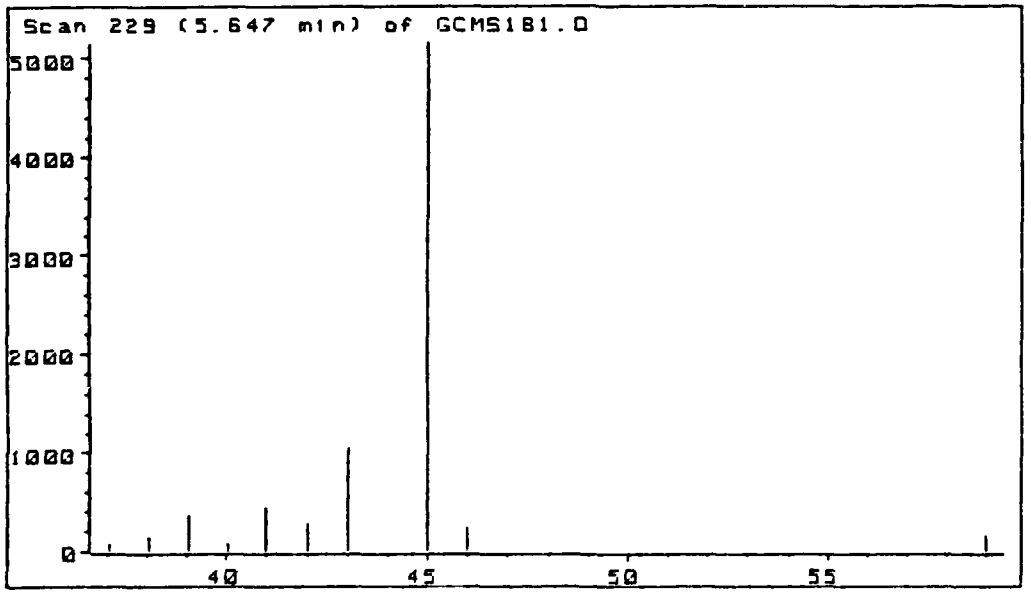

Figure 136. Typical Mass Spectrum of Chromatographic Peak at ca 5.6 Minutes, $K_2B_{10}H_{10}$, 800°C

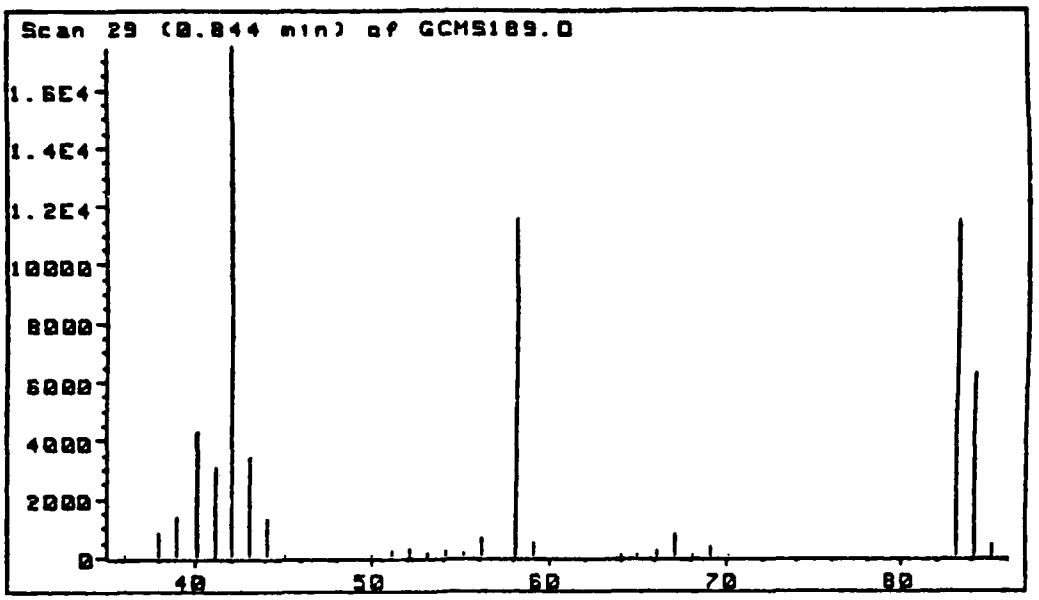

Figure 137. Typical Mass Spectrum of Authentic Sample of N,N-Dimethylaminoacetonitrile

INTENTIONALLY LEFT BLANK.

Table 1. Table of Peaks in Total Ion Chromatograms from GAP 5-3-0 Decomposed 20 Sec at 325°C

Average Time Min.	Figure	Remarks
5.64m	18	Strongest m/e 43,44,58,45.
5.70s	19	Mixture: 43,58; 45.
5.83m	20	Looks like 1,3,5-triazine.
5.97w		
6.02w		
6.30s,v	21	Strongest m/e 43,45,60.
6.33w		
6.52w		
6.61vi		
6.70w		
6.81w		
6.96w		
7.08w		
7.18w		
7.25w		
7.31w		
7.42w		
7.49w		
7.64w		
7.75w		
7.90w		
8.09w		
8.16w		
8.28w,vo		
8.45w		
8.58w		
8.78w		
8.94w		
9.08m		
9.30w		
11.34w		
12.19w		
13.220w		
14.29w		
14.41w		
15.62w,vo		
15.67w,vo		

Table 2. Table of Peaks in Total Ion Chromatograms from GAP 5-3-0 Decomposed 20 Sec at 800°C

Average Time Min.	Figure	Remarks
5.63s	22	Little but m/e 44.
5.68s	23	Most intense: 44,45,43,57,58.
5.73s	24	Mainly m/e 44,43.
5.79s	25	Looks like 1,3,5-triazine.
5.93w		
5.991w		
6.50w		
6.76m,vo		
6.82vi	26	Strongest m/e: 43,45,60,42,44.
6.96m,vo		
7.06m		
7.09m	27	Mixture: 83,56; 45,43,44.
7.15w		
7.25w		
7.29w,vi		
7.35w		
7.43w		
7.54w		
7.70w		
7.93w		
7.98w		
8.09w		
8.20w		
8.78w		
11.42w		

Table 3. Table of Peaks in Total Ion Chromatograms from PEG 5-3-0 Decomposed 20 Sec at 325°C

Average Time Min.	Figure	Remarks
5.67s	28	
5.76s	29	
5.82s	30	Looks like mostly 1,3,5-triazine.
5.97m	31	
6.02m	32	Most intense m/e: 70,43,80,42.
6.13w		
6.23w		
6.31m	33	Most intense m/e: 43,45,60.
6.38m,vo		
6.45w		
6.54m	34	Most intense m/e: 60,44,43.
6.67w,vo		
6.73w		
6.82s,vi	35	
6.97s,vi	36	Most intense m/e: 60,44,43.
7.08vio		
7.14w		
7.29m,vo		
7.36m,vo		
7.42m,vo		
7.51w,vo		
7.72m,vo		
7.80w		
7.88m		
7.96m,vo		
8.02w		
8.15w,vo		
8.21m,vo		
8.25m	37	Most intense m/e: 73,45,43.
8.31m,vo		
8.38w		
8.45w		
8.55w,vo		
8.67w		
8.78w		
8.96w		
9.05w		
10.12m	38	Most intense m/e: 73,45,43.
11.35w		
11.45wvo		
12.20w		

Table 4. Table of Peaks in Total Ion Chromatograms from PEG 5-3-0 Decomposed 20 Sec at 600°C

Average Time Min.	Figure	Remarks
5.68s	39	Strongest by far: m/e 44.
5.83m	40	Mostly 1,3,5-triazine.
5.96m	41	Strongest: 42,58,83,84 $(CH_3)_2NCH_2CN$.
6.91w		
7.00w		
7.10w		
7.24w		
7.34w		
7.44w		
7.52w		
7.88w		
8.06w		
8.51m	42	Strongest: m/e 73.
8.89w		

Table 5. Table of Peaks in Total Ion Chromatograms from PEG 5-3-0 Decomposed 20 Sec at 800°C

Average Time Min.	Figure	Remarks
5.62m	43	
5.68s,vo	44	Same material(s) as following peak?
5.75s,vi	45	Same material(s) as preceding peak?
5.85s,vi	46	Mostly 1,3,5-triazine (m/e 54, 81).
5.94s,vi	47	Mixt., $(CH_3)_2NCH_2CN$ + sym-triazine?
6.02w		
6.13m	48	Most intense are m/e 73,45.
6.19w		
6.51vi	49	
6.75w		
6.89w		
7.01s,vi	50	
7.12w		
7.32m	51	
7.42w		
7.61w		
7.75w		
7.88w		
7.99w		
8.34w		
8.52w		
8.57w,vo		
8.80s,vi	52	
9.38w		
9.48w		
9.79w		
10.33w		
10.86wvo		
11.48w		
12.11wvo		
12.98wvo		

Table 6. Table of Peaks in Total Ion Chromatograms from GAP 5-3-15 Decomposed 20 Sec at 325°C

Average Time Min.	Figure	Remarks
5.54m	53	Little but m/e 44.
5.64s	54	Most intense: m/e 43,44,58.
5.75s	55	Most intense: m/e 43,58.
5.83m,v	56	Looks like 1,3,5-triazine.
5.94m	57	Biggest: 42,83,58,84. $(CH_3)_2NCH_2CN$
6.03w		
6.15m,vo		
6.30m,vo		
6.38w		
6.42w		
6.52w		
6.70w		
6.80w		
6.98s,v	58	Biggest: 55,42,69,44,56,70. $(CH_3)_2NCN$?
7.00w		
7.11w		
7.20w		
7.56w		
7.71w		
7.96w		
8.78w		
9.06w		
9.29w		
11.19w		
11.46w		
12.45m,vo		
12.24w		
13.21w		
14.40m,vo		

Table 7. Table of Peaks in Total Ion Chromatograms from GAP 5-3-15 Decomposed 20 Sec at 800°C

Average Time Min.	Figure	Remarks
5.61s	59	Hardly anything but m/e 44.
5.67s	60	Also has m/e 45,43.
5.75m	61	Mostly 1,3,5-triazine, also m/e 44.
5.91s	62	Most intense: 42,83,58,84. $(CH_3)_2NCH_2CN$.
6.21w		
6.48w		
6.65m,v	63	Strongest: 44,45,59,73; 43,45,60,42.
6.74w		
6.82m	64	Strongest: 55,56,40,53; 83,43,56.
6.90w		
6.96w		
7.04w		
7.16w		
7.27w		
7.34w		
7.45w		
7.53w		
8.03w,vo		
8.79m	65	Most intense: m/e 43,57,71,85.
11.46w		
12.14w,vo		

Table 8. Table of Peaks in Total Ion Chromatograms from PEG 5-3-15 Decomposed 20 Sec at 325°C

Average Time Min.	Figure	Remarks
5.61s	66	A: m/e 44; B: 43,58; C: 45.
5.69s	67	A: m/e 43; B: 58.
5.83s,v	68	Looks like mostly 1,3,5-triazine.
5.98s	69	$(CH_3)_2NCH_2CN$.
6.06w		
6.23w		
6.32w		
6.46s,v	70	Is this CH_3NHCH_2CN or $(CH_3)_2NCN$? Occurs irregularly.
6.51w		
6.64s,v	71	Is this CH_3NHCN_2CN or $(CH_3)_2NCN$? Occurs irregularly.
6.73w		
6.79w		
6.83w,vo		
6.88w,vo		
6.99w		
7.08w,vo		
7.16w		
7.27w		
7.35w		
7.50w		
7.59w		
7.66w		
7.79w		
7.91w		
7.97w		
8.17w		
8.37w		
8.76w		
9.09w		
9.76w		
9.88w		
10.06w		
11.42w		
11.59m		
11.70w		
12.14w		

Table 9. Table of Peaks in Total Ion Chromatograms from PEG 5-3-15 Decomposed 20 Sec at 600°C

Average Time Min.	Figure	Remarks
5.07w		
5.30s,v	72	Strongest is m/e 44, 30 also present.
5.48s,v	73	Strongest: m/e 44.
5.59m,v	74	Strongest: m/e 27; 26,44 also present.
5.67m	75	Mixture: A, 27,26; B, 44.
5.78w		
5.84w		
5.97m	76	Strongest: 42,83,58,84. $(CH_3)_2NCH_2CN$.
6.38m	77	Strongest: 42,69,44,70. $(CH_3)_2NCN$ or CH_3NHCH_2CN?
6.59m	78	
6.69w		
7.17w		
7.79w		
7.88w		
8.89w		
11.58w		
11.68w		
11.88w		

Table 10. Table of Peaks in Total Ion Chromatograms from PEG 5-3-15 Decomposed 20 Sec at 800°C

Average Time Min.	Figure	Remarks
5.60m	79	Almost only m/e is at 44.
5.67m	80	Highest m/e are 45,44,43.
5.72	81	Most intense m/e are 44,43.
5.91w		
5.93m	82	Most intense are 42,58,83,84; $(CH_3)_2NCH_2CN$.
6.06w,vo		
6.11w		
6.22w		
6.39w		
6.44w		
6.53s,v	83	Is this styrene?
6.62s,vi		
6.78w		
6.93w		
7.03w		
7.06m,vi		
7.15w		
7.27w		
7.34w		
7.44w		
7.55w		
7.66w,vo		
7.82w		
7.91w,vo		
8.31w		
8.56w		
8.80m	84	
9.49w		
9.78w,vo		
10.92w,vo		
11.53w		
11.79w,vo		
12.22w,vo		
13.36w		
14.54w,vo		

Table 11. Table of Peaks in Total Ion Chromatograms from HMX Decomposed 20 Sec at 325°C

Average Time Min.	Figure	Remarks
5.71s	85	Unknown A (1,2,4-oxadiazole?)
5.92w		
6.04m	86	Most intense m/e 68,95,38,43.
6.15w		
7.23s	87	
7.34m	88	Most intense m/e 42,58,83,84,40,43,41.
7.42w		
7.61w		
7.70w		
7.95m		
8.67w		
8.74w		

Table 12. Table of Peaks in Total Ion Chromatograms from HMX Decomposed 20 Sec at 400°C

Average Time Min.	Figure	Remarks
5.75s	89	Unknown A (1,2,4-oxadiazole?)
5.88m	90	Contains 1,3,5-triazine.
6.06s	91	Is this $(CH_3)_2NCH_2CN$?
6.84w		
6.96w		
7.04w		
7.14w		
7.56w		
7.87w		
8.02w		
8.51w		
8.88w		

Table 13. Table of Peaks in Total Ion Chromatograms from HMX Decomposed 20 Sec at 600°C

Average Time Min.	Figure	Remarks
5.71s	92	Unknown A (1,2,4-oxadiazole?)
5.86w	93	1,3,5-triazine is present.
5.98m	94	Highest: m/e 42,83,58,84. $(CH_3)_2NCH_2CN$.
6.89w		
6.99w		
7.08w		
7.28w		
7.37w		
7.51w		
7.94w		
8.43w		
8.87w		

Table 14. Table of Peaks in Total Ion Chromatograms from HMX Decomposed 20 Sec at 800°C

Average Time Min.	Figure	Remarks
5.60sh		
5.69s	95	Mostly Unknown A (1,2,4-oxadiazole?)
5.82w	96	Appears to be mostly 1,3,5-triazine.
5.92w		
6.02m,v	97	$(CH_3)_2NCH_2CN$.
6.55w		
6.67w		
6.91w		
6.99w		
7.04m,vo		
7.19w		
7.28w		
7.38w		
7.54m,v	98	Most intense: 45,44,43,42.
7.65w		
7.75m,v	99	
7.76m	100	Is this $CH_3N(CH_2CN)_2$?
7.88w		
8.02w		
8.29w		
8.58w		
8.77w		
8.92w		
11.37w		

Table 15. Table of Peaks in Total Ion Chromatograms from RDX Decomposed 20 Sec at 600°C

Average Time Min.	Figure	Remarks
5.68s,vi	101	Unknown A, (1,2,4-oxadiazole?)
5.88s	102	1,3,5-triazine.
6.60w		
6.80w		
6.97w		
7.39w		
8.90w		

Table 16. Table of Peaks in Total Ion Chromatograms from PEG Decomposed 20 Sec at 325°C

Average Time Min.	Figure	Remarks
5.70m	103	
5.79w		
5.88m	104	
5.94w		
6.02sh	105	
6.12s	106	
6.22m	107	
6.25m	108	
6.31w		
6.41m		
6.48m	109	
6.61w,vo		
6.72w		
6.88w		
6.95w		
7.00w		
7.14w,vo		
7.20w,vo		
7.28w		
7.42w		
7.63m		
7.69w,vo		
7.75w,vo		
7.87s	110	
8.00w		
8.10w		
8.17w		
8.35w		
8.47w		
8.79w,vo		
8.92w,vo		
9.09w,vo		
9.17w		
9.31w,vo		
9.37m		
9.55m	111	
9.70m,vo		
9.81m,vo		
9.94m,vo		
9.99w,vo		
10.11m		
10.20w,vo		
10.33w,vo		
10.40w,vo		
10.60w		
10.73w		
10.83w		
10.94w		

Table 16. Table of Peaks in Total Ion Chromatograms from PEG Decomposed 20 Sec at 325°C (CONT'D)

Average Time Min.	Figure	Remarks
11.14w		
11.22w		
11.37w		
11.58m		
11.79w		
12.05w		
12.19w		
12.41w		
12.57m	112	
12.70w		
12.89m		
13.04m		
13.23w,vo		
13.65w,vo		
13.93w,vo		

Table 17. Table of Peaks in Total Ion Chromatograms from PEG Decomposed 20 Sec at 800°C

Average Time Min.	Figure	Remarks
5.37w,vo		
5.42w,vo		
5.56w,vo		
5.70s	113	
5.83m	114	
5.95m	115	
6.05s	116	
6.14s	117	
6.22w		
6.30w		
6.47w		
6.58w		
6.75m		
6.78w,vo		
6.88w		
6.96w,vo		
7.01w		
7.11w		
7.16w		
7.27w		
7.36m	118	
7.50w,vo		
7.70w		
7.87s	119	
8.00w		
8.08m		
8.43w		
8.69w		
8.79w		
8.89w		
9.06w		
9.34m	120	
9.65w		
9.74w,vo		
9.87m,v	121	
10.00w		
10.39w		
10.81w		
10.90w,vo		
11.07w		
11.25w,vo		
11.39w,vo		
11.49m,vo		
11.65w		
11.72w		
12.06w,vo		
12.21w,vo		
12.39w		

Table 17. Table of Peaks in Total Ion Chromatograms from PEG Decomposed 20 Sec at 800°C (CONT'D)

Average Time Min.	Figure	Remarks
12.57w		
13.00w		
12.64w		
13.94w		
14.21w		

Table 18. Table of Peaks in Total Ion Chromatograms from TAGN Decomposed 20 Sec at 325°C

Average Time Min.	Figure	Remarks
5.60s	122	Mostly m/e 44.
5.66s	123	Mostly 44 and 45.
5.78m	124	May have traces of 1,3,5-triazine.
5.92w		
6.55s,v	125	Mostly 43.
6.65s,v	126	Mostly 43.
6.78s,v	127	Most intense: 44,45,43,42,59,73.
6.86m,v	128	Most intense: 44,43,42,73.
6.95w	129	Most intense: 45,43,42,83,56.
7.01w,vo		
7.08m	130	Most intense: 44,43,45,42.
7.22w		
7.30w		
7.50w		
7.86w		
7.93w		
8.07w		
8.42w		
8.49w		
8.57w		
8.79w		
11.24w		
11.37w		

Table 19. Table of Peaks in Total Ion Chromatograms from TAGN Decomposed 20 Sec at 800°C

Average Time Min.	Figure	Remarks
5.65s	131	Little but m/e 27,26,44,28.
5.67s	132	Little but m/e 44.
5.79w	133	Little if any 1,3,5-triazine.
5.90w	134	Little if any 1,3,5-triazine.
6.01w		
6.21w		
6.86w,vo		
7.00w,vo		
7.16w		
7.28w		
7.41w		
7.55w,vo		
7.98w		
8.07w,vo		
8.20w,vo		
8.31w,vo		
8.44w,vo		
8.70w		
8.77w		
9.43w		
9.92w,vo		
10.12w,vo		
11.37w		
13.22w		

Table 20. Table of Peaks in Total Ion Chromatograms from $K_2B_{10}H_{10}$ Decomposed 20 Sec at 325°C

Average Time Min.	Figure	Remarks
5.45w		
5.64m	135	
5.81w		
5.93w		
6.16w		
6.57w		
6.74w		
7.926w,vo		
8.68w		
10.16w		
11.34w		
11.42w		

Table 21. Table of Peaks in Total Ion Chromatograms from $K_2B_{10}H_{10}$ Decomposed 20 Sec at 800°C

Average Time Min.	Figure	Remarks
5.64m	136	
5.82w,v		
5.93w		
6.00w		
6.53w		
7.20w		
8.77w		
9.41w		
10.75w		
11.59w		

Table 22. Areas and Area Ratios of Some Mass-Spectral Peaks in the Poorly-Retained Products, Pyroprobe at 250°C for 20 Seconds, RDX and RDX-$K_2B_{12}H_{12}$ Mixtures

Run	Cat.?	Peak Areas ($x10^6$) at m/e			Area Ratios		
		Tot	44	70	44/Tot	70/Tot	70/44
46[a]	No	5.443	2.838	0.432	0.534	7.96	15.3
50[a]	No	4.936	2.824	0.237	0.584	4.80	8.39
58[a]	No	4.900	2.56	0.236	0.522	4.82	9.22
72[b]	No	42.299	5.039	0.520	0.119	1.23	10.3
61[a]	Yes	4.490	3.014	0.106	0.677	2.36	3.52
67[a]	Yes	6.577	4.054	0.244	0.616	3.71	6.02
74[b]	Yes	5.247	0.763	0.0414	0.145	0.789	5.43
78[b]	Yes	11.563	1.753	0.0670	0.152	0.579	3.82

a - Masses 35-400 scanned
b - Masses 3-400 scanned

Table 23. Areas and Area Ratios of Some Mass-Spectral Peaks in the Poorly-Retained Products, Pyroprobe at 400°C for 20 Seconds, RDX and RDX-$K_2B_{12}H_{12}$ Mixtures

Run	Cat.?	Peak Areas ($x10^6$) at m/e			Area Ratios		
		Tot	44	70	44/Tot	70/Tot	70/44
49[a]	No	5.247	2.742	0.548	0.522	10.4	20.0
51[a]	No	4.445	2.211	0.431	0.506	9.70	19.5
56[a]	No	5.413	2.488	0.357	0.505	6.60	14.3
71[b]	No	34.602	3.241	0.594	0.0936	1.72	18.3
63[a]	Yes	6.263	3.702	0.166	0.637	2.65	4.48
66[a]	Yes	7.824	4.770	0.299	0.610	3.82	6.27
75[b]	Yes	11.647	1.206	0.146	0.104	1.25	12.1

a - Masses 35-400 scanned
b - Masses 3-400 scanned

Table 24. Areas and Area Ratios of Some Mass-Spectral Peaks in the Poorly-Retained Products, Pyroprobe at 600°C for 20 Seconds, RDX and RDX-$K_2B_{12}H_{12}$ Mixtures

Run	Cat.?	Peak Areas ($x10^6$) at m/e			Area Ratios		
		Tot	44	70	44/Tot	70/Tot	70/44
44[a]	No	4.358	1.651	0.213	0.378	4.89	12.9
52[a]	No	4.56	1.901	0.367	0.428	8.05	19.3
57[a]	No	6.578	2.587	0.360	0.398	5.47	13.9
70[b]	No	59.715	4.199	0.155	0.0703	0.26	3.69
43[a]	Yes	5.470	2.420	0.253	0.428	4.62	10.4
45[a]	Yes	5.333	2.443	0.260	0.458	4.88	10.6
64[a]	Yes	6.722	3.585	0.271	0.536	4.03	7.56
68[a]	Yes	7.908	3.895	0.318	0.492	4.02	8.16
76[b]	Yes	14.563	1.333	0.179	0.0913	1.23	13.4

a - Masses 35-400 scanned
b - Masses 3-400 scanned

Table 25. Areas and Area Ratios of Some Mass-Spectral Peaks in the Poorly-Retained Products, Pyroprobe at 800°C for 20 Seconds, RDX and RDX-$K_2B_{12}H_{12}$ Mixtures

Run	Cat.?	Peak Areas ($x10^6$) at m/e			Area Ratios		
		Tot	44	70	44/Tot	70/Tot	70/44
53[a]	No	4.046	1.869	0.043	0.470	1.06	2.30
54[a]	No	5.067	2.336	0.0549	0.462	1.08	2.35
59[a]	No	3.690	2.088	0.0308	0.566	0.835	1.48
69[b]	No	44.462	4.313	0.151	0.0969	0.34	3.50
73[b]	No	49.992	4.896	0.170	0.0980	0.34	3.47
62[a]	Yes	5.344	3.076	0.127	0.582	2.38	4.13
65[a]	Yes	6.559	3.775	0.151	0.559	2.30	4.00
77[b]	Yes	16.110	1.291	0.0934	0.0801	0.580	7.23

a - Masses 35-400 scanned
b - Masses 3-400 scanned

Table 26. Areas and Area Ratios of Some Mass-Spectral Peaks in the Poorly-Retained Products, Pyroprobe at Indicated Temperature for 20 Seconds, RDX and RDX-$K_2B_{12}H_{12}$ Mixtures

Run	Cat.?	Temp (°C)	Peak Areas ($x10^6$) at m/e			Area Ratios		
			Tot	44	70	44/Tot	70/Tot	70/44
31[a]	Yes	600	1.25	1.02	------	0.816	----	-----
32[a]	No	600	8.08	4.59	0.526	0.568	6.51	11.5
33[a]	Yes	600	6.04	4.50	0.0820	0.745	1.36	1.82
34[a]	No	600	2.25	1.24	0.02	0.551	3.92	7.12
35[a]	Yes	600	12.92	7.79	0.402	0.603	3.11	5.16
36[a,b]	No	600	11.80	7.26	0.05	0.621	0.4	0.7
43[a]	Yes	600	5.66	2.42	0.249	0.428	4.40	10.29
44[a]	No	600	4.36	1.65	0.208	0.378	4.77	12.61
45[a]	Yes	600	5.33	2.44	0.259	0.458	4.86	10.6
23[a,c]	Yes	250	8.08	4.76	0.447	0.589	5.53	9.39
25[a,d]	No	250	9.15	5.44	0.539	0.594	5.89	9.91
27[a,e]	Yes	250	11.30	7.24	0.481	0.641	4.26	6.64
29[a,c]	No	250	6.83	3.65	0.474	0.534	6.94	12.99

a - Masses 35-400 scanned.
b - Atypical run - helium leak caused broad peaks and long retention times.
c - Fresh tube.
d - Tube used for run 23, probably contaminated with $K_2B_{12}H_{12}$ residue, therefore atypical uncatalyzed run.
e - Tube used for runs 23-25.

Table 27. Intensity of 1,3,5-Triazine Peaks, Normalized Against Highest Peaks in Chromatogram

Run	Sample	Temp (°C)	Height of Major 1,3,5-Triazine Peaks m/e 54	m/e 81	Ratio to Highest Chromatog. Peaks m/e 54	m/e 81
107	RDX	600	12,000	12,000	0.43	0.43
108	RDX	600	14,800	15,400	0.42	0.42
109	RDX	600	7,800	8,200	0.37	0.39
110	RDX	600	42,000	16,000	0.38	0.38
111	HMX	800	120	120	0.0055	0.0055
112	HMX	600	1,200	1,000	0.0261	0.0217
113	HMX	400	4,200	4,000	0.072	0.069
114	PEG-5-3-0	600	1,200	1,300	0.0231	0.0250
115	PEG-5-3-15	600	700	800	0.0560	0.0640
116	PEG-5-3-0	600	2,000	2,000	0.0625	0.0625
117	PEG-5-3-15	600	450	500	0.0132	0.0147
118	PEG-5-3-0	800	950	950	0.0194	0.0194
119	PEG-5-3-15	800	160	180	0.0021	0.0023
120	PEG-5-3-0	320	3,000	3,000	0.3191	0.3191
121	PEG-5-3-15	320	150	180	0.0158	0.0189
122	PEG-5-3-0	800	300	300	0.0667	0.0667
123	PEG-5-3-15	800	160	160	0.0032	0.0032
124	PEG-5-3-0	800	400	400	0.1600	0.1600
125	PEG-5-3-15	800	222	222	0.0222	0.0222
127	PEG-5-3-0	325	1,400	1,400	0.0933	0.0933
128	PEG-5-3-15	325	1,300	1,300	0.0394	0.0394
129	PEG-5-3-0	325	2,696	2,696	0.2696	0.2696
130	PEG-5-3-15	325	1,800	1,800	0.0391	0.0391
131	GAP-5-3-0	325	3,200	3,200	0.1143	0.1143
132	GAP-5-3-15	325	600	600	0.0075	0.0075
133	GAP-5-3-0	325	8,685	8,685	0.2171	0.2171
134	GAP-5-3-15	325	200	200	0.0118	0.0118
135	GAP-5-3-0	800	1,400	1,800	0.2333	0.30
136	GAP-5-3-15	800	170	190	0.0567	0.0633
137	GAP-5-3-0	800	550	600	0.0611	0.0667
138	GAP-5-3-15	800	400	500	0.0571	0.0714
139	PEG-5-3-0	325	1,300	1,300	0.2321	0.2321
140	PEG-5-3-0	800	1,700	1,700	0.2833	0.2833
141	PEG-5-3-15	325	500	500	0.0156	0.0156
142	PEG-5-3-15	800	600	600	0.060	0.060
143	GAP-5-3-0	325	5,000	5,000	0.333	0.333
144	GAP-5-3-0	800	2,627	2,627	0.2388	0.2388
145	GAP-5-3-15	325	1,000	1,000	0.2000	0.2000
146	GAP-5-3-15	800	450	450	0.0375	0.0375

Table 27. Intensity of 1,3,5-Triazine Peaks, Normalized Against Highest Peaks in Chromatogram (CONT'D)

Run	Sample	Temp (°C)	Height of Major 1,3,5-Triazine Peaks m/e 54	m/e 81	Ratio to Highest Chromatog. Peaks m/e 54	m/e 81
147	GAP-5-3-0	800	410	350	0.0059	0.0050
148	PEG-5-3-15	800	600	600	0.0214	0.0214
149	GAP-5-3-15	325	1,000	1,200	0.0050	0.0050
150	PEG-5-3-0	325	1,800	1,800	0.1059	0.1059
151	PEG-5-3-0	800	1,200	1,500	0.0522	0.0652
152	PEG-5-3-6	800	1,800	1,800	0.0300	0.0300
153	PEG-5-3-12	800	2,400	2,400	0.0343	0.0343
154	GAP-5-3-3	800	1,500	1,500	0.0366	0.0366
155	GAP-5-3-9	800	3,000	3,000	0.0732	0.0732
156	GAP-5-3-15	800	1,700	1,700	0.0243	0.0243
157	TAGN	800	20	--	0.0011	--
158	TAGN	800	40	30	0.0013	0.0010
159	TAGN	800	--	--	--	--
160	TAGN	325	290	290	0.026	0.026
161	GAP-5-3-0	325	4,500	4,500	0.1800	0.1800
162	GAP-5-3-6	325	6,000	6,000	0.3539	0.3539
163	GAP-5-3-12	325	1,500	1,500	0.0882	0.0882
164	PEG-5-3-3	325	6,000	6,000	0.333	0.333
165	PEG-5-3-9	325	1,800	1,800	0.0720	0.0720
166	PEG-5-3-15	325	500	500	0.0156	0.0156
167	TAGN	800	50	50	0.0038	0.0038
168	TAGN	325	206	206	0.034	0.034
169	TAGN	325	100	100	0.011	0.011
170	TAGN	800	70	--	0.0018	--
171	TAGN	325	310	310	0.016	0.016
172	HMX	800	1,700	1,900	0.053	0.059
173	HMX	800	800	800	0.20	0.22
174	HMX	800	800	800	0.016	0.016
175	HMX	325	100	--	0.0017	--
176	PEG	800	<30	<40	<0.0007	<0.0009
177	PEG	325	--	--	--	--
178	PEG	800	<40	<50	<0.0006	<0.0007
179	PEG	325	--	--	--	--
180	$K_2B_{10}H_{10}$	800	--	--	--	--
181	$K_2B_{10}H_{10}$	800	--	--	--	--
182	$K_2B_{10}H_{10}$	325	--	--	--	--
183	$K_2B_{10}H_{10}$	325	--	--	--	--

Table 27. Intensity of 1,3,5-Triazine Peaks, Normalized Against Highest Peaks in Chromatogram (CONT'D)

Run	Sample	Temp (°C)	Height of Major 1,3,5-Triazine Peaks m/e 54	m/e 81	Ratio to Highest Chromatog. Peaks m/e 54	m/e 81
184	TAGN	800	40	35	0.0031	0.0027
185	TAGN	325	180	220	0.020	0.024
186	HMX	325	175	--	0.0025	--

No of Copies	Organization
...ss, unlimited) 12	Administrator
...ss, limited) 2	Defense Technical Info Center
...sified) 2	ATTN: DTIC-DDA Cameron Station Alexandria, VA 22304-6145
1	HQDA (SARD-TR) WASH DC 20310-0001
1	Commander US Army Materiel Command ATTN: AMCDRA-ST 5001 Eisenhower Avenue Alexandria, VA 22333-0001
1	Commander US Army Laboratory Command ATTN: AMSLC-DL Adelphi, MD 20783-1145
2	Commander Armament RD&E Center US Army AMCCOM ATTN: SMCAR-MSI Picatinny Arsenal, NJ 07806-5000
2	Commander Armament RD&E Center US Army AMCCOM ATTN: SMCAR-TDC Picatinny Arsenal, NJ 07806-5000
1	Director Benet Weapons Laboratory Armament RD&E Center US Army AMCCOM ATTN: SMCAR-CCB-TL Watervliet, NY 12189-4050
1	Commander US Army Armament, Munitions and Chemical Command ATTN: SMCAR-ESP-L Rock Island, IL 61299-5000
1	Commander US Army Aviation Systems Command ATTN: AMSAV-DACL 4300 Goodfellow Blvd. St. Louis, MO 63120-1798
1	Director US Army Aviation Research and Technology Activity Ames Research Center Moffett Field, CA 94035-1099

No of Copies	Organization
1	Commander US Army Missile Command ATTN: AMSMI-RD-CS-R (DOC) Redstone Arsenal, AL 35898-5010
1	Commander US Army Tank-Automotive Command ATTN: AMSTA-TSL (Technical Library) Warren, MI 48397-5000
1	Director US Army TRADOC Analysis Command ATTN: ATAA-SL White Sands Missile Range, NM 88002-5502
(Class. only) 1	Commandant US Army Infantry School ATTN: ATSH-CD (Security Mgr.) Fort Benning, GA 31905-5660
(Unclass. only) 1	Commandant US Army Infantry School ATTN: ATSH-CD-CSO-OR Fort Benning, GA 31905-5660
(Class. only) 1	The Rand Corporation P.O. Box 2138 Santa Monica, CA 90401-2138
1	Air Force Armament Laboratory ATTN: AFATL/DLODL Eglin AFB, FL 32542-5000

Aberdeen Proving Ground

Dir, USAMSAA
ATTN: AMXSY-D
AMXSY-MP, H. Cohen

Cdr, USATECOM
ATTN: AMSTE-TO-F

Cdr, CRDEC, AMCCOM
ATTN: SMCCR-RSP-A
SMCCR-MU
SMCCR-MSI

Dir, VLAMO
ATTN: AMSLC-VL-D

No. of Copies	Organization
4	Commander US Army Research Office ATTN: R. Ghirardelli D. Mann R. Singleton R. Shaw P.O. Box 12211 Research Triangle Park, NC 27709-2211
2	Commander Armament RD&E Center US Army AMCCOM ATTN: SMCAR-AEE-B, D.S. Downs SMCAR-AEE, J.A. Lannon Picatinny Arsenal, NJ 07806-5000
1	Commander Armament RD&E Center US Army AMCCOM ATTN: SMCAR-AEE-BR, L. Harris Picatinny Arsenal, NJ 07806-5000
2	Commander US Army Missile Command ATTN: AMSMI-RK, D.J. Ifshin W. Wharton Redstone Arsenal, AL 35898
1	Commander US Army Missile Command ATTN: AMSMI-RKA, A.R. Maykut Redstone Arsenal, AL 35898-5249
1	Office of Naval Research Department of the Navy ATTN: R.S. Miller, Code 432 800 N. Quincy Street Arlington, VA 22217
1	Commander Naval Air Systems Command ATTN: J. Ramnarace, AIR-54111C Washington, DC 20360
1	Commander Naval Surface Weapons Center ATTN: J.L. East, Jr., G-23 Dahlgren, VA 22448-5000
2	Commander Naval Surface Weapons Center ATTN: R. Bernecker, R-13 G.B. Wilmot, R-16 Silver Spring, MD 20902-5000
5	Commander Naval Research Laboratory ATTN: M.C. Lin J. McDonald E. Oran J. Shnur R.J. Doyle, Code 6110 Washington, DC 20375
1	Commanding Officer Naval Underwater Systems Center Weapons Department ATTN: R.S. Lazar, Code 36301 Newport, RI 02840
1	Superintendent Naval Postgraduate School Department of Aeronautics ATTN: D.W. Netzer Monterey, CA 93940
3	AL/LSCF ATTN: R. Geisler J. Levine D. Weaver Edwards AFB, CA 93523-5000
1	AL/MKPB ATTN: B. Goshgarian Edwards AFB, CA 93523-5000
1	AFOSR ATTN: J.M. Tishkoff Bolling AFB Washington, DC 20332
1	OSD/SDIO/UST ATTN: L.H. Caveny Pentagon Washington, DC 20301-7100
1	Commandant USAFAS ATTN: ATSF-TSM-CN Fort Sill, OK 73503-5600

No. of Copies | Organization

1 | [illegible] Research Lab (AFSC)
ATTN: S.A. Shackleford
USAF Academy, CO 80840-6528

1 | University of Dayton Research Institute
ATTN: D. Campbell
AL/PAP
Edwards AFB, CA 93523

1 | NASA
Langley Research Center
Langley Station
ATTN: G.B. Northam, MS 168
Hampton, VA 23365

4 | National Bureau of Standards
ATTN: J. Hastie
M. Jacox
T. Kashiwagi
H. Semerjian
US Department of Commerce
Washington, DC 20234

1 | Aerojet Solid Propulsion Co.
ATTN: P. Micheli
Sacramento, CA 95813

1 | Applied Combustion Technology, Inc.
ATTN: A.M. Varney
P.O. Box 17885
Orlando, FL 32860

2 | Applied Mechanics Reviews
The American Society of
Mechanical Engineers
ATTN: R.E. White
A.B. Wenzel
345 E. 47th Street
New York, NY 10017

1 | Atlantic Research Corporation
ATTN: M.K. King
5390 Cherokee Avenue
Alexandria, VA 22314

1 | Atlantic Research Corporation
ATTN: R.H.W. Waesche
7511 Wellington Road
Gainesville, VA 22065

No. of Copies | Organization

1 | AVCO Everett Research Laboratory
Division
ATTN: D. Stickler
2385 Revere Beach Parkway
Everett, MA 02149

1 | Battelle Memorial Institute
Tactical Technology Center
ATTN: J. Huggins
505 King Avenue
Columbus, OH 43201

1 | Cohen Professional Services
ATTN: N.S. Cohen
141 Channing Street
Redlands, CA 92373

1 | Exxon Research & Engineering Co.
ATTN: A. Dean
Route 22E
Annandale, NJ 08801

1 | Ford Aerospace and Communications
Corporation
DIVAD Division
Division Headquarters, Irvine
ATTN: D. Williams
Main Street & Ford Road
Newport Beach, CA 92663

1 | General Applied Science Laboratories, Inc.
77 Raynor Avenue
Ronkonkama, NY 11779-6649

1 | General Electric Armament &
Electrical Systems
ATTN: M.J. Bulman
Lakeside Avenue
Burlington, VT 05401

1 | General Electric Ordnance Systems
ATTN: J. Mandzy
100 Plastics Avenue
Pittsfield, MA 01203

2 | General Motors Research Labs
Physics Department
ATTN: T. Sloan
R. Teets
Warren, MI 48090

No. of Copies	Organization
2	Hercules, Inc. Allegheny Ballistics Laboratory ATTN: W.B. Walkup E.A. Yount P.O. Box 210 Rocket Center, WV 26726
1	Honeywell, Inc. Government and Aerospace Products ATTN: D.E. Broden, MS MN50-2000 600 2nd Street NE Hopkins, MN 55343
1	Honeywell, Inc. ATTN: R.E. Tompkins MN38-3300 10400 Yellow Circle Drive Minnetonka, MN 55343
1	IBM Corporation ATTN: A.C. Tam Research Division 5600 Cottle Road San Jose, CA 95193
1	IIT Research Institute ATTN: R.F. Remaly 10 West 35th Street Chicago, IL 60616
2	Director Lawrence Livermore National Laboratories ATTN: C. Westbrook M. Costantino P.O. Box 808 Livermore, CA 94550
1	Lockheed Missiles & Space Co. ATTN: George Lo 3251 Hanover Street Dept. 52-35/B204/2 Palo Alto, CA 94304
1	Los Alamos National Laboratories ATTN: B. Nichols, T7, MS-B284 P.O. Box 1663 Los Alamos, NM 87545
1	National Science Foundation ATTN: A.B. Harvey Washington, DC 20550
1	Olin Corporation Smokeless Powder Operations ATTN: V. McDonald P.O. Box 222 St. Marks, FL 32355
1	Paul Gough Associates, Inc. ATTN: P.S. Gough 1048 South Street Portsmouth, NH 03801-5423
2	Princeton Combustion Research Laboratories, Inc. ATTN: M. Summerfield N.A. Messina 475 US Highway One Monmouth Junction, NJ 08852
1	Hughes Aircraft Company ATTN: T.E. Ward 8433 Fallbrook Avenue Canoga Park, CA 91303
1	Rockwell International Corporation Rocketdyne Division ATTN: J.E. Flanagan/HB02 6633 Canoga Avenue Canoga Park, CA 91304
4	Sandia National Laboratory Combustion Sciences Department ATTN: R. Cattolica S. Johnston P. Mattern D. Stephenson Livermore, CA 94550
1	Science Applications, Inc. ATTN: R.B. Edelman 23146 Cumorah Crest Woodland Hills, CA 91364
3	SRI International ATTN: G. Smith D. Crosley D. Golden 333 Ravenswood Avenue Menlo Park, CA 94025
1	Stevens Institute of Technology Davidson Laboratory ATTN: R. McAlevy, III Hoboken, NJ 07030

No. of Copies	Organization
1	Thiokol Corporation Elkton Division ATTN: S.F. Palopoli P.O. Box 241 Elkton, MD 21921
1	Thiokol Corporation Huntsville Division ATTN: R. Glick Huntsville, AL 35807
3	Thiokol Corporation Wasatch Division ATTN: S.J. Bennett P.O. Box 524 Brigham City, UT 84302
1	United Technologies ATTN: A.C. Eckbreth East Hartford, CT 06108
3	United Technologies Corporation Chemical Systems Division ATTN: R.S. Brown T.D. Myers (2 copies) P.O. Box 49028 San Jose, CA 95161-9028
1	Universal Propulsion Company ATTN: H.J. McSpadden Black Canyon Stage 1 Box 1140 Phoenix, AZ 85029
1	Veritay Technology, Inc. ATTN: E.B. Fisher 4845 Millersport Highway P.O. Box 305 East Amherst, NY 14051-0305
1	Brigham Young University Department of Chemical Engineering ATTN: M.W. Beckstead Provo, UT 84601
1	California Institute of Technology Jet Propulsion Laboratory ATTN: MS 125/159 4800 Oak Grove Drive Pasadena, CA 91103
1	California Institute of Technology ATTN: F.E.C. Culick/MC 301-46 204 Karman Lab. Pasadena, CA 91125

No. of Copies	Organization
1	University of California, Berkeley Mechanical Engineering Department ATTN: J. Daily Berkeley, CA 94720
1	University of California Los Alamos Scientific Lab. P.O. Box 1663, Mail Stop B216 Los Alamos, NM 87545
1	University of California, San Diego ATTN: F.A. Williams Department of Applied Mechanics & Engineering Sciences, B010 La Jolla, CA 92093
2	University of California, Santa Barbara Quantum Institute ATTN: K. Schofield M. Steinberg Santa Barbara, CA 93106
2	University of Southern California Department of Chemistry ATTN: S. Benson C. Wittig Los Angeles, CA 90007
1	Case Western Reserve University Division of Aerospace Sciences ATTN: J. Tien Cleveland, OH 44135
1	Cornell University Department of Chemistry ATTN: T.A. Cool Baker Laboratory Ithaca, NY 14853
1	University of Florida Department of Chemistry ATTN: J. Winefordner Gainesville, FL 32611
3	Georgia Institute of Technology School of Aerospace Engineering ATTN: E. Price W.C. Strahle B.T. Zinn Atlanta, GA 30332

No. of Copies	Organization
1	University of Illinois Department of Mechanical Engineering ATTN: H. Krier 144MEB, 1206 W. Green Street Urbana, IL 61801
1	Johns Hopkins University/APL Chemical Propulsion Information Agency ATTN: T.W. Christian Johns Hopkins Road Laurel, MD 20707
1	University of Michigan Gas Dynamics Lab Aerospace Engineering Bldg. ATTN: G.M. Faeth Ann Arbor, MI 48109-2140
1	University of Minnesota Department of Mechanical Engineering ATTN: E. Fletcher Minneapolis, MN 55455
3	Pennsylvania State University Applied Research Laboratory ATTN: K.K. Kuo H. Palmer M. Micci University Park, PA 16802
1	Pennsylvania State University Department of Mechanical Engineering ATTN: V. Yang University Park, PA 16802
1	Polytechnic Institute of NY Graduate Center ATTN: S. Lederman Route 110 Farmingdale, NY 11735
2	Princeton University Forrestal Campus Library ATTN: K. Brezinsky I. Glassman P.O. Box 710 Princeton, NJ 08540
1	Purdue University School of Aeronautics and Astronautics ATTN: J.R. Osborn Grissom Hall West Lafayette, IN 47906

No. of Copies	Organization
1	Purdue University Department of Chemistry ATTN: E. Grant West Lafayette, IN 47906
2	Purdue University School of Mechanical Engineering ATTN: N.M. Laurendeau S.N.B. Murthy TSPC Chaffee Hall West Lafayette, IN 47906
1	Rensselaer Polytechnic Institute Department of Chemical Engineering ATTN: A. Fontijn Troy, NY 12181
1	Stanford University Department of Mechanical Engineering ATTN: R. Hanson Stanford, CA 94305
1	University of Texas Department of Chemistry ATTN: W. Gardiner Austin, TX 78712
1	University of Utah Department of Mechanical Engineering ATTN: G. Flandro Salt Lake City, UT 84112
1	Virginia Polytechnic Institute and State University ATTN: J.A. Schetz Blacksburg, VA 24061
1	Freedman Associates ATTN: E. Freedman 2411 Diana Road Baltimore, MD 21209-1525

USER EVALUATION SHEET/CHANGE OF ADDRESS

This Laboratory undertakes a continuing effort to improve the quality of the reports it publishes. Your comments/answers to the items/questions below will aid us in our efforts.

1. BRL Report Number TR-3078 Date of Report FEB 90

2. Date Report Received _____

3. Does this report satisfy a need? (Comment on purpose, related project, or other area of interest for which the report will be used.) _____

4. How specifically, is the report being used? (Information source, design data, procedure, source of ideas, etc.) _____

5. Has the information in this report led to any quantitative savings as far as man-hours or dollars saved, operating costs avoided or efficiencies achieved, etc? If so, please elaborate. _____

6. General Comments. What do you think should be changed to improve future reports? (Indicate changes to organization, technical content, format, etc.)

_____

_____

_____

CURRENT ADDRESS

_____
Name

_____
Organization

_____
Address

_____
City, State, Zip

7. If indicating a Change of Address or Address Correction, please provide the New or Correct Address in Block 6 above and the Old or Incorrect address below.

OLD ADDRESS

_____
Name

_____
Organization

_____
Address

_____
City, State, Zip

(Remove this sheet, fold as indicated, staple or tape closed, and mail.)

FOLD HERE

Director
U.S. Army Ballistic Research Laboratory
ATTN: SLCBR-DD-T
Aberdeen Proving Ground, MD 21005-5066

NO POSTAGE
NECESSARY
IF MAILED
IN THE
UNITED STATES

OFFICIAL BUSINESS

BUSINESS REPLY MAIL
FIRST CLASS PERMIT NO 12062 WASHINGTON, DC
POSTAGE WILL BE PAID BY DEPARTMENT OF THE ARMY

Director
U.S. Army Ballistic Research Laboratory
ATTN: SLCBR-DD-T
Aberdeen Proving Ground, MD 21005-9989

FOLD HERE